

SUPPORTING INFORMATION

Cooperativity in luminescent heterobimetallic diphosphine- β -diketiminato complexes

Frederic Krätschmer,^a Xiaofei Sun,^a David Frick,^a Christina Zovko,^a Wim Klopper^b and Peter W. Roesky^{*a}

^a Institute of Inorganic Chemistry, Karlsruhe Institute of Technology, Engesserstr. 15, 76131 Karlsruhe, Germany; E-mail: roesky@kit.edu

^b Institute of Physical Chemistry, Karlsruhe Institute of Technology, Fritz-Haber-Weg 2, 76131 Karlsruhe, Germany.

Table of Contents

Synthesis and characterization.....	S2
General procedures.....	S2
Synthesis of complexes	S3
Synthesis of [PNacAu] (1)	S3
Synthesis of [PNacAg] (2)	S3
Synthese von [PNacAuCu] (3).....	S4
Synthesis of [PNacAuZn] (4)	S5
Synthesis of [PNacAuCd] (5)	S5
Synthesis of [PNacAuHg] (6).....	S6
Synthesis of [PNacAgZn] (7)	S7
Synthesis of [PNacAgCd] (8)	S7
NMR Spectra.....	S9
IR spectra.....	S22
Raman Spectra	S26
UV/Vis spectra.....	S30
Photoluminescence	S34
General methods.....	S34
Photoluminescence spectra	S34
Photoluminescence decay curves	S40
X-ray crystallography.....	S42
General methods.....	S42
Summary of crystal data.....	S43
Crystal structures.....	S46
Quantum chemical calculations	S50
References.....	S64

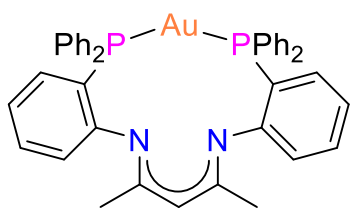
Synthesis and characterization¹

General procedures

All air- and moisture-sensitive manipulations were performed under dry N₂ or Ar atmosphere using standard Schlenk techniques or in an argon-filled *MBraun* glovebox, unless otherwise stated. Prior to use, CH₂Cl₂ and MeCN were dried by refluxing over P₂O₅ and CaH₂, respectively, and distilled under a nitrogen atmosphere. Other solvents (THF, Et₂O and toluene) were dried using an *MBraun* solvent purification system (SPS-800) and degassed. THF was additionally distilled under nitrogen from potassium benzophenone ketyl before storage over 4 Å molecular sieve. THF-d₈ and C₆D₆ was dried over Na-K alloy and CDCl₃ was dried over 4 Å molecular sieves. All deuterated solvents were degassed by freeze-pump-thaw cycles. P_Nac-H, [AuCl(tht)], [Au(C₆F₅)(tht)] and [Ag(C₆F₅)(MeCN)] were prepared according to the literature procedures.² All other chemicals were obtained from commercial sources and used without further purification. NMR spectra were recorded on *Bruker* spectrometers (Avance Neo 300 MHz, Avance Neo 400 MHz or Avance III 400 MHz). Chemical shifts are referenced using signals of the residual protio solvent (¹H) or the solvent (¹³C) and are reported relative to tetramethylsilane (¹H, ¹³C, ²⁹Si), phosphoric acid (³¹P) and dimethylcadmium (¹¹³Cd). All NMR spectra were measured at 298 K, unless otherwise specified. The multiplicity of the signals is indicated as s = singlet, d = doublet, t = triplet, m = multiplet and br = broad. Assignments were determined on the basis of unambiguous chemical shifts, coupling patterns and ¹³C-DEPT experiments or 2D correlations (¹H¹H COSY, ¹H¹³C HSQC, ¹H¹³C HMBC). Infrared (IR) spectra were recorded in the region 3600–400 cm⁻¹ on a *Bruker* Tensor 37 FTIR spectrometer equipped with a room temperature DLaTGS detector and a diamond attenuated total reflection (ATR) unit and a nitrogen-flushed chamber. In terms of their absolute intensity, the signals were classified into different categories (0.0-0.1 vs = very strong, 0.1-0.4 s = strong, 0.4-0.7 m = medium, 0.7-0.9 w = weak, 0.9-1.0 vw = very weak). Raman spectra were recorded in the region 4000-20 cm⁻¹ on a *Bruker* MultiRam spectrometer equipped with a Nd:YAG laser (λ = 1064 nm) and a germanium detector at a resolution of 2 cm⁻¹. The powdered crystalline sample materials were flame sealed in a glass tube. The laser energy was adjusted to values between 20 and 200 mW depending on the FID amplitude and laser focusing. In terms of their intensity, the signals were classified into different categories (vs = very strong, s = strong, m = medium, w = weak, vw = very weak). Elemental analyses were carried out with an *Elementar* Vario Micro Cube. Ultraviolet-visible (UV-Vis) spectra were recorded on an *Ocean Optics* USB-ISS-UV/VIS Spectrophotometer.

Synthesis of complexes

Synthesis of [PNacAu] (1)



PNac-H (200.0 mg, 0.32 mmol, 1.00 eq) and K(BTSA) (60.0 mg, 0.32 mmol, 1.00 eq) were dissolved in 10 mL of THF and stirred at ambient temperatures for 16 hours. Subsequently, [AuCl(tht)] (100.0 mg, 0.32 mmol, 1.00 eq) was added and the suspension was stirred for another 16 hours in the dark. The reaction mixture was filtered and the solvent was reduced to approximate 3 ml. The solution was layered with *n*-pentane to yield [PNacAu] as orange crystals, suitable for X-ray analysis. Crystalline yield: 0.13 g (0.16 mmol, 49%).

$^1\text{H NMR}$ (THF- d_8 , 400 MHz): δ [ppm] = 7.63-7.58 (m, 8 H, H_{Ar}), 7.46-7.38 (m, 12 H, H_{Ar}), 7.20-7.15 (m, 2 H, H_{Ar}), 6.70-6.66 (m, 6 H, H_{Ar}), 4.25 (s, 1 H, $\text{CH}_{\text{NacNac}}$), 1.57 (s, 6 H, CH_3).

$^{13}\text{C}\{^1\text{H}, ^{31}\text{P}\}$ NMR (THF- d_8 , 100 MHz): δ [ppm] = 160.7 ($\text{C}_{\text{NacNac}}^{\text{q}}$), 158.8 ($\text{C}_{\text{N-Ar}}^{\text{q}}$), 135.0 (C_{Ph}), 133.9 ($\text{C}_{\text{Ph-P}}^{\text{q}}$), 133.4 (C_{Ph}), 132.3 (C_{Ph}), 131.5 (C_{Ph}), 129.6 (C_{Ph}), 122.0 (C_{Ph}), 121.0 ($\text{C}_{\text{Ar-P}}^{\text{q}}$), 118.6 (C_{Ph}), 96.2 ($\text{CH}_{\text{NacNac}}$), 22.3 (CH_3).

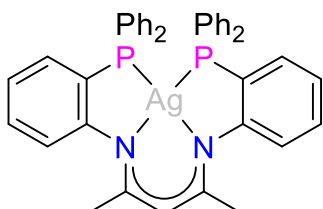
$^{31}\text{P}\{^1\text{H}\}$ NMR (THF- d_8 , 162 MHz): δ [ppm] = 28.6 (s, 2 P, Ar- PPh_2).

IR (ATR): ($\tilde{\nu}$) [cm^{-1}] = 3053 (vw), 2972 (vw), 2872 (vw), 2165 (vw), 1982 (vw), 1651 (vw), 1618 (vw), 1558 (vw), 1529 (vw), 1525 (vw), 1478 (vw), 1456 (vw), 1432 (vw), 1383 (w), 1305 (vw), 1290 (vw), 1256 (vw), 1180 (vw), 1124 (vw), 1098 (vw), 1067 (vw), 1026 (vw), 1001 (vw), 939 (vw), 920 (vw), 873 (vw), 855 (vw), 823 (vw), 797 (vw), 745 (vw), 691 (vw), 492 (w), 403 (w).

Raman: ($\tilde{\nu}$) [cm^{-1}] = Spectra shows broad Raman fluorescence, therefore intensities are not given. 1583, 1388, 1307, 1279, 1178, 1158, 1099, 1032, 999, 791, 410, 342, 283, 230.

EA Calcd (%) for $[\text{C}_{41}\text{H}_{35}\text{AuN}_2\text{P}_2]$ ($814.66 \text{ g mol}^{-1}$): C 60.45, H 4.33, N 3.44; found C 60.63, H 4.24, N 3.14.

Synthesis of [PNacAg] (2)



PNac-H (50.0 mg, 0.08 mmol, 1.00 eq) and AgBF_4 (15.7 mg, 0.32 mmol, 1.00 eq) were dissolved in 10 mL of THF and stirred at ambient temperatures for 16 hours. Subsequently, K(BTSA) (16.1 mg, 0.08 mmol, 1.00 eq) was added and the suspension was stirred for another 16 hours in the dark. The reaction mixture was filtered and the solvent was reduced to approximate 3 ml. The solution was layered with *n*-pentane to yield [PNacAg] as yellow crystals, suitable for X-ray analysis.

Crystalline yield: 14.0 mg (0.02 mmol, 24%).

Supplementary Information

¹H NMR (THF-d₈, 400 MHz): δ [ppm] = 7.47 (dtd, $^3J_{H,H} = 7.6$ Hz, 5.6 Hz, 1.8 Hz, 8 H, H_{Ar}), 7.38-7.35 (m, 12 H, H_{Ar}), 7.19 (ddd, $^3J_{H,H} = 8.4$ Hz, 7.2 Hz, 1.6 Hz, 2 H, H_{Ar}), 6.81 (dtd, $^3J_{H,H} = 7.6$ Hz, 3.9 Hz, 1.6 Hz, 2 H, H_{Ar}), 6.78-6.75 (m, 2 H, Ar-H), 6.72 (t, $^3J_{H,H} = 7.3$ Hz, 2 H, H_{Ar}), 4.31 (s, 1 H, CH_{NacNac}), 1.66 (s, 6 H, CH_3).

¹³C{¹H, ³¹P} NMR (THF-d₈, 100 MHz): δ [ppm] = 162.1 (C^q_{NacNac}), 158.9 (C^q_{N-Ar}), 135.0 (d, $J_{C,Ag} = 1.5$ Hz, C_{Ph}), 134.9 (C_{Ph}), 133.2 (C^q_{Ph-P}), 133.1 (d, $J_{C,Ag} = 1.1$ Hz, C_{Ph}), 131.1 (C_{Ph}), 130.7 (C_{Ph}), 129.6 (C_{Ph}), 123.1 (C_{Ph}), 121.7 (C^q_{Ar-P}), 119.9 (C_{Ph}), 97.2 (CH_{NacNac}), 22.8 (CH_3).

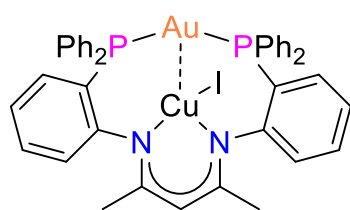
³¹P{¹H} NMR (THF-d₈, 162 MHz): δ [ppm] = -10.7 (dd, $^1J_{P,Ag(107)} = 391.7$ Hz, $^1J_{P,Ag(109)} = 452.2$ Hz, 2 P, Ar-PPh₂).

IR (ATR): ($\tilde{\nu}$) [cm^{-1}] = 3058 (vw), 3002 (vw), 2965 (vw), 2951 (vw), 2912 (vw), 2869 (vw), 1578 (vw), 1539 (w), 1477 (vw), 1456 (vw), 1432 (w), 1382 (m), 1299 (w), 1253 (vw), 1175 (w), 1156 (vw), 1121 (w), 1095 (w), 1065 (vw), 1026 (vw), 1003 (vw), 939 (vw), 919 (vw), 857 (vw), 800 (vw), 741 (w), 690 (w), 618 (vw), 542 (vw), 484 (w), 412 (w).

Raman: ($\tilde{\nu}$) [cm^{-1}] = Spectra shows broad Raman fluorescence, peaks are not visible.

EA Calcd (%) for [C₄₁H₃₅AgN₂P₂] (724.56 g mol⁻¹): C 67.87, H 4.86, N 3.86; found C 67.64, H 4.45, N 3.58.

Synthese von [PNacAuCu] (3)



PNac-H (50.0 mg, 0.08 mmol, 1.00 eq), [Au(C₆F₅)(tbt)] (36.5 mg, 0.08 mmol, 1.00 eq) and copper iodide (15.4 mg, 0.08 mmol, 1.00 eq) were dissolved in 5 mL of THF and stirred at ambient temperatures for 16 hours. The solvent was removed in vacuum, 4 ml DCM were added, and the mixture was filtered. Orange crystals of **3** suitable for X-ray analysis could be obtained by layering the solution with *n*-pentane. Crystalline yield: 55.0 mg (0.05 mmol, 68%).

¹H NMR (THF-d₈, 400 MHz): δ [ppm] = 7.80 (q, $^3J_{H,H} = 6.2$ Hz, 4 H, H_{Ar}), 7.70 (q, $^3J_{H,H} = 7.9$ Hz, 7.2 Hz, 4 H, H_{Ar}), 7.56-7.35 (m, 14 H, H_{Ar}), 7.04-6.92 (m, 4 H, H_{Ar}), 6.88-6.81 (m, 2 H, H_{Ar}), 4.10 (s, 1 H, CH_{NacNac}), 1.20 (s, 6 H, CH_3).

¹³C{¹H, ³¹P} NMR (THF-d₈, 100 MHz): δ [ppm] = 162.7 (C^q_{NacNac}), 156.7 (C^q_{N-Ar}), 136.3 (C_{Ph}), 135.3 (C_{Ph}), 134.7 (C_{Ph}), 132.8 (C^q_{Ph-P}), 132.7 (C_{Ph}), 132.4 (C_{Ph}), 131.6 (C_{Ph}), 131.1 (C^q_{Ph-P}), 129.8 (C_{Ph}), 129.7 (C_{Ph}), 128.5 (C^q_{Ar-P}), 125.9 (C_{Ph}), 122.8 (C_{Ph}), 93.8 (CH_{NacNac}), 22.9 (CH_3).

³¹P{¹H} NMR (THF-d₈, 162 MHz): δ [ppm] = 27.1 (s, 2 P, Ar-PPh₂).

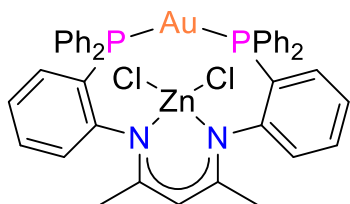
IR (ATR): ($\tilde{\nu}$) [cm^{-1}] = 3049 (vw), 2977 (vw), 2908 (vw), 1614 (vw), 1578 (vw), 1525 (w), 1481 (vw), 1430 (w), 1386 (m), 1258 (vw), 1184 (w), 1158 (vw), 1124 (vw), 1096 (w), 1067 (vw), 1025 (vw), 997 (vw), 921 (vw), 871 (vw), 848 (vw), 824 (vw), 744 (w), 690 (w), 695 (vw), 550 (vw), 492 (w), 415 (w).

Supplementary Information

Raman: ($\tilde{\nu}$) [cm^{-1}] = 3051 (m), 2912 (vw), 1583 (vs), 1553 (w), 1528 (w), 1437 (vw), 1394 (vw), 1290 (w), 1186 (vw), 1161 (w), 1127 (vw), 1097 (w), 1069 (vw), 1035 (s), 1000 (vs), 700 (w), 619 (vw), 556 (vw), 500 (vw), 359 (vw), 252 (vw), 224 (vw), 172 (m).

EA Calcd (%) for $[\text{C}_{41}\text{H}_{35}\text{AuCuIN}_2\text{P}_2] \cdot (\text{CH}_2\text{Cl}_2)$ ($1090.04 \text{ g mol}^{-1}$): C 46.28, H 3.42, N 2.57; found C 46.49, H 3.45, N 2.60.

Synthesis of [PNacAuZn] (4)



PNac-H (50.0 mg, 0.08 mmol, 1.00 eq), $[\text{Au}(\text{C}_6\text{F}_5)(\text{tht})]$ (36.5 mg, 0.08 mmol, 1.00 eq) and zinc chloride (11.0 mg, 0.08 mmol, 1.00 eq) were dissolved in 5 mL of THF and stirred at ambient temperatures for 16 hours. The solvent was removed in vacuum, 4 ml of DCM were added, and the mixture was filtered. Light yellow crystals of **4** suitable for X-ray diffraction analysis could be obtained by layering the solution with *n*-pentane. Crystalline yield: 47.0 mg (0.05 mmol, 61%).

^1H NMR (THF- d_8 , 400 MHz): δ [ppm] = 7.85-7.80 (m, 4 H, H_{Ar}), 7.70-7.65 (m, 4 H, H_{Ar}), 7.61-7.48 (m, 8 H, H_{Ar}), 7.45-7.35 (m, 8 H, H_{Ar}), 7.18 (t, $^3J_{\text{H,H}} = 8.0 \text{ Hz}$, 2 H, H_{Ar}), 6.97 (q, $^3J_{\text{H,H}} = 6.3 \text{ Hz}$, 2 H, H_{Ar}), 4.31 (s, 1 H, $\text{CH}_{\text{NacNac}}$), 1.12 (s, 6 H, CH_3).

$^{13}\text{C}\{^1\text{H}, ^{31}\text{P}\}$ NMR (THF- d_8 , 100 MHz): δ [ppm] = 168.4 ($\text{C}^{\text{q}}_{\text{NacNac}}$), 154.3 ($\text{C}^{\text{q}}_{\text{N-Ar}}$), 136.4 (C_{Ph}), 135.3 (C_{Ph}), 134.5 (C_{Ph}), 133.6 (C_{Ph}), 132.9 (C_{Ph}), 132.8 ($\text{C}^{\text{q}}_{\text{Ph-P}}$), 131.8 (C_{Ph}), 130.3 (C_{Ph}), 130.1 ($\text{C}^{\text{q}}_{\text{Ph-P}}$), 129.9 (C_{Ph}), 128.5 ($\text{C}^{\text{q}}_{\text{Ar-P}}$), 128.4 (C_{Ph}), 125.7 (C_{Ph}), 94.3 ($\text{CH}_{\text{NacNac}}$), 23.2 (CH_3).

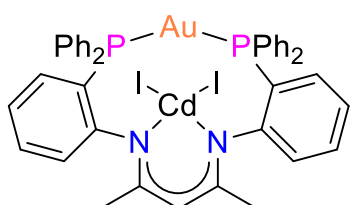
$^{31}\text{P}\{^1\text{H}\}$ NMR (THF- d_8 , 162 MHz): δ [ppm] = 25.7 (s, 2 P, Ar- PPh_2).

IR (ATR): ($\tilde{\nu}$) [cm^{-1}] = 3052 (vw), 3005 (vw), 2883 (vw), 2837 (vw), 2163 (vw), 1980 (vw), 1583 (vw), 1551 (w), 1524 (w), 1480 (vw), 1458 (vw), 1433 (w), 1381 (w), 1311 (vw), 1283 (vw), 1231 (vw), 1184 (vw), 1160 (vw), 1126 (vw), 1096 (vw), 1072 (vw), 1027 (vw), 997 (vw), 939 (vw), 877 (vw), 833 (vw), 744 (w), 691 (w), 622 (vw), 554 (vw), 534 (vw), 500 (w), 491 (w), 419 (w).

Raman: ($\tilde{\nu}$) [cm^{-1}] = 3057 (m), 2928 (vw), 1586 (s), 1554 (w), 1466 (vw), 1438 (vw), 1399 (vw), 1370 (vw), 1288 (w), 1233 (w), 1185 (vw), 1161 (vw), 1129 (vw), 1099 (w), 1034 (w), 1000 (s), 696 (vw), 667 (vw), 620 (vw), 565 (vw), 505 (vw), 363 (w), 306 (vw), 240 (w), 179 (w), 134 (vs).

EA Calcd (%) for $[\text{C}_{41}\text{H}_{35}\text{AuCl}_2\text{N}_2\text{P}_2\text{Zn}]$ ($950.94 \text{ g mol}^{-1}$): C 51.79, H 3.71, N 2.95; found C 51.66, H 3.56, N 2.75.

Synthesis of [PNacAuCd] (5)



[PNacAu] (50.0 mg, 0.06 mmol, 1.00 eq) and cadmium iodide (22.5 mg, 0.06 mmol, 1.00 eq) were dissolved in 4 mL of THF and stirred for 16 hours at ambient temperatures. The reaction mixture was filtered and layered with *n*-pentane, yielding

Supplementary Information

colourless crystals suitable for X-ray diffraction analysis of **5**.
Crystalline yield: 28.0 mg (0.02 mmol, 39%).

^1H NMR (THF- d_8 , 400 MHz): δ [ppm] = 7.82 (q, $^3J_{\text{H,H}} = 6.6$ Hz, 4 H, H_{Ar}), 7.72 (q, $^3J_{\text{H,H}} = 6.8$ Hz, 4 H, H_{Ar}), 7.58-7.41 (m, 14 H, H_{Ar}), 7.32-7.29 (m, 2 H, H_{Ar}), 7.16 (td, $^3J_{\text{H,H}} = 7.8$ Hz, 1.1 Hz, 2 H, H_{Ar}), 6.98 (ddd, $^3J_{\text{H,H}} = 12.9$ Hz, 5.1 Hz, 1.1 Hz, 2 H, H_{Ar}), 4.25 (s, $^4J_{\text{H,Cd}(111/113)} = 1.5$ Hz, 1 H, $\text{CH}_{\text{NacNac}}$), 1.13 (s, 6 H, CH_3).

$^{13}\text{C}\{^1\text{H},^{31}\text{P}\}$ NMR (THF- d_8 , 100 MHz): δ [ppm] = 167.9 ($\text{C}_{\text{NacNac}}^{\text{q}}$), 153.9 ($\text{C}_{\text{N-Ar}}^{\text{q}}$), 135.4 (C_{Ph}), 133.8 (C_{Ph}), 133.7 (C_{Ph}), 132.5 (C_{Ph}), 131.5 (C_{Ph}), 130.9 ($\text{C}_{\text{Ph-P}}^{\text{q}}$), 130.8 (C_{Ph}), 129.6 ($\text{C}_{\text{Ph-P}}^{\text{q}}$), 128.9 (C_{Ph}), 128.7 (C_{Ph}), 128.6 ($\text{C}_{\text{Ar-P}}^{\text{q}}$), 125.5 (C_{Ph}), 124.0 (C_{Ph}), 93.6 ($\text{CH}_{\text{NacNac}}$), 22.3 (s, $^3J_{\text{C,Cd}(111/113)} = 4.2$ Hz, CH_3).

$^{31}\text{P}\{^1\text{H}\}$ NMR (THF- d_8 , 162 MHz): δ [ppm] = 27.4 (s, 2 P, Ar- PPh_2).

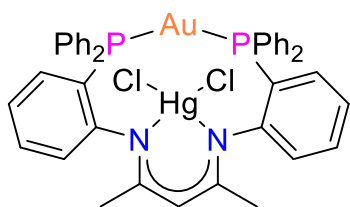
^{113}Cd NMR (THF- d_8 , 67 MHz): δ [ppm] = -273.1 (s).

IR (ATR): ($\tilde{\nu}$) [cm^{-1}] = 3052 (vw), 2968 (vw), 2868 (vw), 2164 (vw), 1980 (vw), 1617 (vw), 1525 (w), 1479 (vw), 1454 (vw), 1432 (w), 1380 (w), 1285 (vw), 1224 (vw), 1184 (vw), 1126 (vw), 1097 (vw), 1066 (vw), 1024 (vw), 998 (vw), 937 (vw), 873 (vw), 822 (vw), 746 (vw), 691 (vw), 619 (vw), 549 (vw), 490 (w), 413 (w).

Raman: ($\tilde{\nu}$) [cm^{-1}] = 3056 (m), 2922 (vw), 1585(vs), 1530 (w), 1437 (w), 1391 (vw), 1284 (w), 1227 (vw), 1185 (w), 1161 (w), 1129 (vw), 1099 (w), 1029 (8m), 1001 (vs), 697 (w), 669 (vw), 619 (w), 557 (w), 500 (vw), 358 (w), 236 (w), 174 (s), 155 (vs).

EA Calcd (%) for $[\text{C}_{41}\text{H}_{35}\text{AuCdI}_2\text{N}_2\text{P}_2]$ (1180.88 g mol $^{-1}$): C 41.70, H 2.99, N 2.37; found C 41.18, H 3.03, N 2.07.

Synthesis of [PNacAuHg] (**6**)



[PNacAu] (50.0 mg, 0.06 mmol, 1.00 eq) and mercury chloride (16.7 mg, 0.06 mmol, 1.00 eq) were dissolved in 4 mL of THF and stirred for 16 hours at ambient temperatures. The reaction mixture was filtered and layered with *n*-pentane, yielding colourless crystals suitable for X-ray diffraction analysis of **6**.

Crystalline yield: 43.0 mg (0.04 mmol, 65%).

^1H NMR (THF- d_8 , 400 MHz): δ [ppm] = 7.78-7.69 (m, 8 H, H_{Ar}), 7.55 (t, $^3J_{\text{H,H}} = 7.3$ Hz, 2 H, H_{Ar}), 7.50-7.43 (m, 12 H, H_{Ar}), 7.13 (t, $^3J_{\text{H,H}} = 7.5$ Hz, 2 H, H_{Ar}), 6.92 (ddd, $^3J_{\text{H,H}} = 12.9$ Hz, 5.3 Hz, 1.3 Hz, 2 H, H_{Ar}), 4.24 (s, $^4J_{\text{H,Hg}(119)} = 5.5$ Hz, 1 H, $\text{CH}_{\text{NacNac}}$), 1.25 (s, 6 H, CH_3).

$^{13}\text{C}\{^1\text{H},^{31}\text{P}\}$ NMR (THF- d_8 , 100 MHz): δ [ppm] = 168.0 ($\text{C}_{\text{NacNac}}^{\text{q}}$), 155.9 ($\text{C}_{\text{N-Ar}}^{\text{q}}$), 136.2 (C_{Ph}), 135.2 (C_{Ph}), 134.9 (C_{Ph}), 133.8 (C_{Ph}), 132.7 (C_{Ph}), 132.6 ($\text{C}_{\text{Ph-P}}^{\text{q}}$), 131.8 (C_{Ph}), 130.9 ($\text{C}_{\text{Ph-P}}^{\text{q}}$), 130.1 (C_{Ph}), 129.9 (C_{Ph}), 128.4 ($\text{C}_{\text{Ar-P}}^{\text{q}}$), 125.9 (C_{Ph}), 124.9 (C_{Ph}), 95.0 ($\text{CH}_{\text{NacNac}}$), 23.8 (CH_3).

$^{31}\text{P}\{^1\text{H}\}$ NMR (THF- d_8 , 162 MHz): δ [ppm] = 27.4 (s, 2 P, Ar- PPh_2).

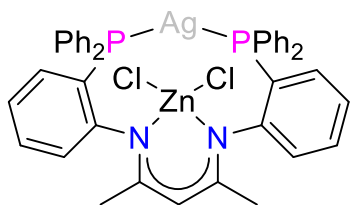
IR (ATR): ($\tilde{\nu}$) [cm^{-1}] = 3052 (vw), 2967 (vw), 2920 (vw), 2857 (vw), 2166 (vw), 1982 (vw), 1894 (vw), 1823 (vw), 1699 (vw), 1616 (vw), 1580 (vw), 1527 (w), 1481 (vw), 1456 (vw), 1432 (w), 1381 (w), 1309 (vw), 1260 (vw), 1182 (vw), 1160 (vw), 1127 (vw), 1098 (w), 1066 (vw), 1026 (vw), 996 (vw), 920 (vw), 874 (vw), 807 (vw), 746 (w), 692 (w), 592 (vw), 552 (vw), 498 (w), 416 (vw).

Supplementary Information

Raman: ($\tilde{\nu}$) [cm^{-1}] = 3055 (w), 1584 (w), 1556 (vw), 1377 (vw), 1283 (vw), 1163 (vw), 1098 (w), 1034 (vw), 1000 (w), 820 (vw), 700 (vw), 619 (vw), 555 (vw), 355 (vw), 324 (w), 268 (m), 172 (vs).

EA Calcd (%) for $[\text{C}_{41}\text{H}_{35}\text{AuCl}_2\text{HgN}_2\text{P}_2]$ (1086.15 g mol^{-1}): C 45.34, H 3.25, N 2.58; found C 45.90, H 3.30, N 2.48.

Synthesis of [PNacAgZn] (7)



PNac-H (50.0 mg, 0.08 mmol, 1.00 eq), $[\text{Ag}(\text{C}_6\text{F}_5)(\text{MeCN})]$ (25.5 mg, 0.08 mmol, 1.00 eq) and zinc chloride (11.0 mg, 0.08 mmol, 1.00 eq) were dissolved in 5 mL of THF and stirred at ambient temperatures for 16 hours. The mixture was filtered and layered with *n*-pentane yielding light yellow crystals of **7** suitable for X-ray diffraction analysis. Crystalline yield: 56.0 mg (0.065 mmol, 80%).

^1H NMR (THF- d_8 , 400 MHz): δ [ppm] = 7.80-7.75 (m, 4 H, H_{Ar}), 7.58-7.45 (m, 12 H, H_{Ar}), 7.38-7.31 (m, 8 H, H_{Ar}), 7.18 (t, $^3J_{\text{H,H}} = 7.5$ Hz, 2 H, H_{Ar}), 7.04 (ddd, $^3J_{\text{H,H}} = 7.9$ Hz, 5.0 Hz, 1.3 Hz, 2 H, H_{Ar}), 4.30 (s, 1 H, $\text{CH}_{\text{NacNac}}$), 1.01 (s, 6 H, CH_3).

$^{13}\text{C}\{^1\text{H}, ^{31}\text{P}\}$ NMR (THF- d_8 , 100 MHz): δ [ppm] = 169.9 ($\text{C}_{\text{NacNac}}^{\text{q}}$), 154.6 ($\text{C}_{\text{N-Ar}}^{\text{q}}$), 154.6 (d, $J_{\text{C,Ag}} = 0.8$ Hz, $\text{C}_{\text{N-Ar}}^{\text{q}}$), 136.6 (d, $J_{\text{C,Ag}} = 2.9$ Hz, C_{Ph}), 134.8 (d, $J_{\text{C,Ag}} = 2.7$ Hz, C_{Ph}), 134.0 (C_{Ph}), 134. (d, $J_{\text{C,Ag}} = 1.6$ Hz, C_{Ph}), 132.9 (C_{Ph}), 132.4 (C_{Ph}), 131.0 (C_{Ph}), 130.6 (d, $J_{\text{C,Ag}} = 6.9$ Hz, $\text{C}_{\text{Ph-P}}^{\text{q}}$), 130.3 (C_{Ph}), 129.9 (C_{Ph}), 129.2 (d, $J_{\text{C,Ag}} = 1.0$ Hz, $\text{C}_{\text{Ar-P}}^{\text{q}}$), 128.0 (C_{Ph}), 125.9 (C_{Ph}), 95.0 ($\text{CH}_{\text{NacNac}}$), 23.3 (CH_3).

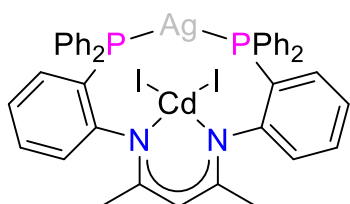
$^{31}\text{P}\{^1\text{H}\}$ NMR (THF- d_8 , 162 MHz): δ [ppm] = -2.3 (dd, $^1J_{\text{P,Ag}(107)} = 496.6$ Hz, $^1J_{\text{P,Ag}(109)} = 572.8$ Hz, 2 P, Ar- PPh_2).

IR (ATR): ($\tilde{\nu}$) [cm^{-1}] = 3053 (vw), 2973 (vw), 2870 (vw), 2165 (vw), 1981 (vw), 1652 (vw), 1617 (vw), 1525 (vw), 1479 (vw), 1455 (vw), 1432 (vw), 1380 (vw), 1285 (vw), 1226 (vw), 1184 (vw), 1127 (vw), 1097 (vw), 1067 (vw), 1025 (vw), 998 (vw), 939 (vw), 875 (vw), 823 (vw), 745 (vw), 691 (vw), 488 (w), 394 (w).

Raman: ($\tilde{\nu}$) [cm^{-1}] = 3054 (w), 2921 (vw), 1585 (s), 1556 (vw), 1436 (vw), 1371 (vw), 1289 (w), 1234 (vw), 1187 (vw), 1163 (vw), 1129 (vw), 1097 (vw), 1030 (w), 1000 (vs), 695 (vw), 618 (vw), 363 (vw), 242 (m), 161 (vs).

EA Calcd (%) for $[\text{C}_{41}\text{H}_{35}\text{AgCl}_2\text{N}_2\text{P}_2\text{Zn}]$ (861.84 g mol^{-1}): C 57.14, H 4.09, N 3.25; found C 56.65, H 4.10, N 2.95.

Synthesis of [PNacAgCd] (8)



PNac-H (50.0 mg, 0.08 mmol, 1.00 eq), $[\text{Ag}(\text{C}_6\text{F}_5)(\text{MeCN})]$ (25.5 mg, 0.08 mmol, 1.00 eq) and cadmium iodide (29.6 mg, 0.08 mmol, 1.00 eq) were dissolved in 5 mL of THF and stirred at ambient temperatures for 16 hours. The mixture was filtered and layered with *n*-pentane yielding light yellow crystals of **8** suitable for X-ray analysis. Crystalline yield: 57.0 mg (0.052 mmol, 65%).

^1H NMR (THF- d_8 , 400 MHz): δ [ppm] = 7.71-7.66 (m, 4 H, H_{Ar}), 7.63-7.58 (m, 4 H, H_{Ar}), 7.55 (t, $^3J_{\text{H,H}} = 7.4$ Hz, 2 H, H_{Ar}), 7.49-7.45 (m, 6 H, H_{Ar}), 7.42-7.38 (m, 6 H, H_{Ar}), 7.26 (dtd, $^3J_{\text{H,H}} = 6.8$ Hz, 3.4 Hz,

Supplementary Information

1.1 Hz, 2 H, H_{Ar}), 7.16 (t, $^3J_{H,H} = 7.5$ Hz, 2 H, H_{Ar}), 7.05 (ddd, $^3J_{H,H} = 7.9$ Hz, 4.8 Hz, 1.4 Hz, 2 H, H_{Ar}), 4.27 (s, $^4J_{H,Cd(111/113)} = 2.0$ Hz, 1 H; CH_{NacNac}), 1.03 (s, 6 H, CH_3).

$^{13}C\{^1H, ^{31}P\}$ NMR (THF- d_8 , 100 MHz): δ [ppm] = 170.8 (s, $^2J_{C,Cd(111/113)} = 2.1$ Hz, C^q_{NacNac}), 155.4 (C^q_{N-Ar}), 155.4 (C^q_{N-Ar}), 136.8 (C_{Ph}), 136.6 (C_{Ph}), 134.4 (C_{Ph}), 134.4 (C_{Ph}), 134.3 (C_{Ph}), 133.6 (C^q_{Ph-P}), 133.5 (C^q_{Ph-P}), 132.9 (C_{Ph}), 132.2 (C_{Ph}), 131.1 (C^q_{Ar-P}), 131.0 (C_{Ph}), 130.1 (C_{Ph}), 129.8 (C_{Ph}), 126.4 (C_{Ph}), 95.9 (s, $^3J_{C,Cd(111/113)} = 11.4$ Hz, CH_{NacNac}), 23.9 (s, $^3J_{C,Cd(111/113)} = 4.1$ Hz, CH_3).

$^{31}P\{^1H\}$ NMR (THF- d_8 , 162 MHz): δ [ppm] = -2.3 (dd, $^1J_{P,Ag(107)} = 470.3$ Hz, $^1J_{P,Ag(109)} = 543.3$ Hz, 2 P, $Ar-PPh_2$).

^{113}Cd NMR (THF- d_8 , 67 MHz): δ [ppm] = -286.1 (s).

IR (ATR): ($\tilde{\nu}$) [cm^{-1}] = 3052 (vw), 2967 (vw), 2867 (vw), 1580 (vw), 1543 (w), 1520 (w), 1479 (vw), 1453 (vw), 1431 (w), 1376 (w), 1309 (vw), 1282 (vw), 1239 (vw), 1180 (vw), 1156 (vw), 1126 (vw), 1095 (vw), 1064 (vw), 1023 (vw), 998 (vw), 983 (vw), 937 (vw), 871 (vw), 848 (vw), 818 (vw), 742 (w), 692 (w), 619 (vw), 550 (vw), 487 (w), 412 (w).

Raman: ($\tilde{\nu}$) [cm^{-1}] = 3055 (w), 2923 (vw), 1584 (m), 1550 (vw), 1436 (vw), 1381 (vw), 1280 (w), 1223 (vw), 1186 (vw), 1160 (vw), 1129 (vw), 1097 (vw), 1071 (vw), 1036 (w), 1002 (m), 694 (vw), 619 (vw), 554 (vw), 493 (vw), 358 (vw), 322 (vw), 294 (vw), 232 (w), 143 (vs).

EA Calcd (%) for $[C_{41}H_{35}AgCdI_2N_2P_2]$ (1091.78 g mol $^{-1}$): C 45.11, H 3.23, N 2.57; found C 45.80, H 3.45, N 2.15.

Supplementary Information

NMR Spectra

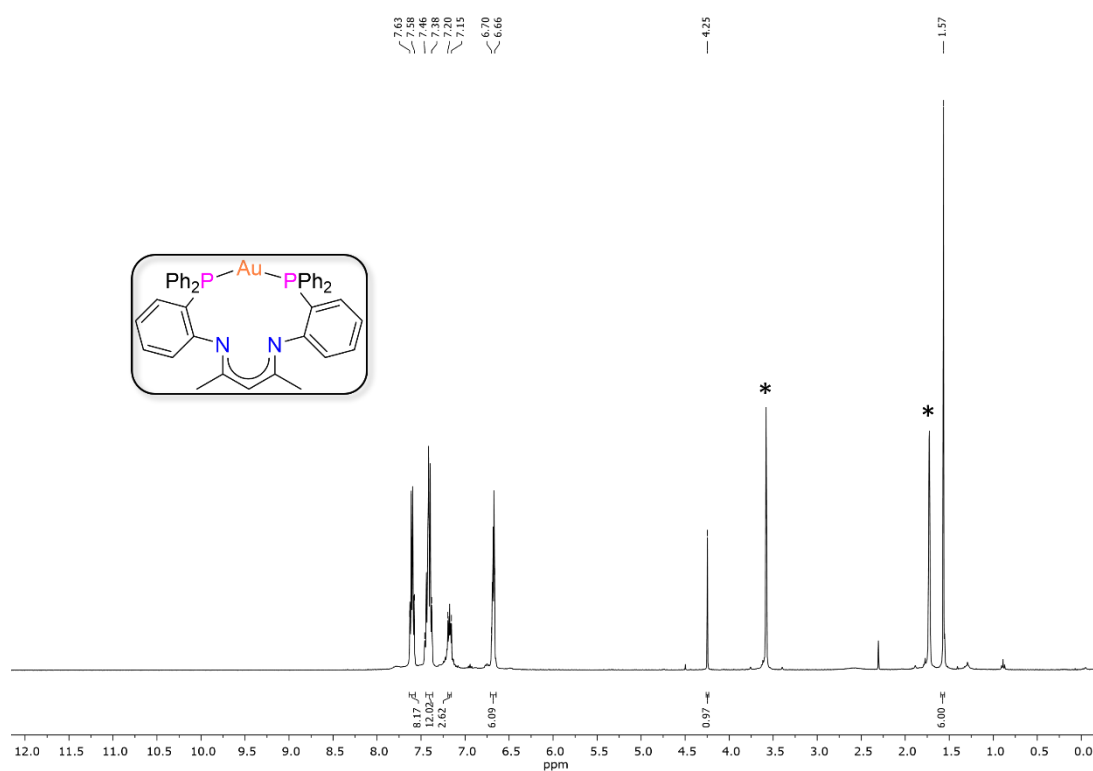


Figure S1: ^1H NMR spectrum of [PNacAu] (1) in THF- d_8 (400 MHz, 298 K): *, residual protio solvent signal.

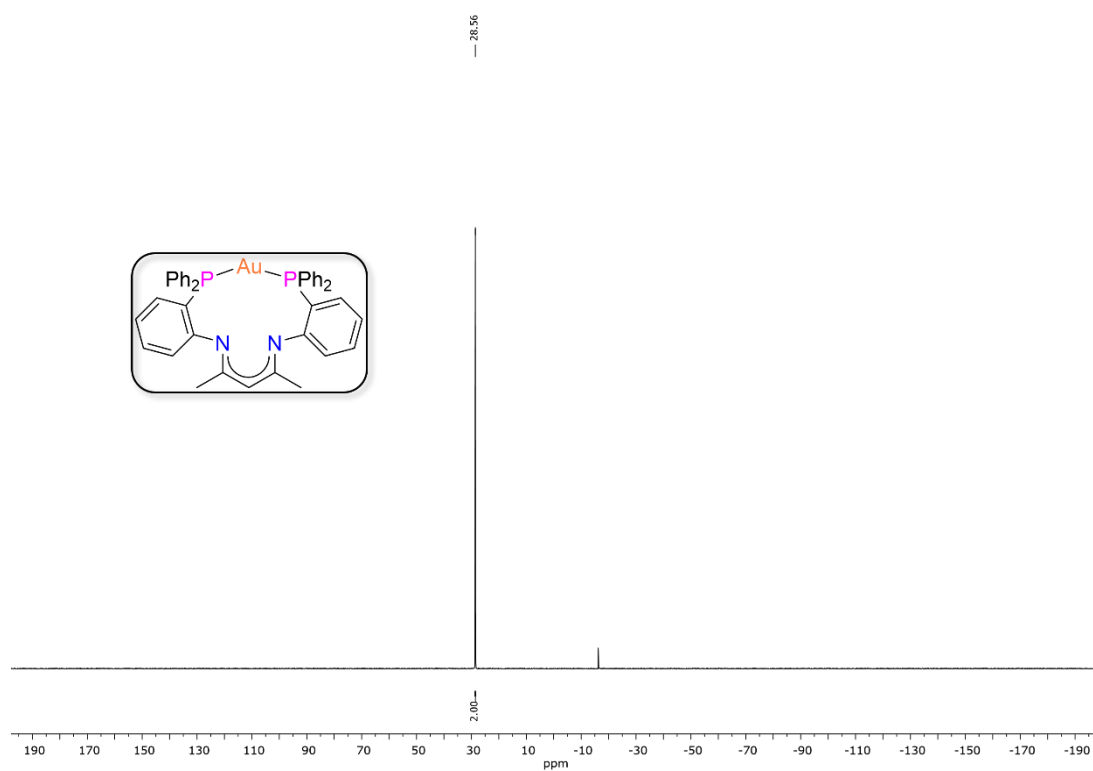


Figure S2: $^{31}\text{P}\{^1\text{H}\}$ NMR spectrum of [PNacAu] (1) in THF- d_8 (162 MHz, 298 K).

Supplementary Information

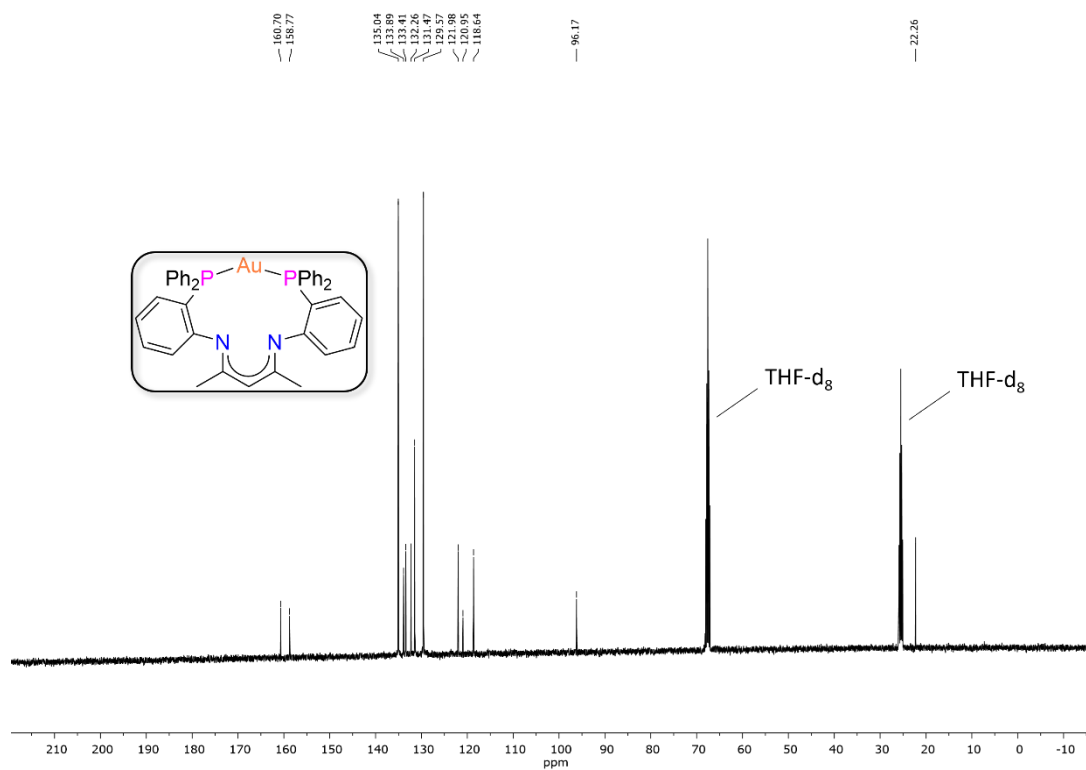


Figure S3: ¹³C{¹H, ³¹P} NMR spectrum of **[PNacAu] (1)** in THF-d₈ (100 MHz, 298 K).

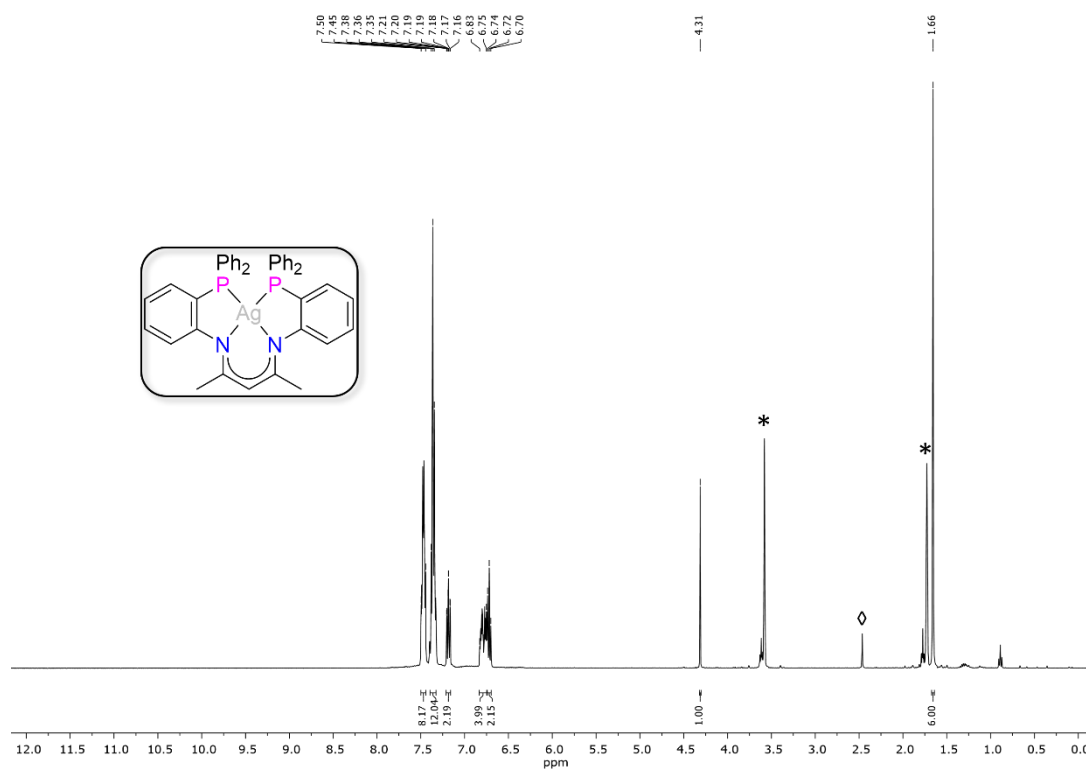


Figure S4: ¹H NMR spectrum of **[PNacAg] (2)** in THF-d₈ (400 MHz, 298 K): *, residual protio solvent signal; ◊, H₂O from the NMR solvent.

Supplementary Information

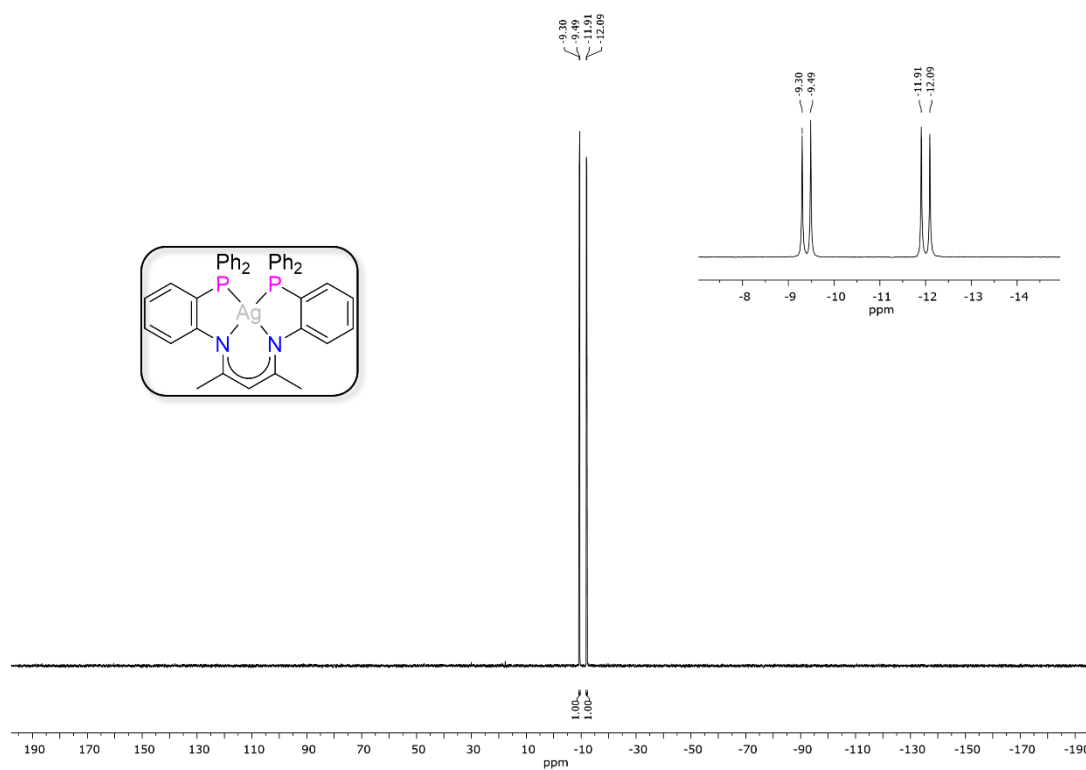


Figure S5: $^{31}\text{P}\{^1\text{H}\}$ NMR spectrum of $[\text{PNacAg}]$ (2) in THF-d_8 (162 MHz, 298 K).

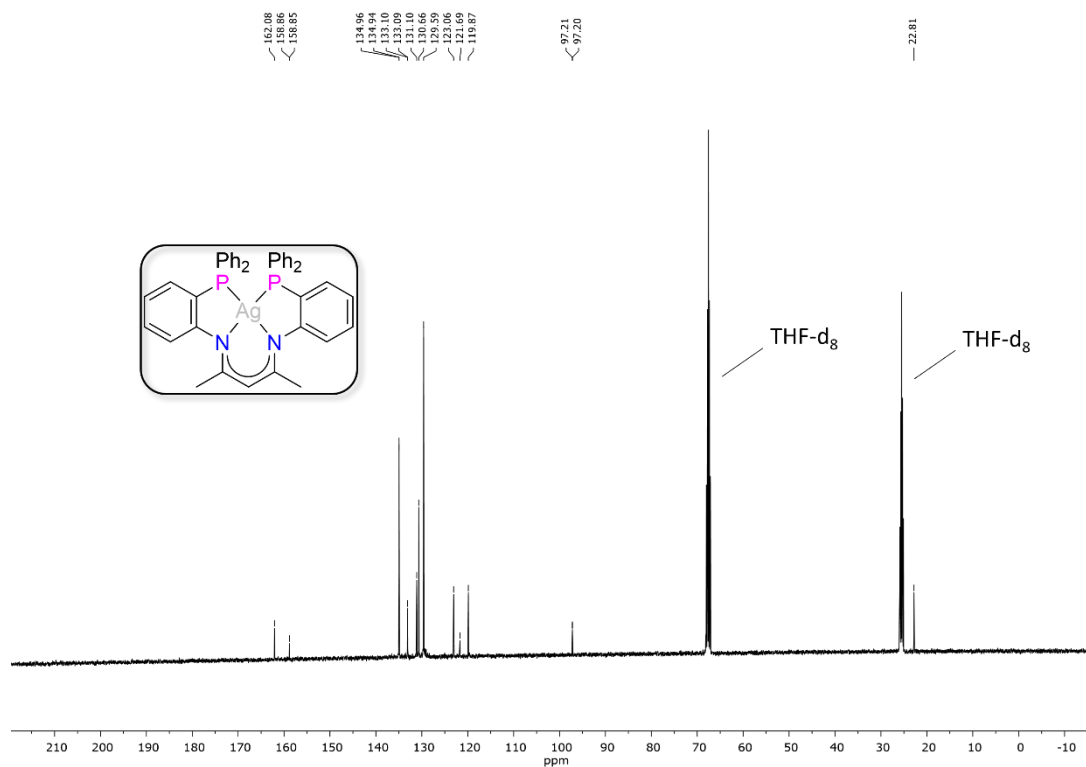


Figure S6: $^{13}\text{C}\{^1\text{H},^{31}\text{P}\}$ NMR spectrum of $[\text{PNacAg}]$ (2) in THF-d_8 (100 MHz, 298 K).

Supplementary Information

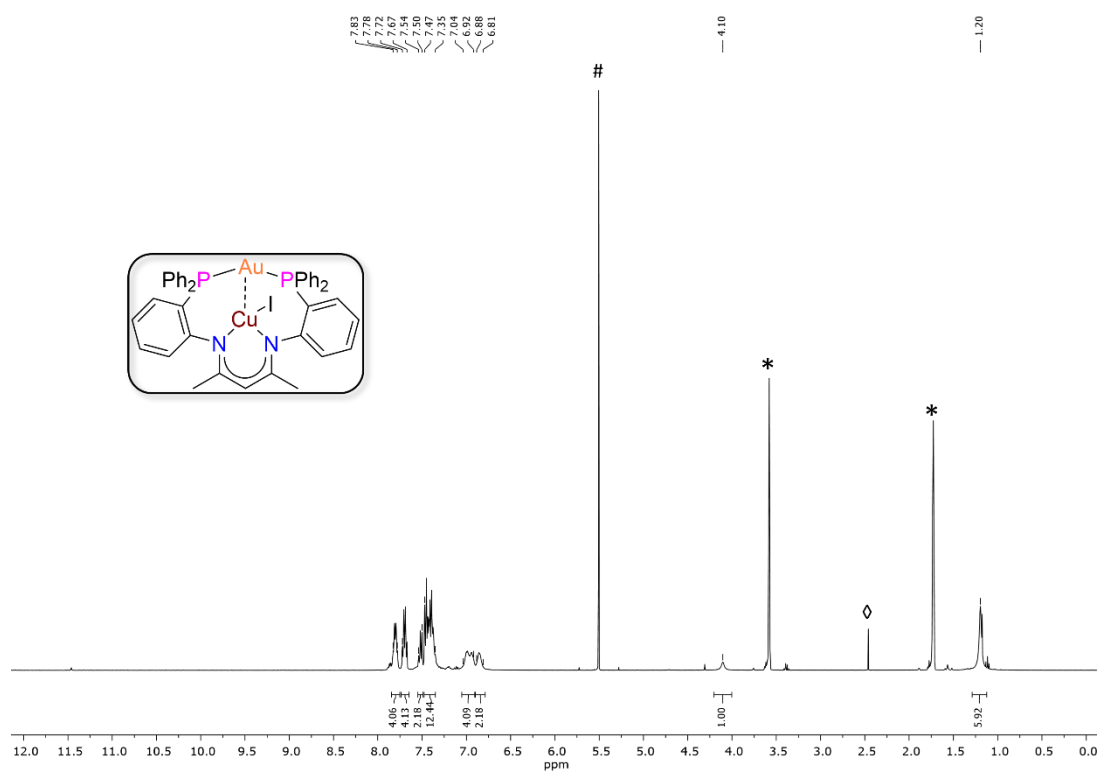


Figure S7: ^1H NMR spectrum of [PNacAuCu] (3) in THF- d_8 (400 MHz, 298 K): *, residual protio solvent signal; #, DCM traces that are originating from the crystals; ◇, H₂O from the NMR solvent.

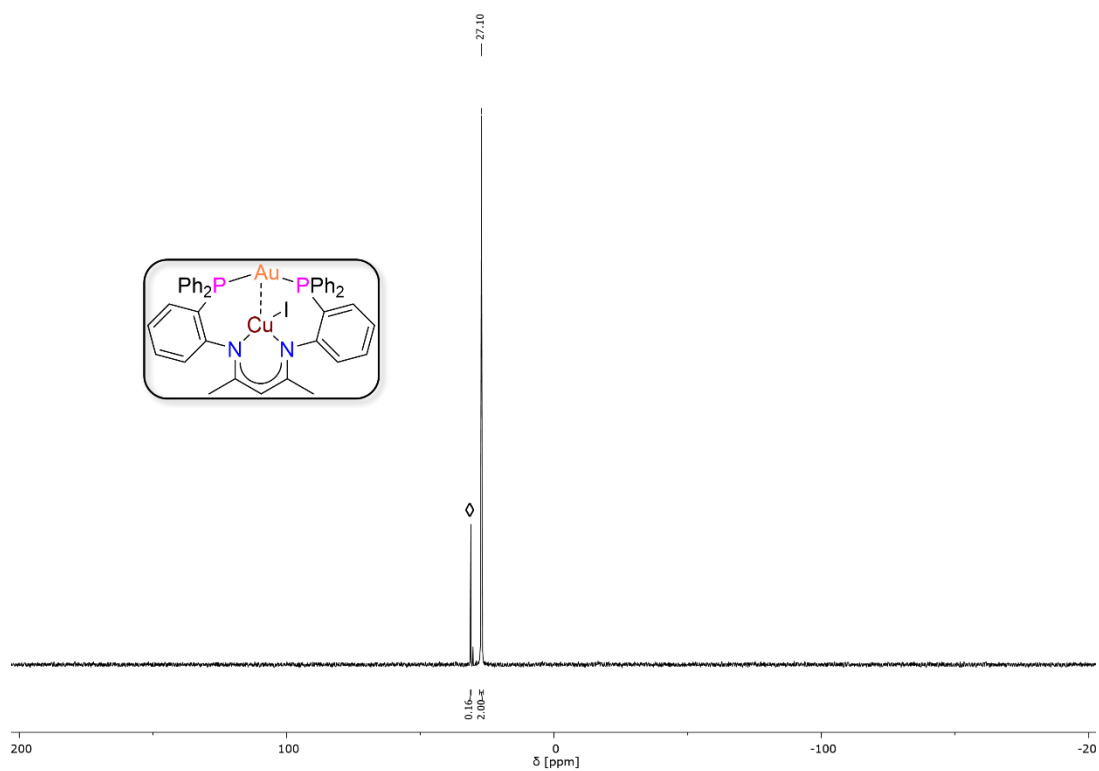


Figure S8: $^{31}\text{P}\{^1\text{H}\}$ NMR spectrum of [PNacAuCu] (3) in THF- d_8 (162 MHz, 298 K): ◇, decomposition product.

Supplementary Information

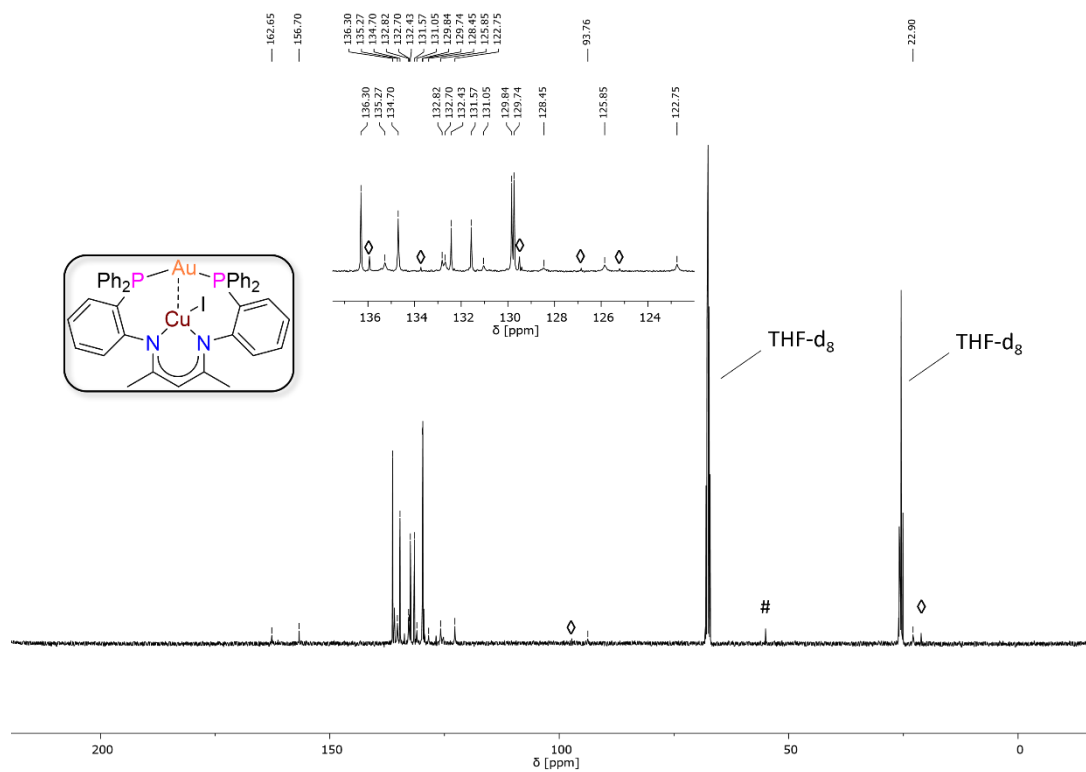


Figure S9: $^{13}\text{C}\{^1\text{H},^{31}\text{P}\}$ NMR spectrum of **[PNacAuCu] (3)** in THF-d_8 (100 MHz, 298 K): #, DCM traces that are originating from the crystals; \diamond , decomposition product.

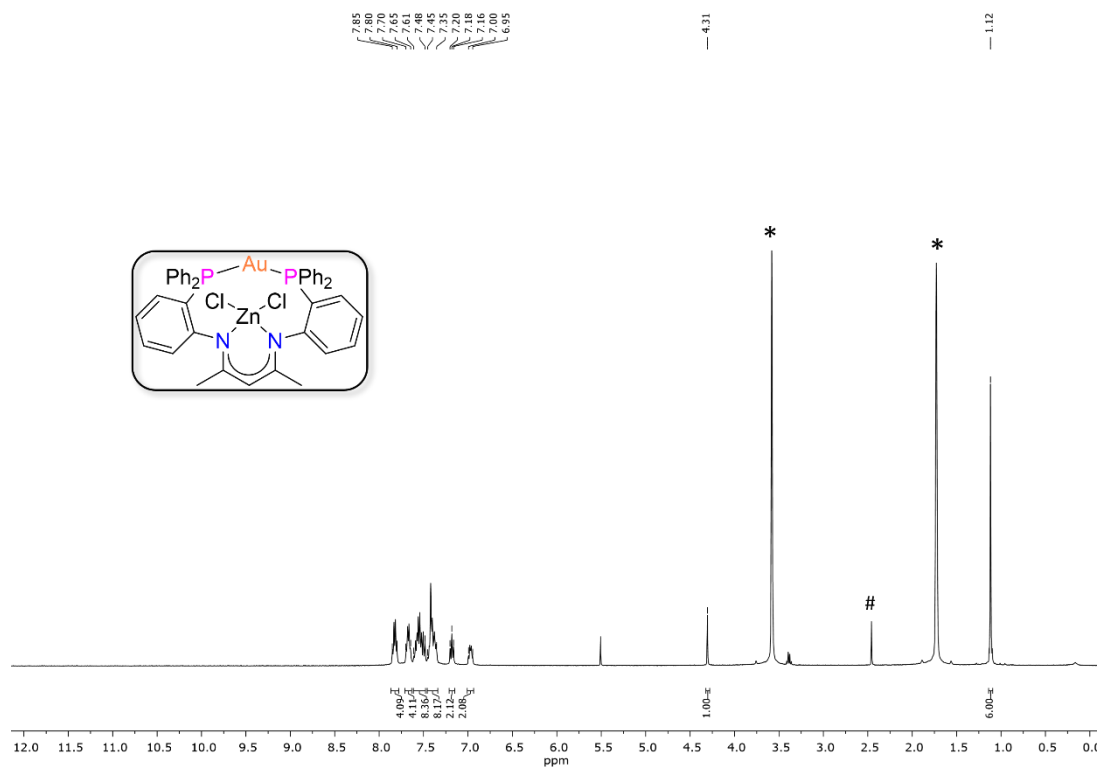


Figure S10: ^1H NMR spectrum of **[PNacAuZn] (4)** in THF-d_8 (400 MHz, 298 K): *, residual protio solvent signal; #, toluene traces that are originating from the crystals.

Supplementary Information

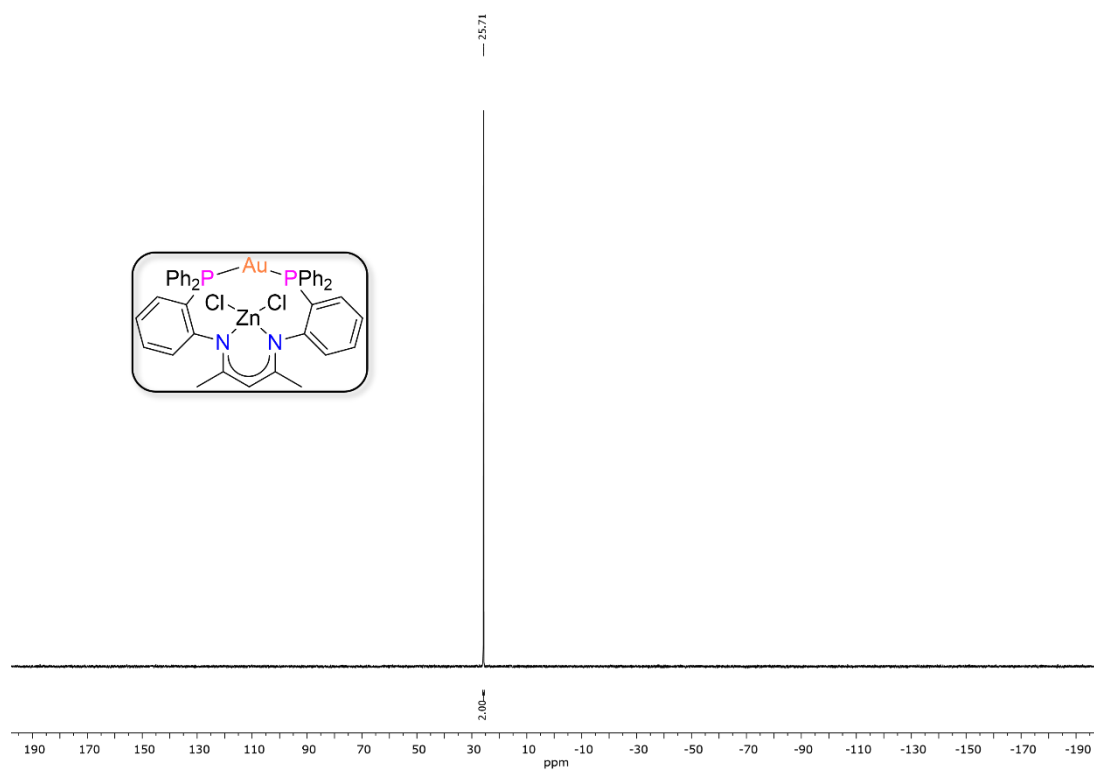


Figure S11: $^{31}\text{P}\{^1\text{H}\}$ NMR spectrum of [PNacAuZn] (4) in THF- d_8 (162 MHz, 298 K).

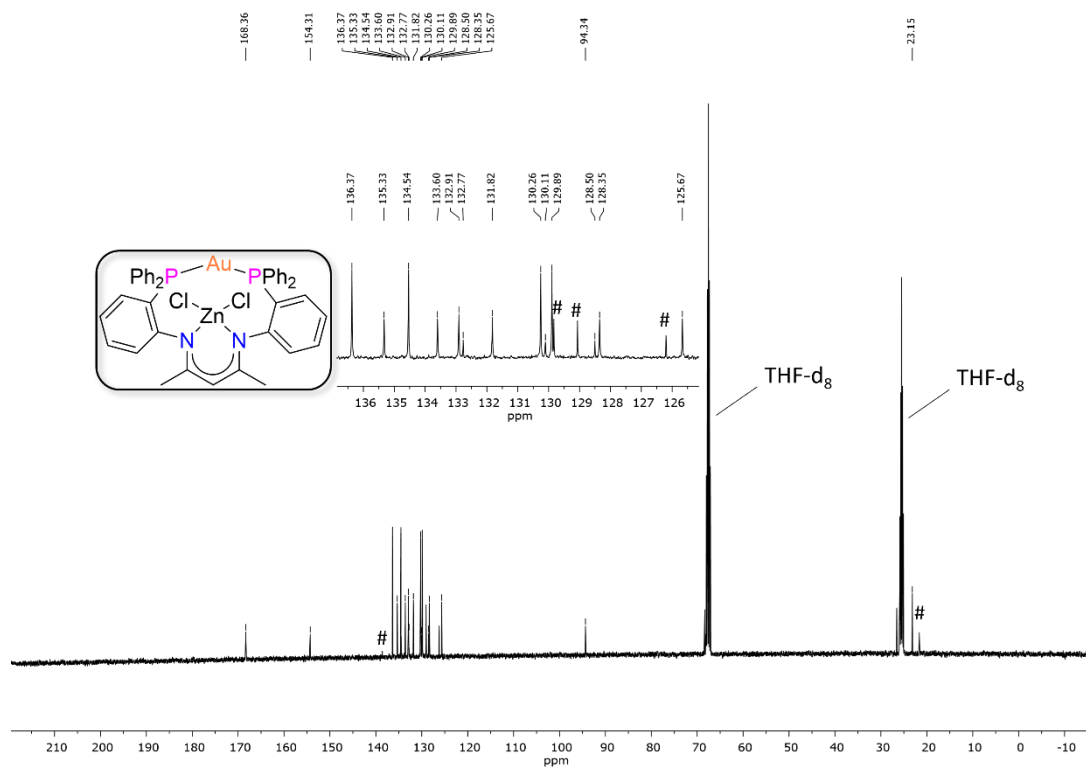
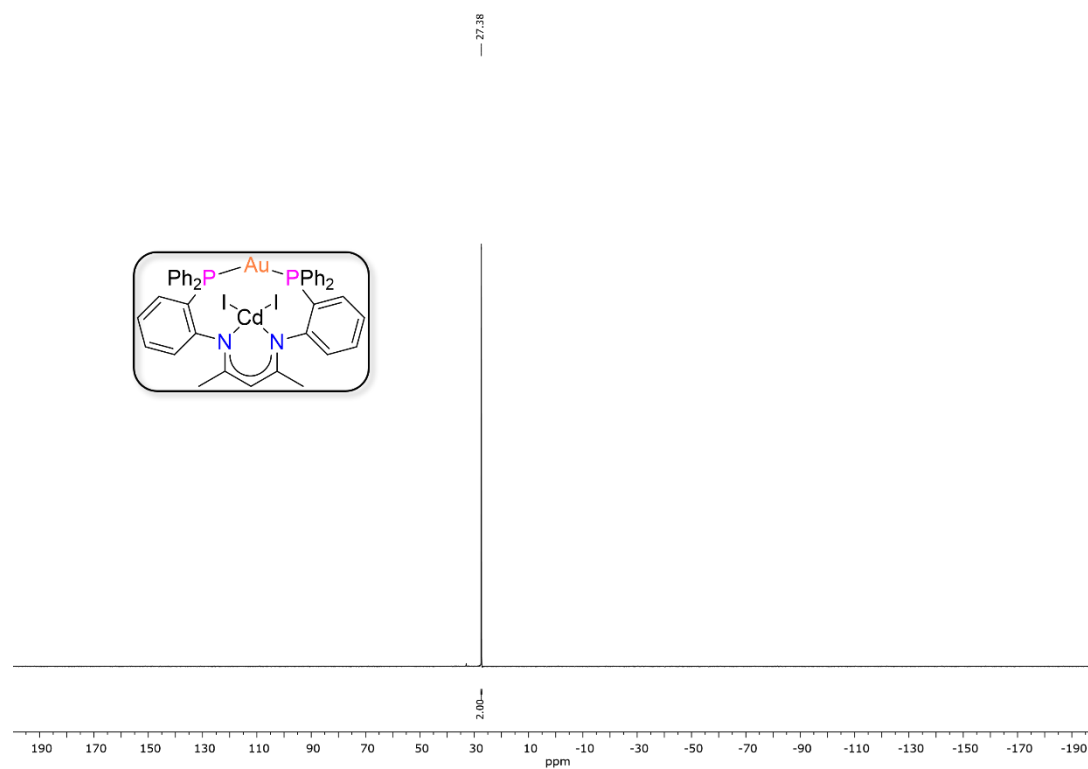
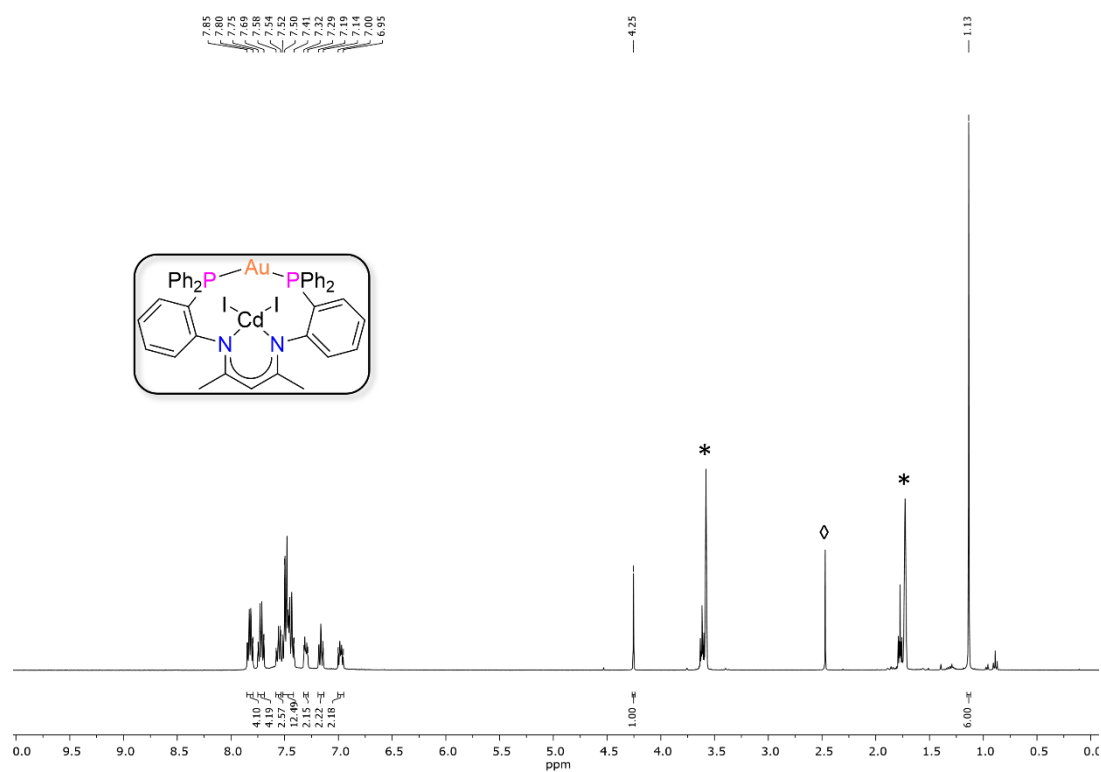


Figure S12: $^{13}\text{C}\{^1\text{H},^{31}\text{P}\}$ NMR spectrum of [PNacAuZn] (4) in THF- d_8 (100 MHz, 298 K): #, toluene traces that are originating from the crystals.

Supplementary Information



Supplementary Information

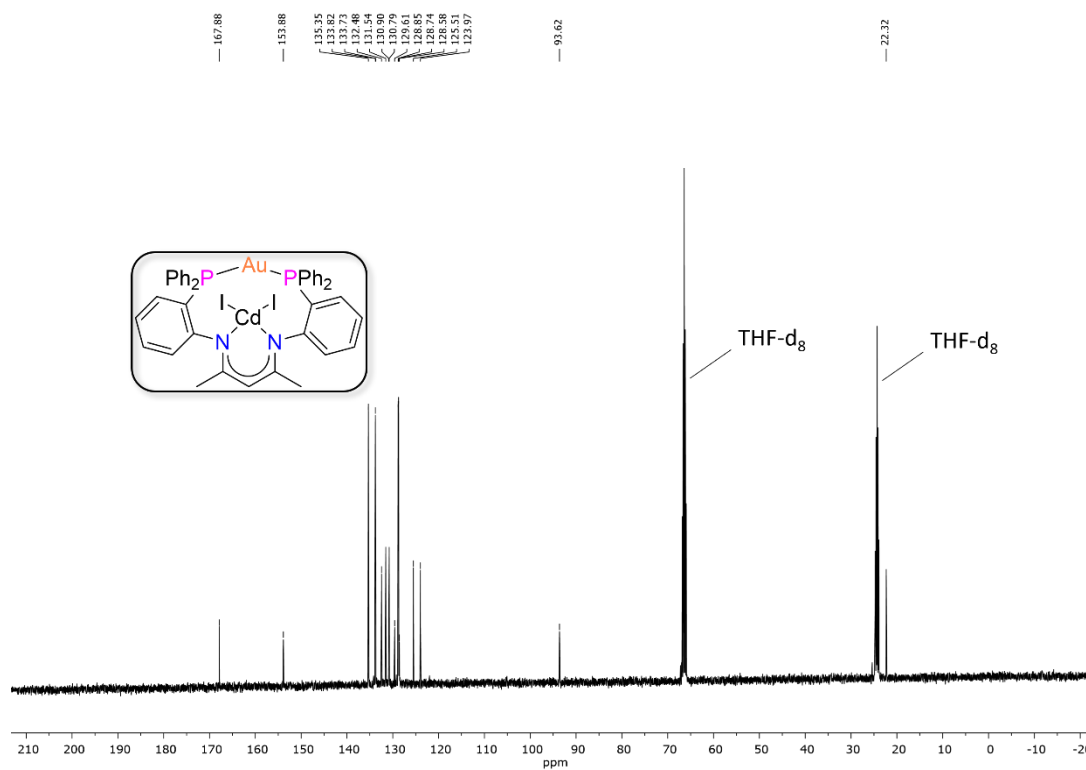


Figure S15: $^{13}\text{C}\{^1\text{H},^{31}\text{P}\}$ NMR spectrum of [PNacAuCd] (5) in THF- d_8 (100 MHz, 298 K).

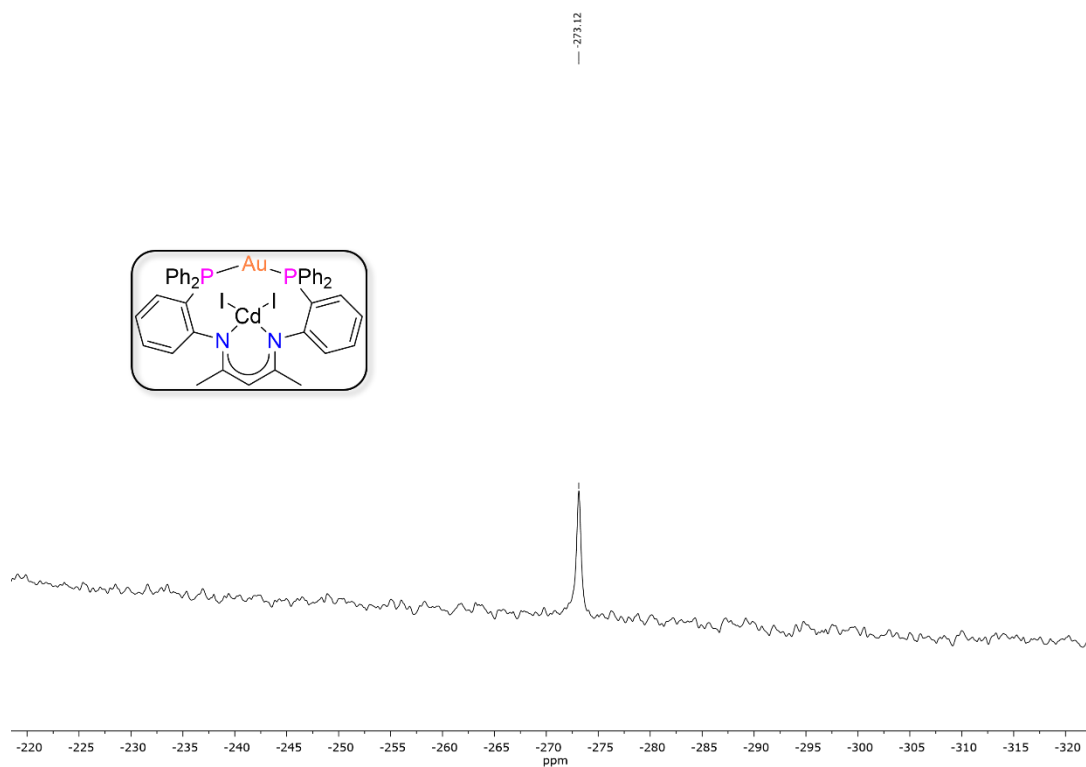


Figure S16: ^{113}Cd NMR spectrum of [PNacAuCd] (5) in THF- d_8 (67 MHz, 298 K).

Supplementary Information

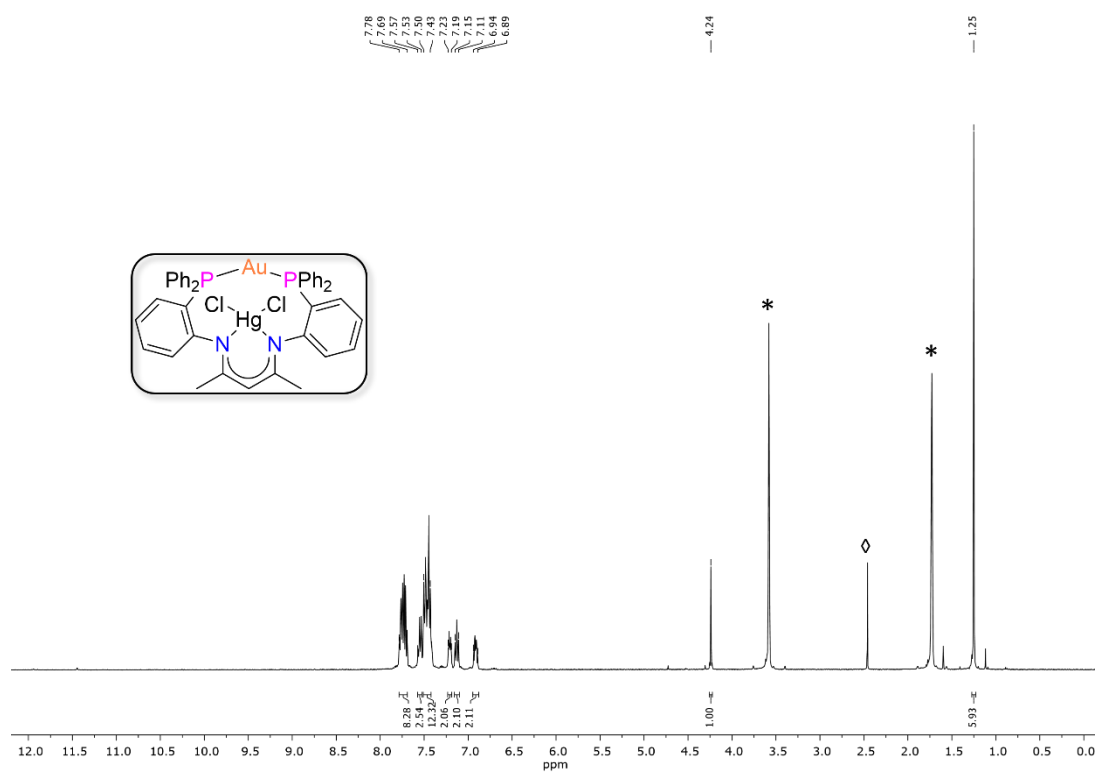


Figure S17: ^1H NMR spectrum of **[PNacAuHg] (6)** in THF- d_8 (400 MHz, 298 K): *, residual protio solvent signal; \diamond , H₂O from the NMR solvent.

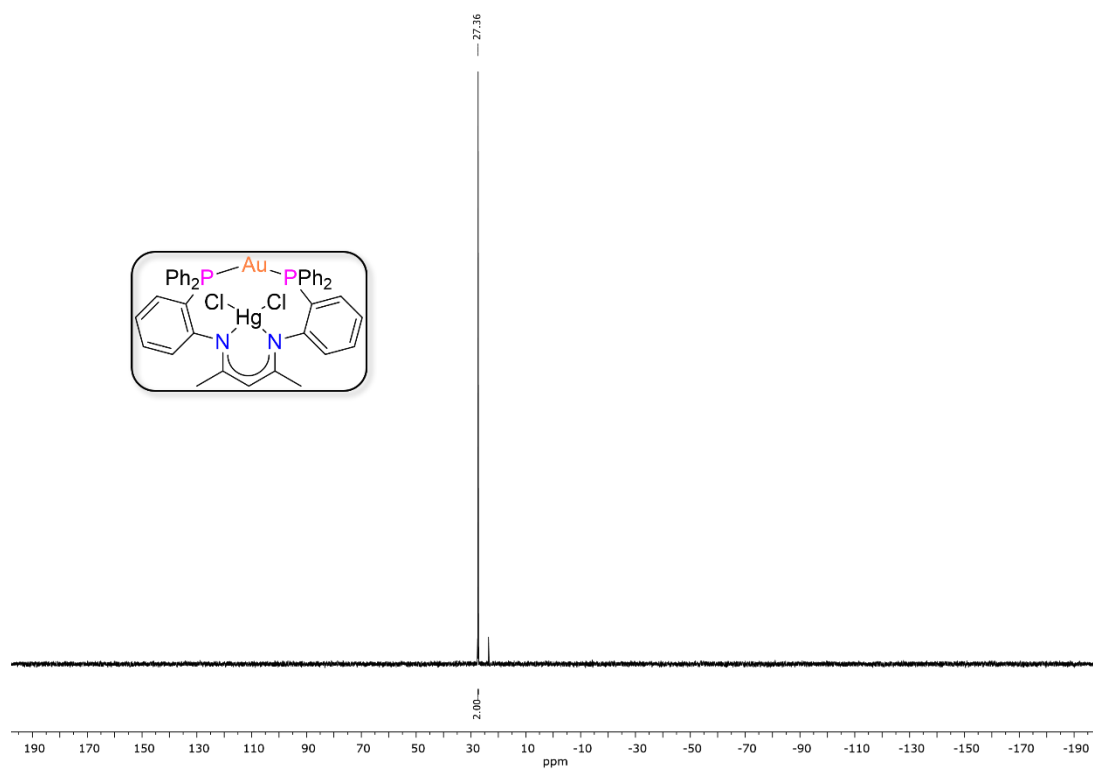
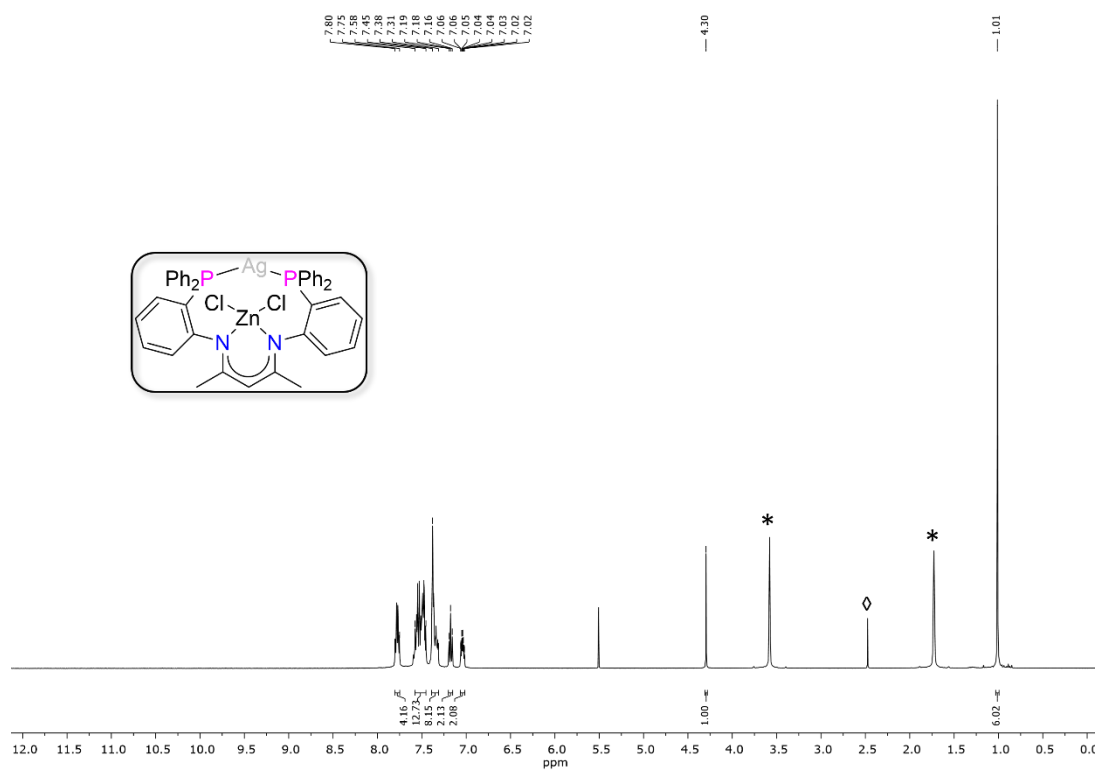
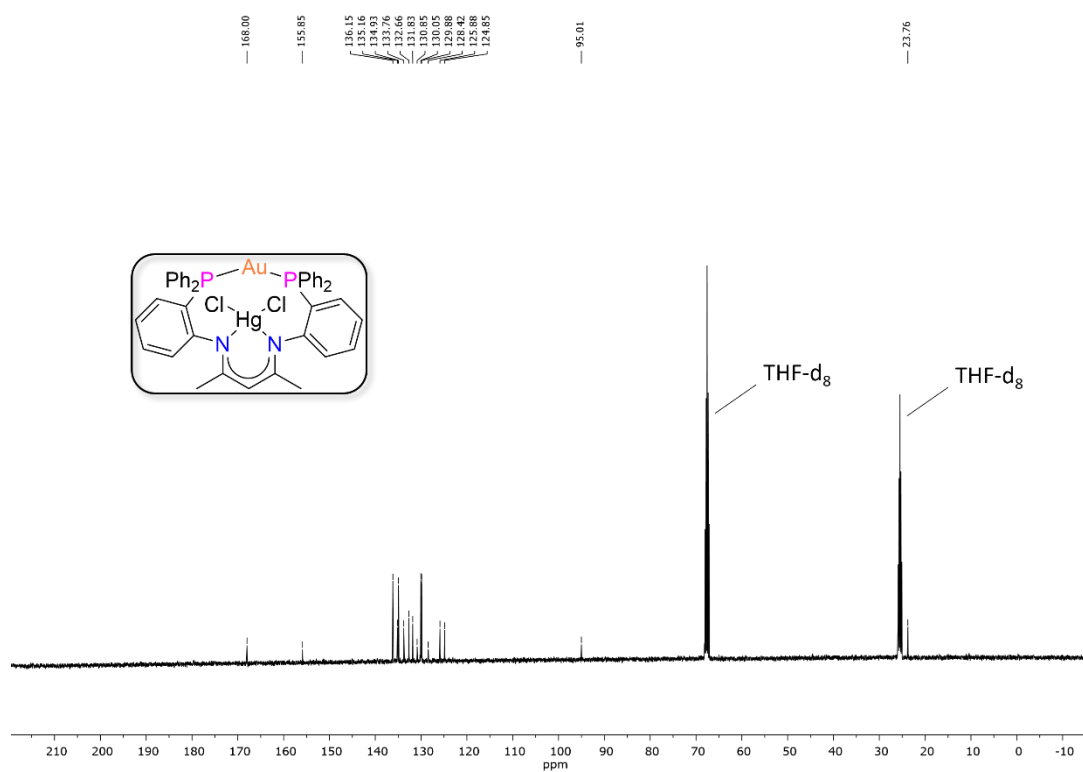


Figure S18: $^{31}\text{P}\{^1\text{H}\}$ NMR spectrum of **[PNacAuHg] (6)** in THF- d_8 (162 MHz, 298 K).

Supplementary Information



Supplementary Information

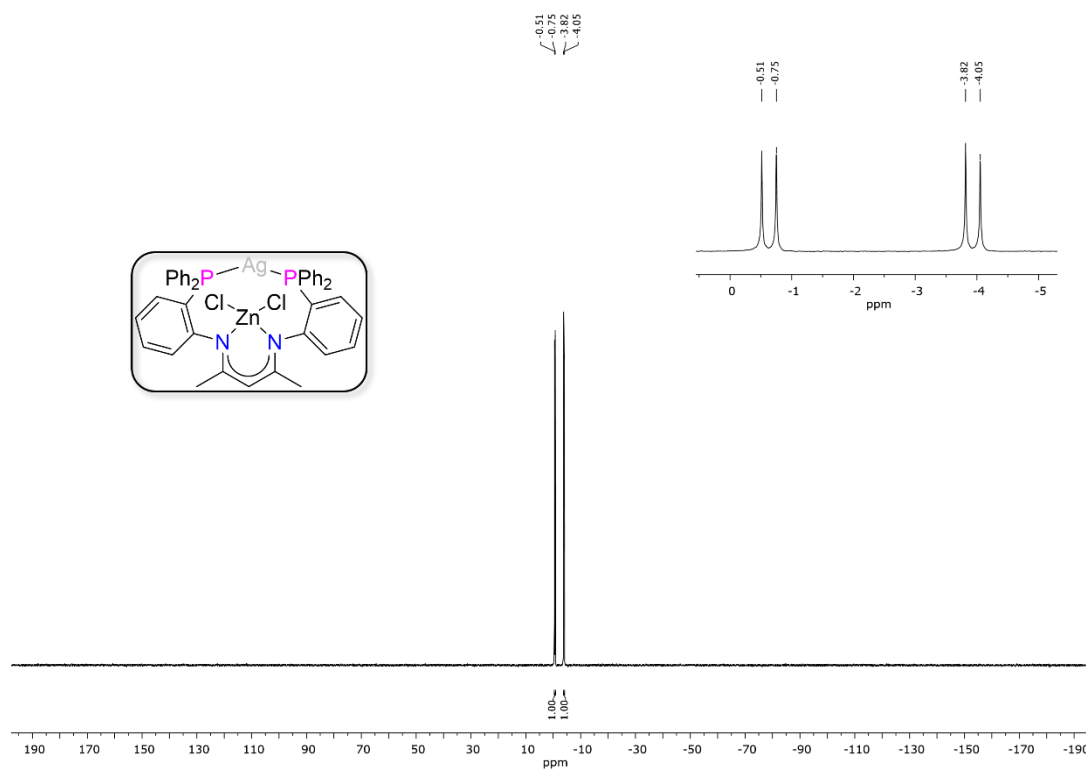


Figure S21: $^{31}\text{P}\{^1\text{H}\}$ NMR spectrum of $[\text{PNacAgZn}]$ (7) in THF-d_8 (162 MHz, 298 K).

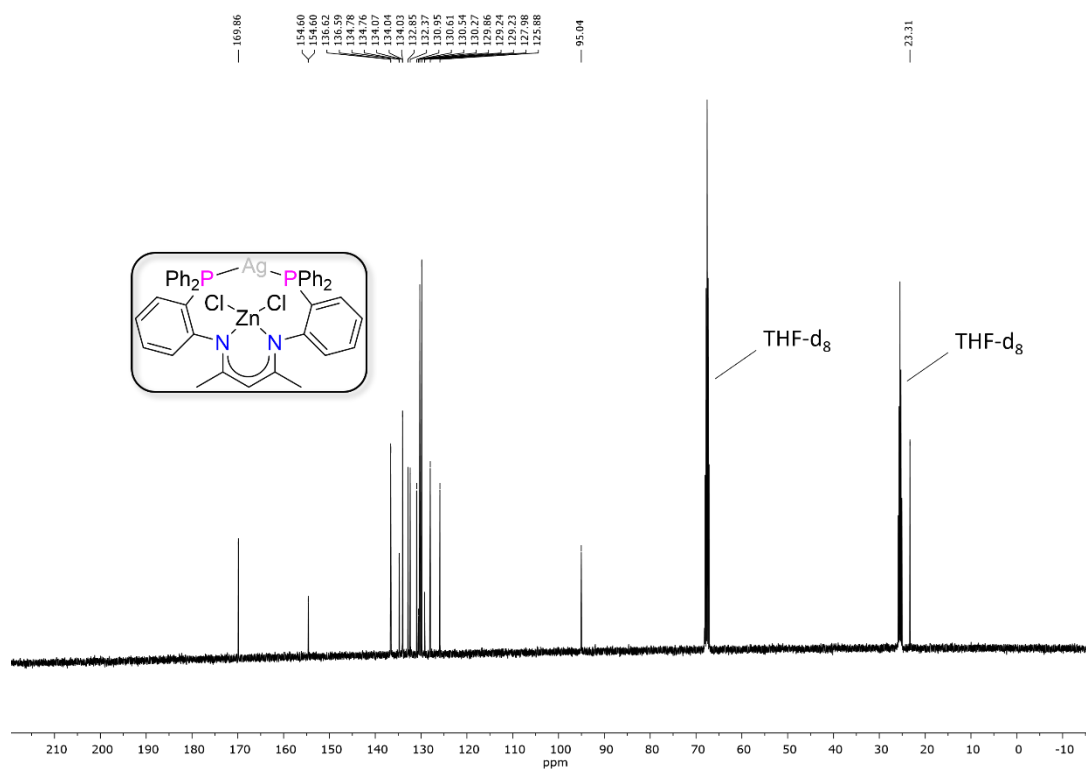


Figure S22: $^{13}\text{C}\{^1\text{H},^{31}\text{P}\}$ NMR spectrum of $[\text{PNacAgZn}]$ (7) in THF-d_8 (100 MHz, 298 K).

Supplementary Information

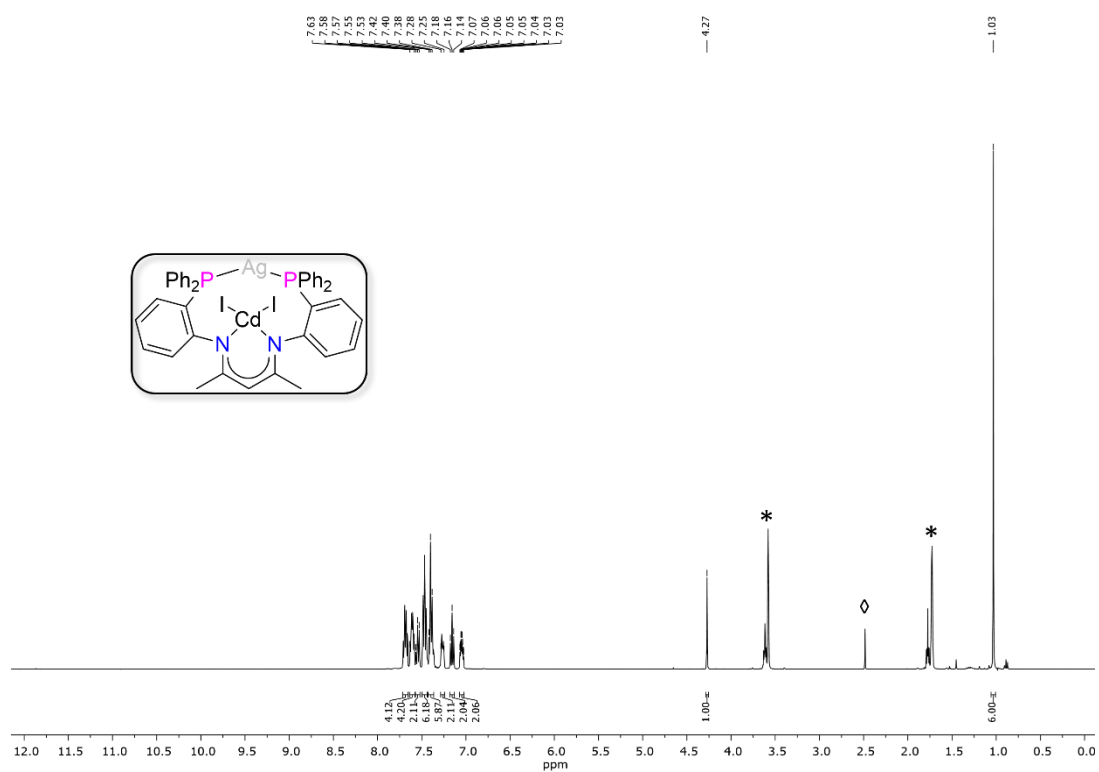


Figure S23: ¹H NMR spectrum of **[PNacAgCd] (8)** in THF-d₈ (400 MHz, 298 K): *, residual protio solvent signal; ◊, H₂O from the NMR solvent.

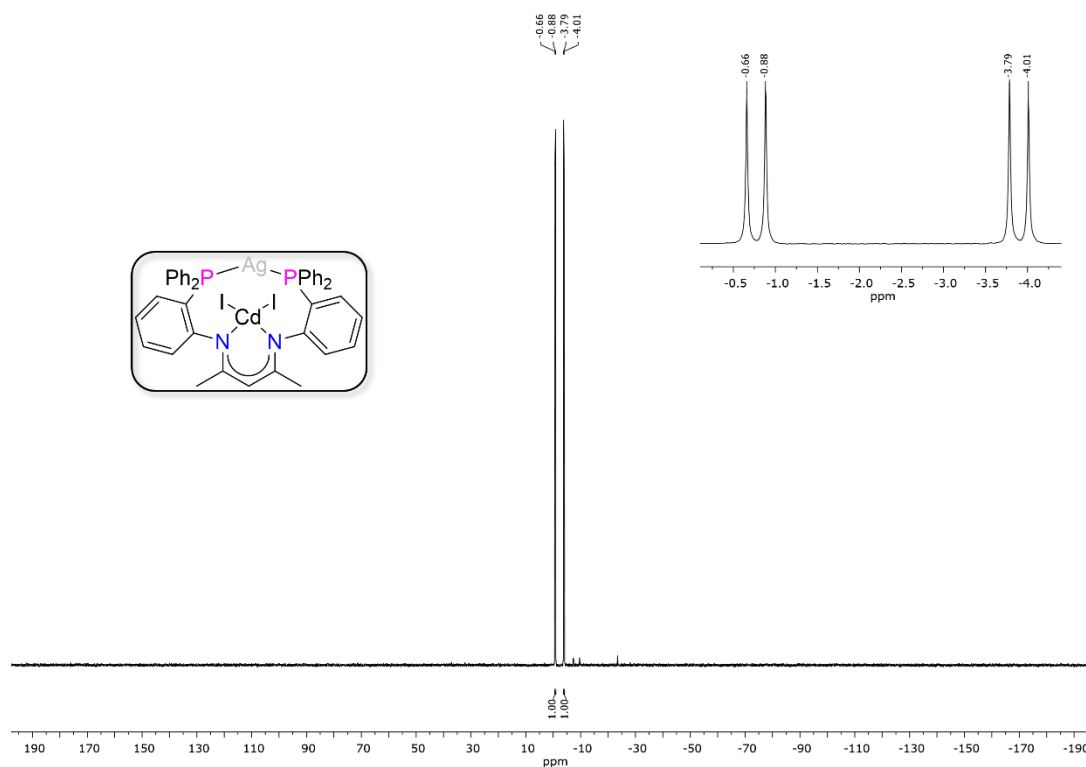


Figure S24: ³¹P{¹H} NMR spectrum of **[PNacAgCd] (8)** in THF-d₈ (162 MHz, 298 K).

Supplementary Information

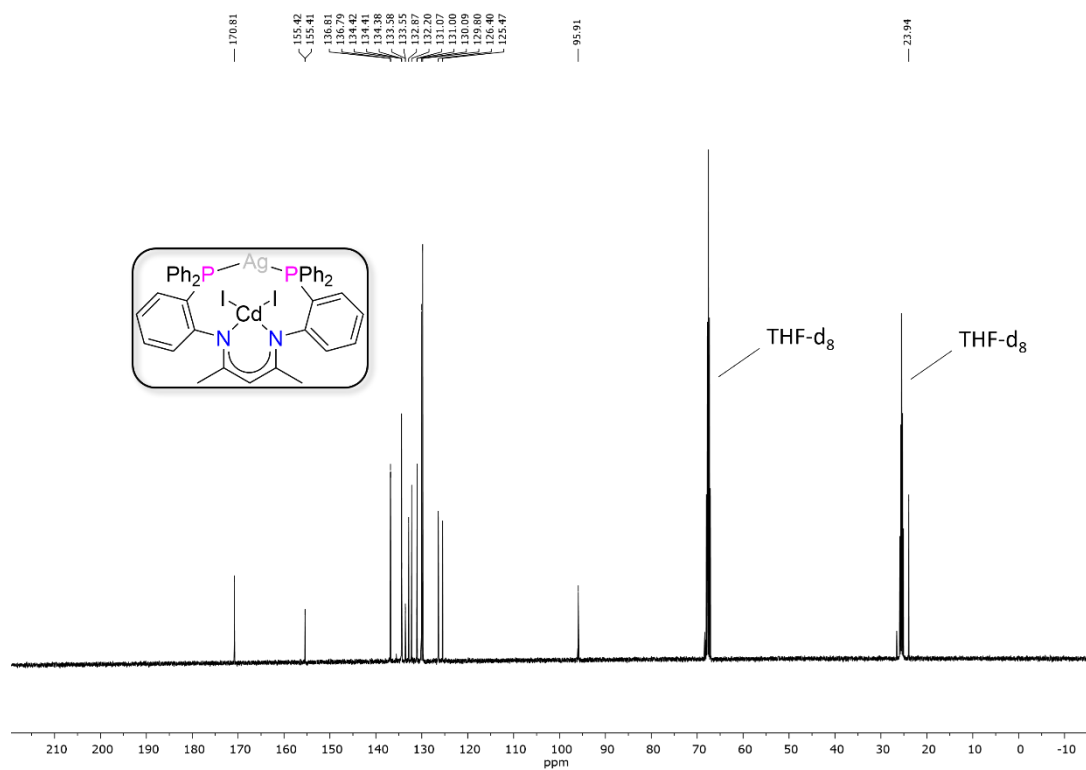


Figure S25: $^{13}\text{C}\{^1\text{H},^{31}\text{P}\}$ NMR spectrum of [PNacAgCd] (8) in THF- d_8 (100 MHz, 298 K).

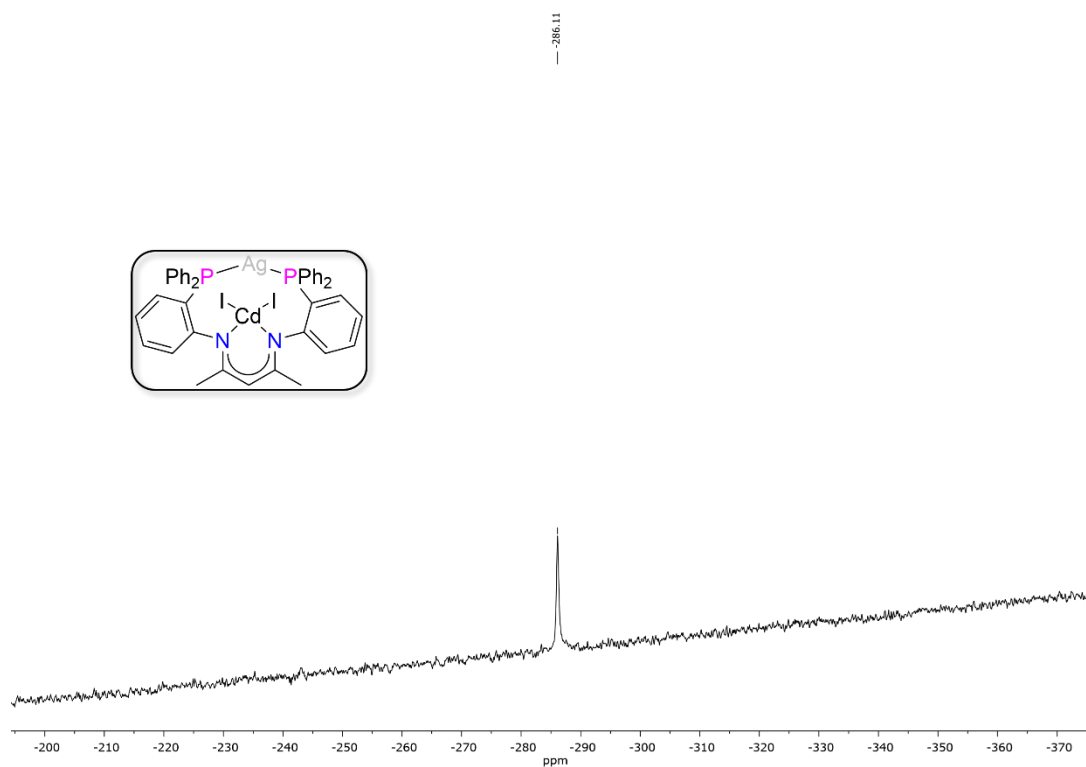


Figure S26: ^{113}Cd NMR spectrum of [PNacAgCd] (8) in THF- d_8 (67 MHz, 298 K).

IR spectra

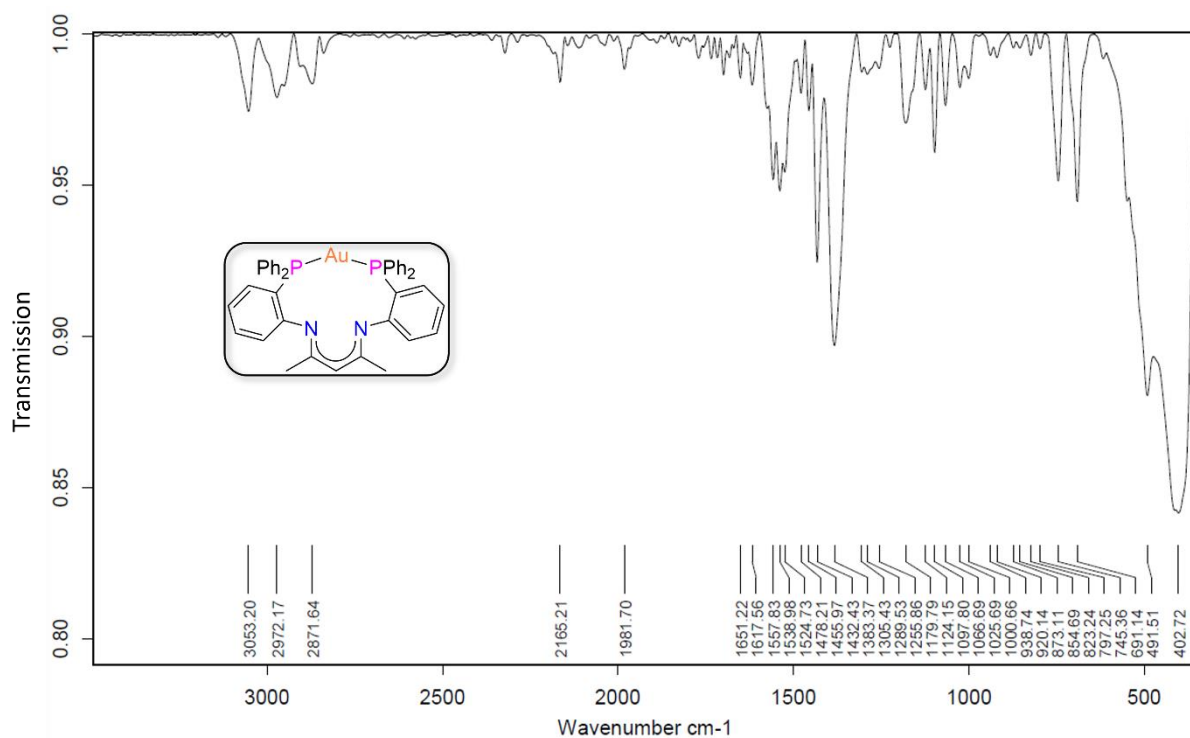


Figure S27: IR spectrum of [PNacAu] (1).

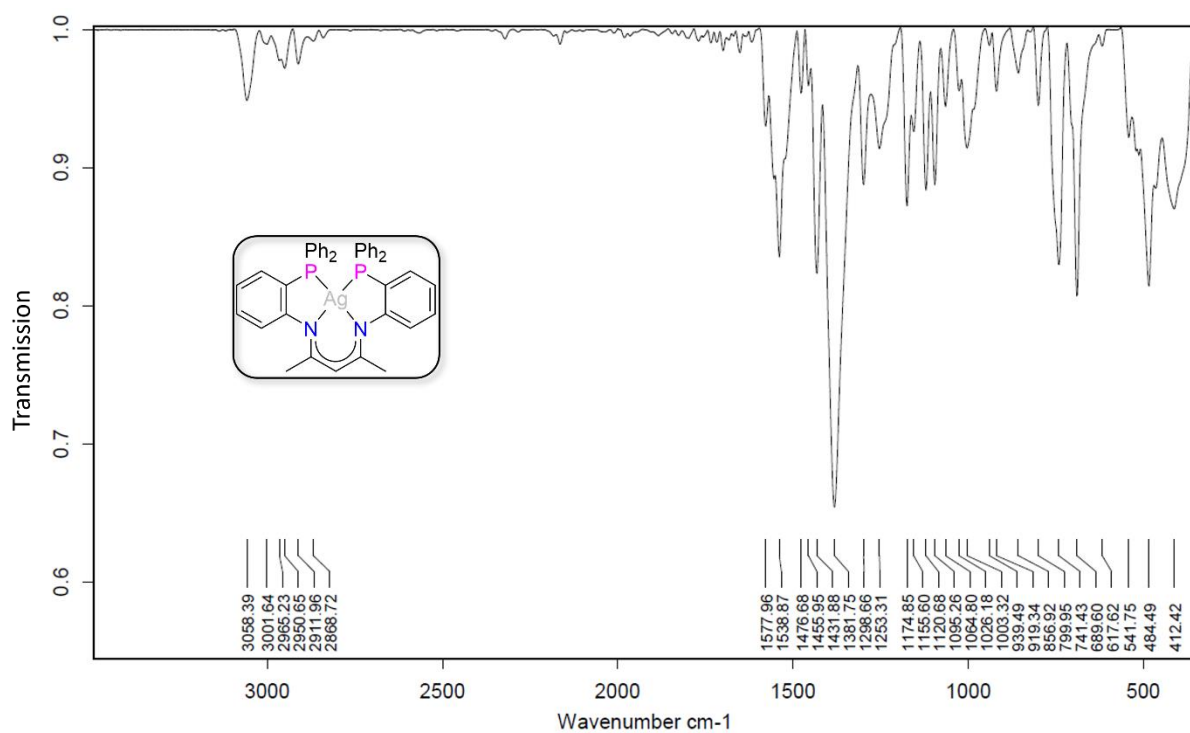


Figure S28: IR spectrum of [PNacAg] (2).

Supplementary Information

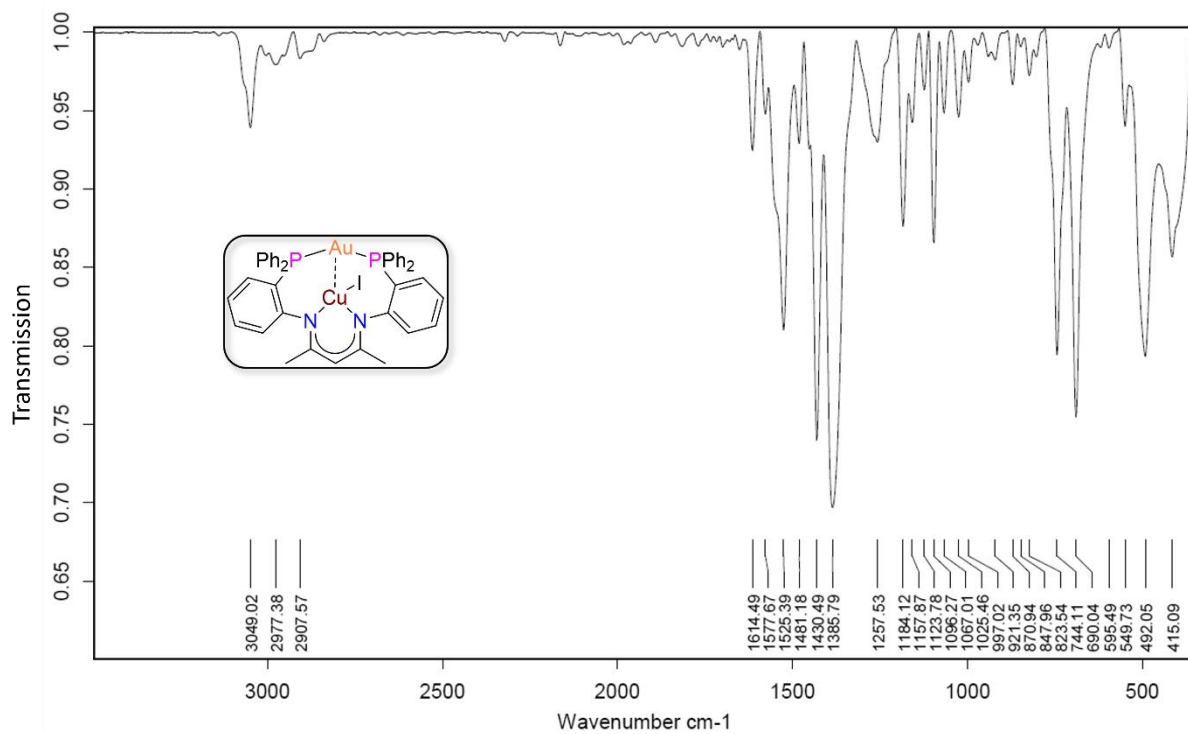


Figure S29: IR spectrum of [PNacAuCu] (3).

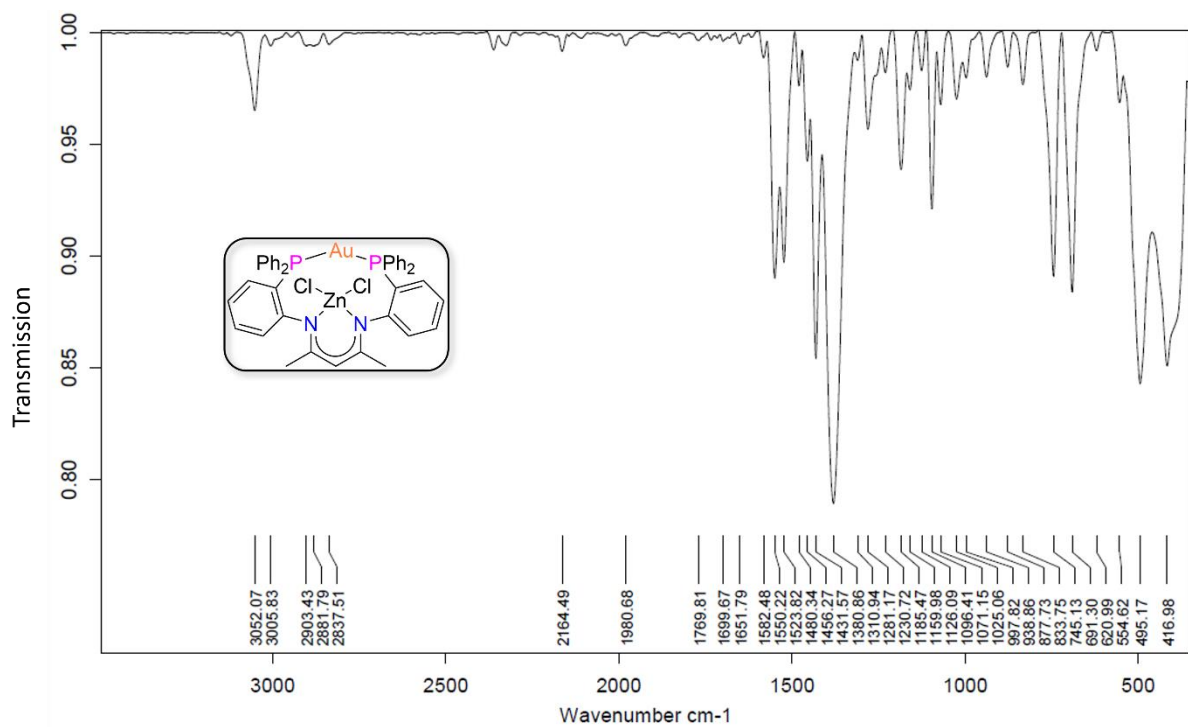


Figure S30: IR spectrum of [PNacAuZn] (4).

Supplementary Information

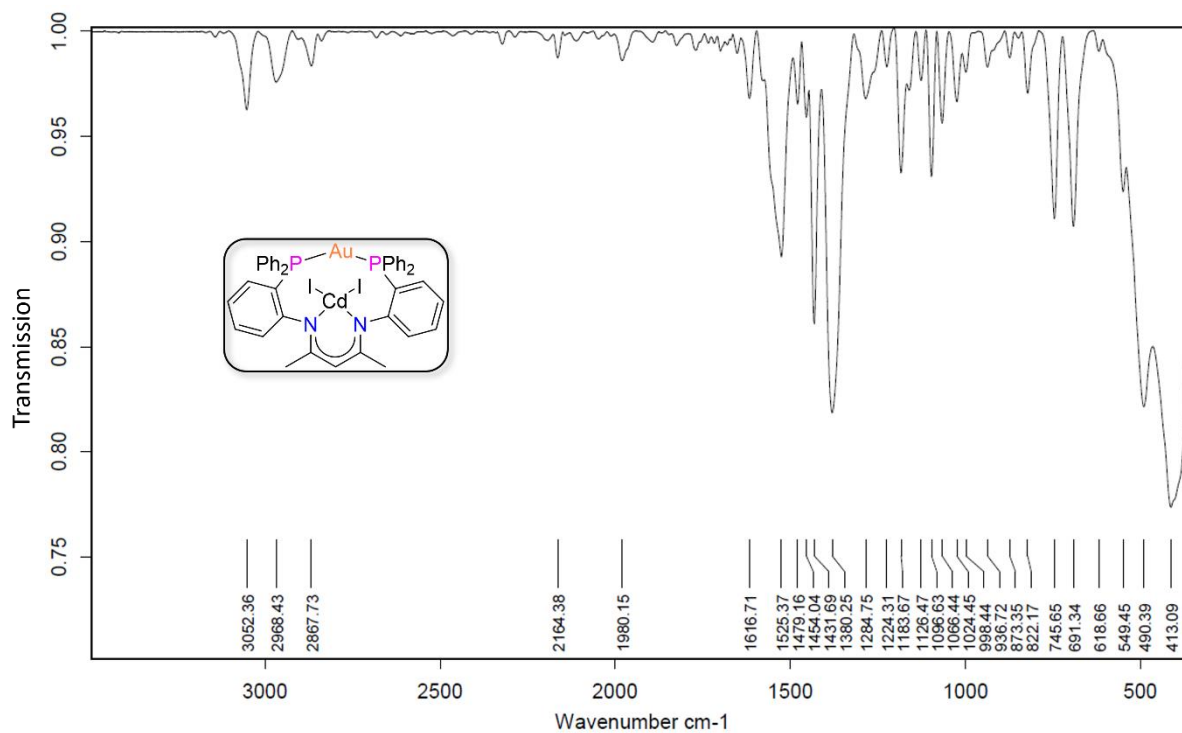


Figure S31: IR spectrum of [PNacAuCd] (5).

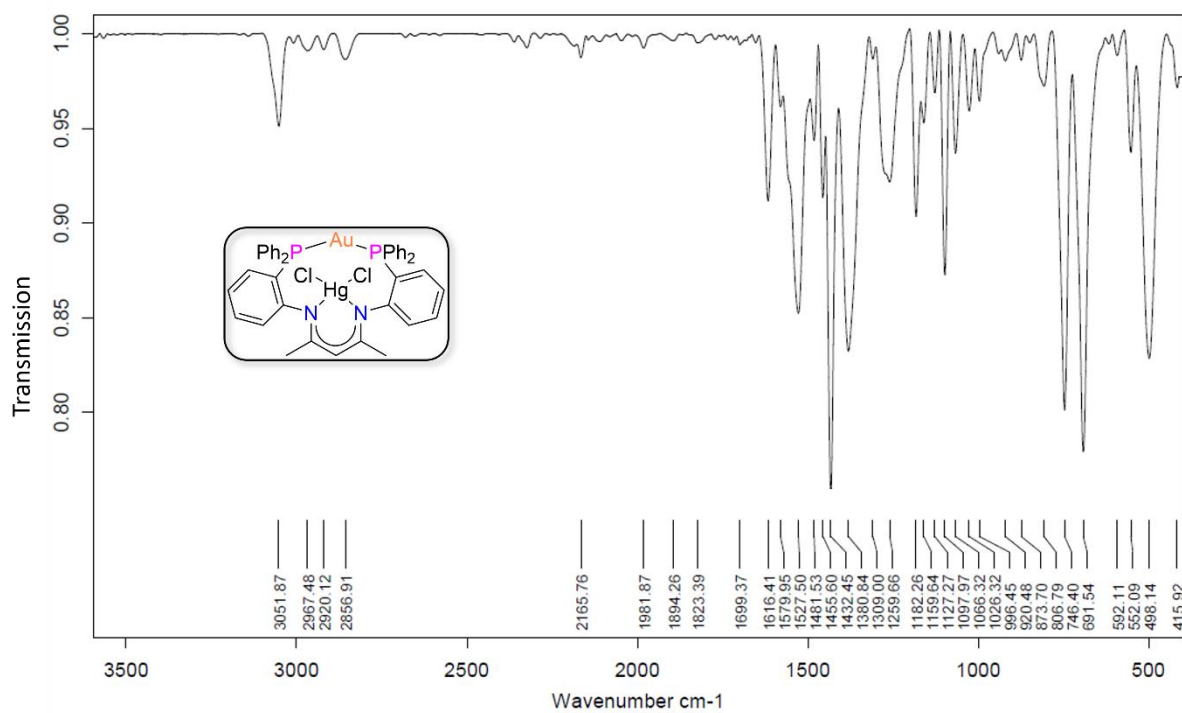


Figure S32: IR spectrum of [PNacAuHg] (6).

Supplementary Information

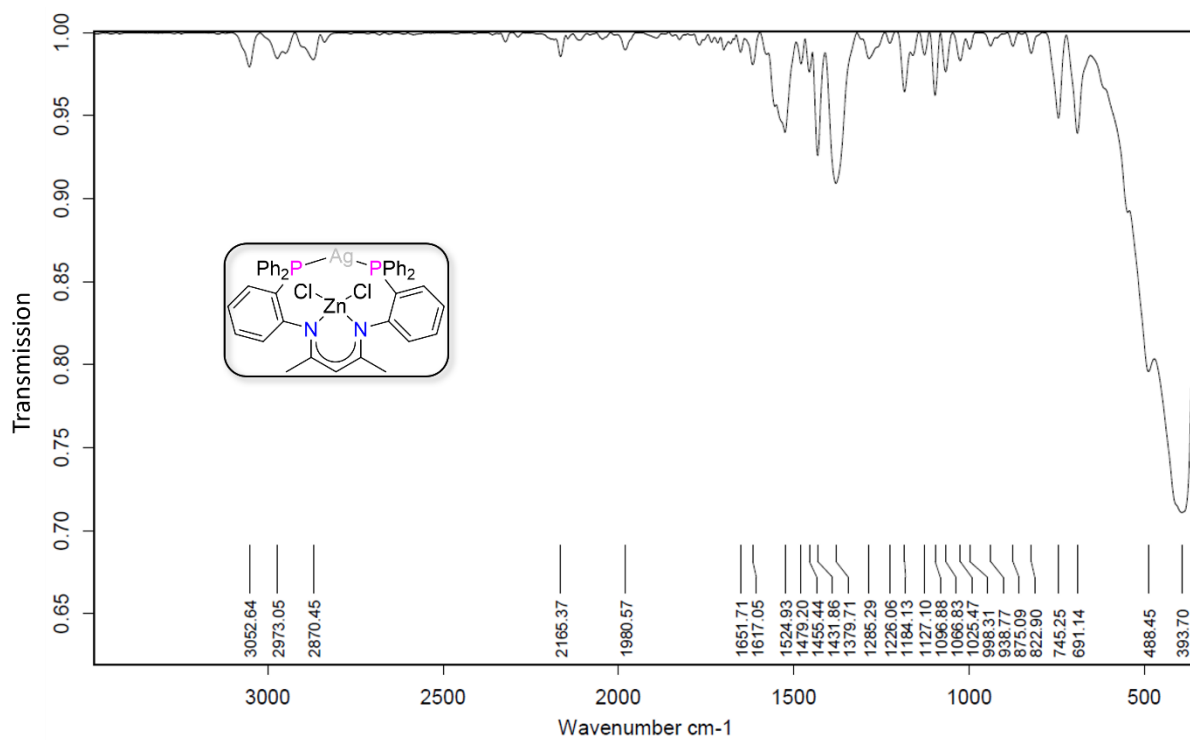


Figure S33: IR spectrum of [PNacAgZn] (6).

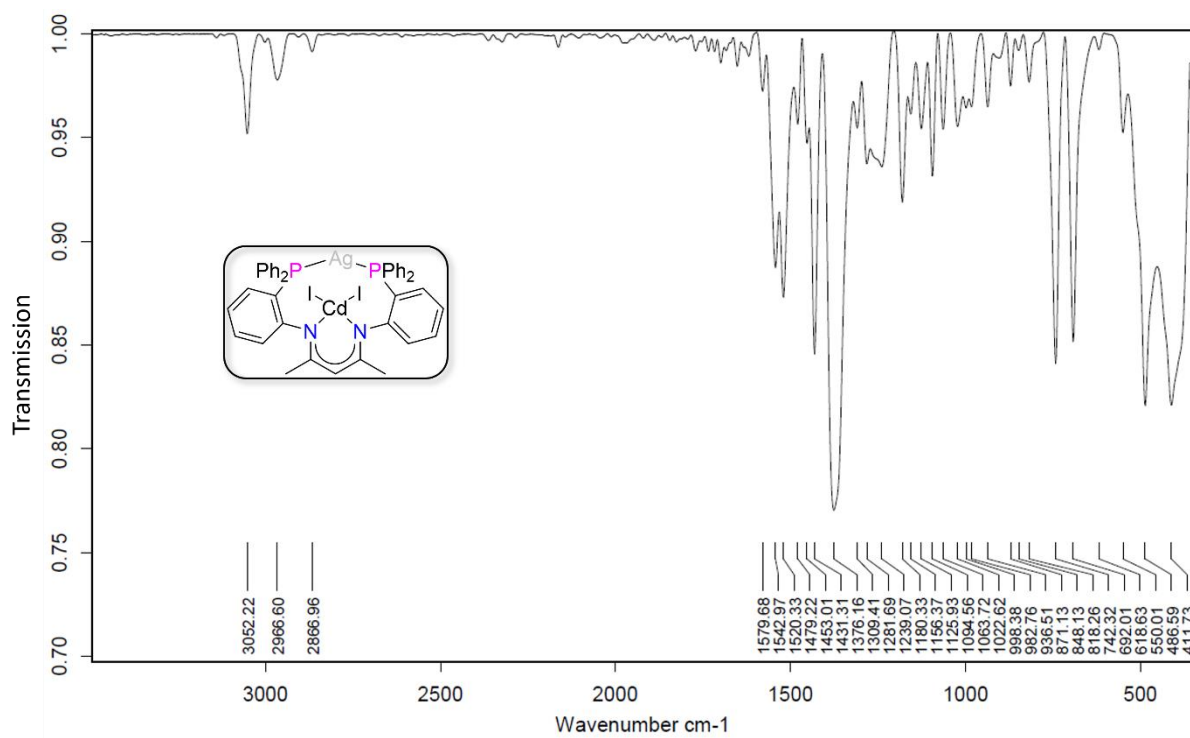


Figure S34: IR spectrum of [PNacAgCd] (7).

Raman Spectra

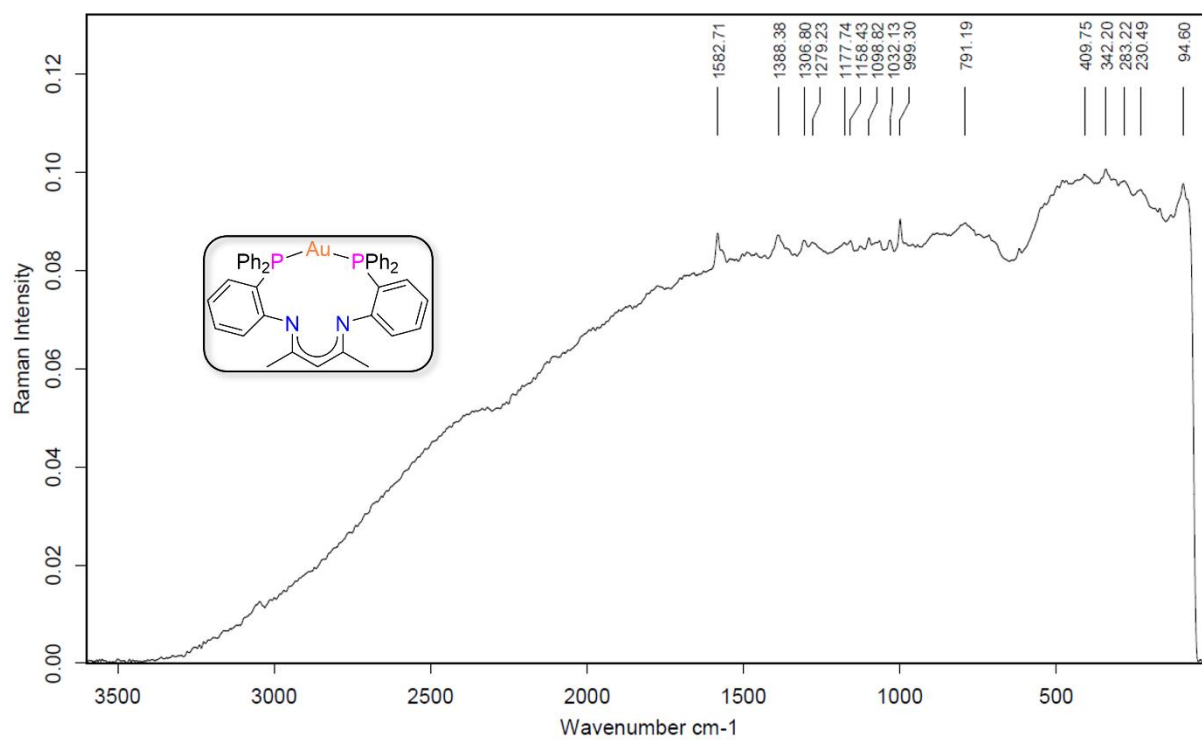


Figure S35: Raman spectrum of [PNacAu] (1). The Spectrum shows Raman fluorescence.

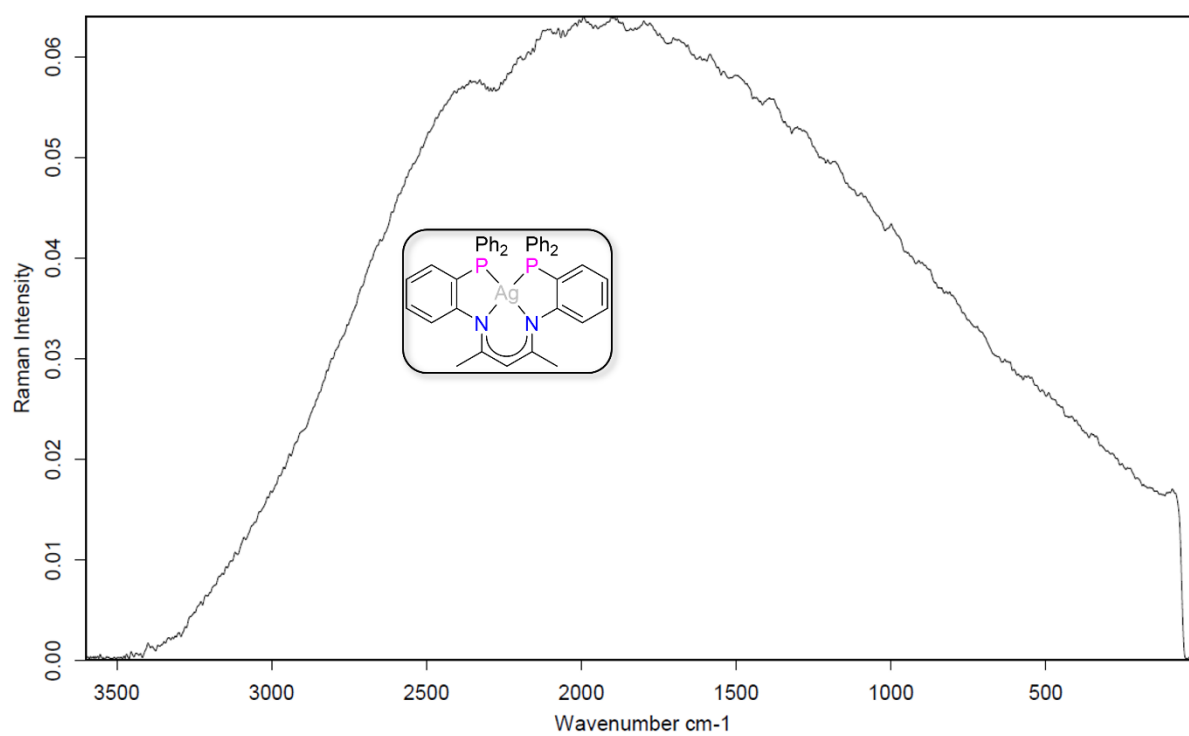


Figure S36: Raman spectrum of [PNacAg] (2). The Spectrum shows Raman fluorescence.

Supplementary Information

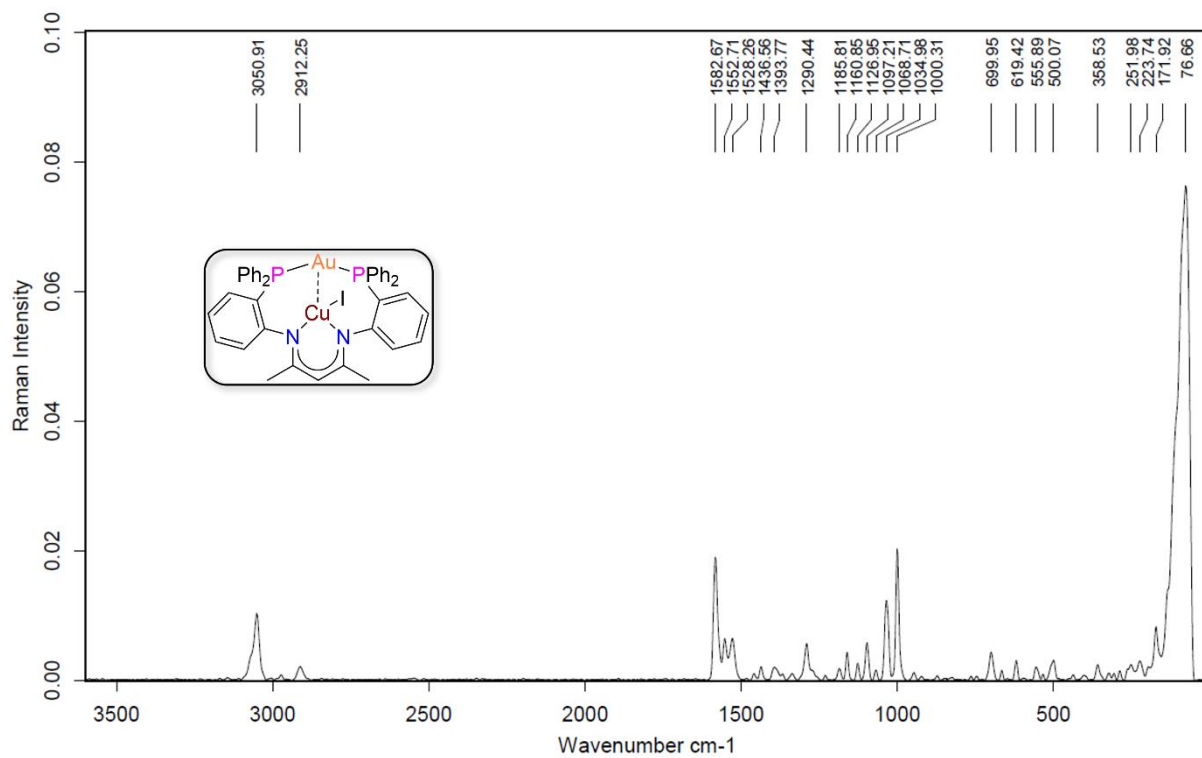


Figure S37: Raman spectrum of [PNacAuCu] (3).

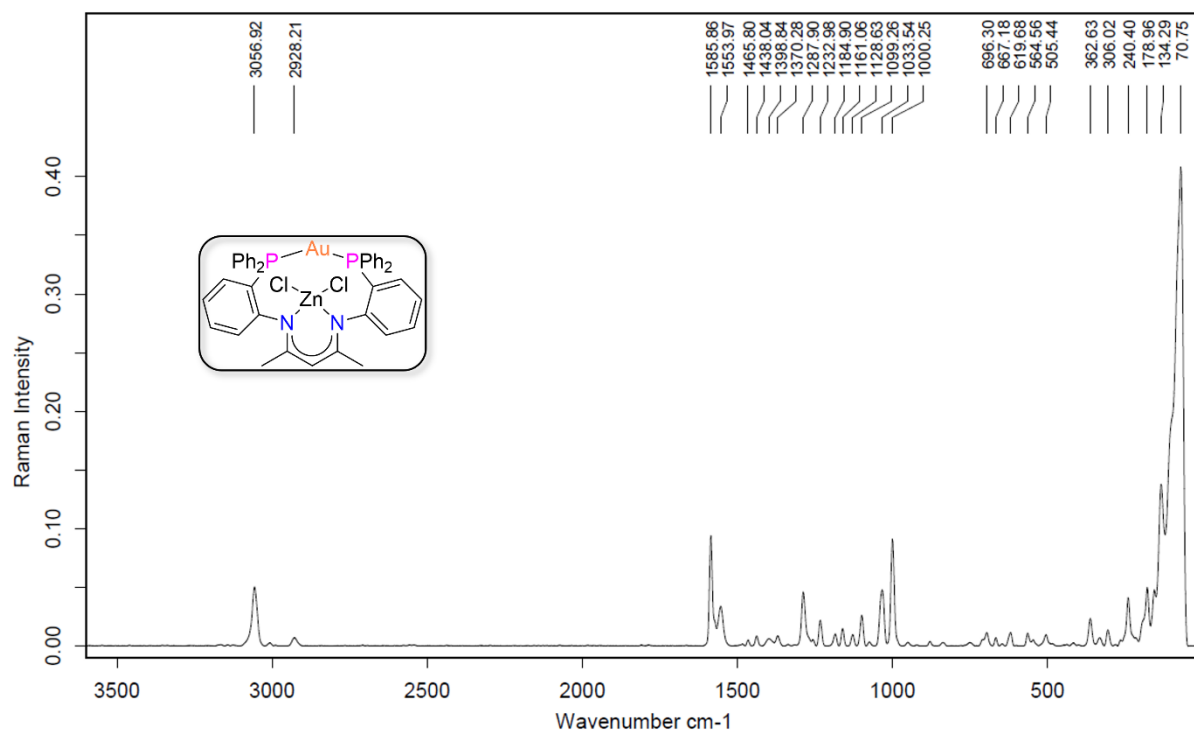


Figure S38: Raman spectrum of [PNacAuZn] (4).

Supplementary Information

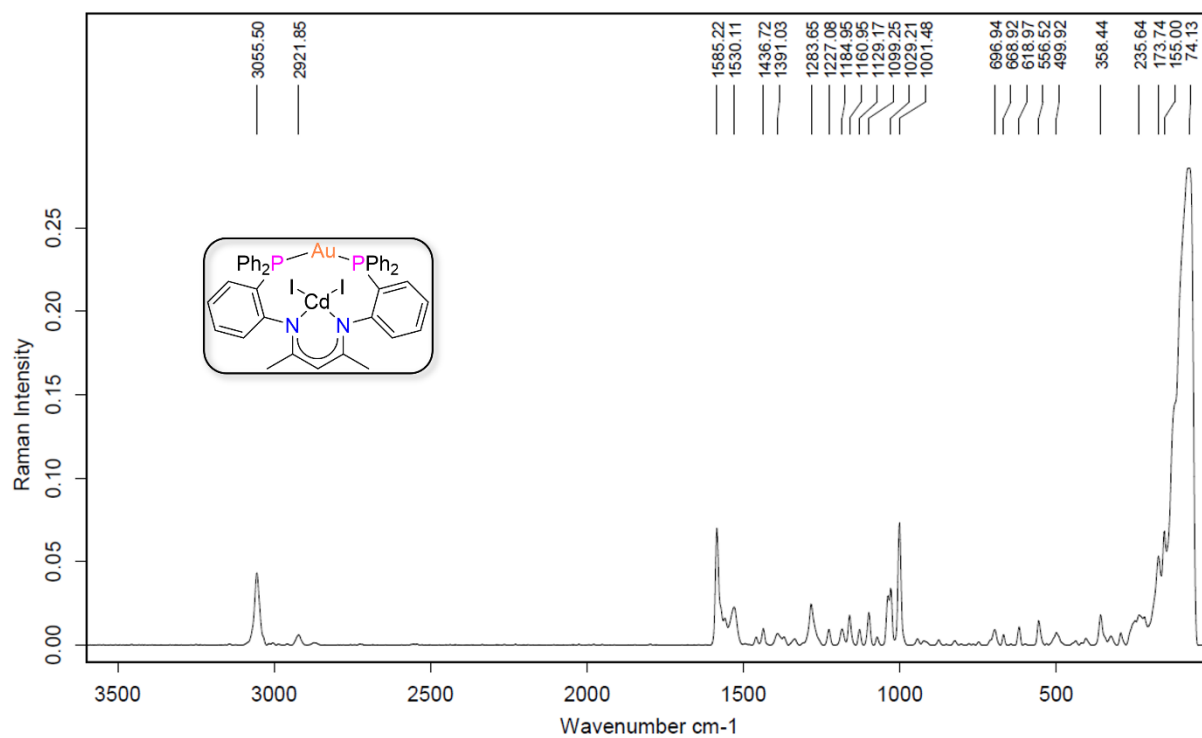


Figure S39: Raman spectrum of [PNacAuCd] (5).

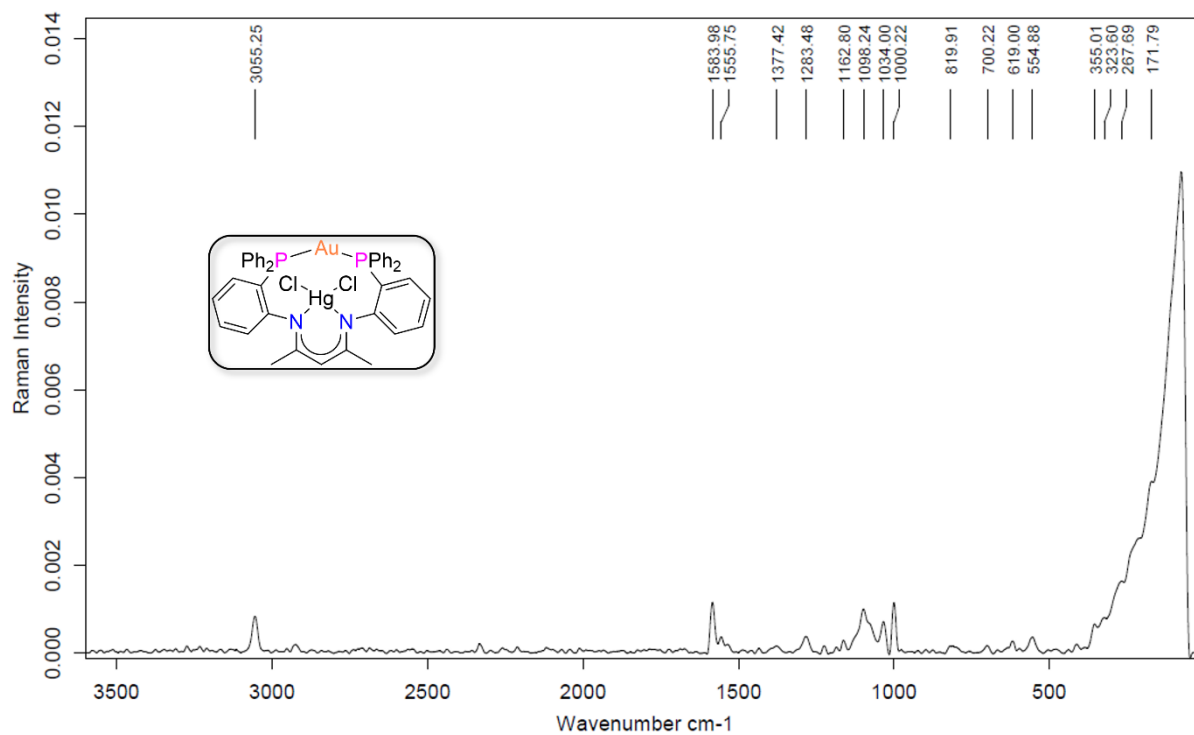


Figure S40: Raman spectrum of [PNacAuHg] (6).

Supplementary Information

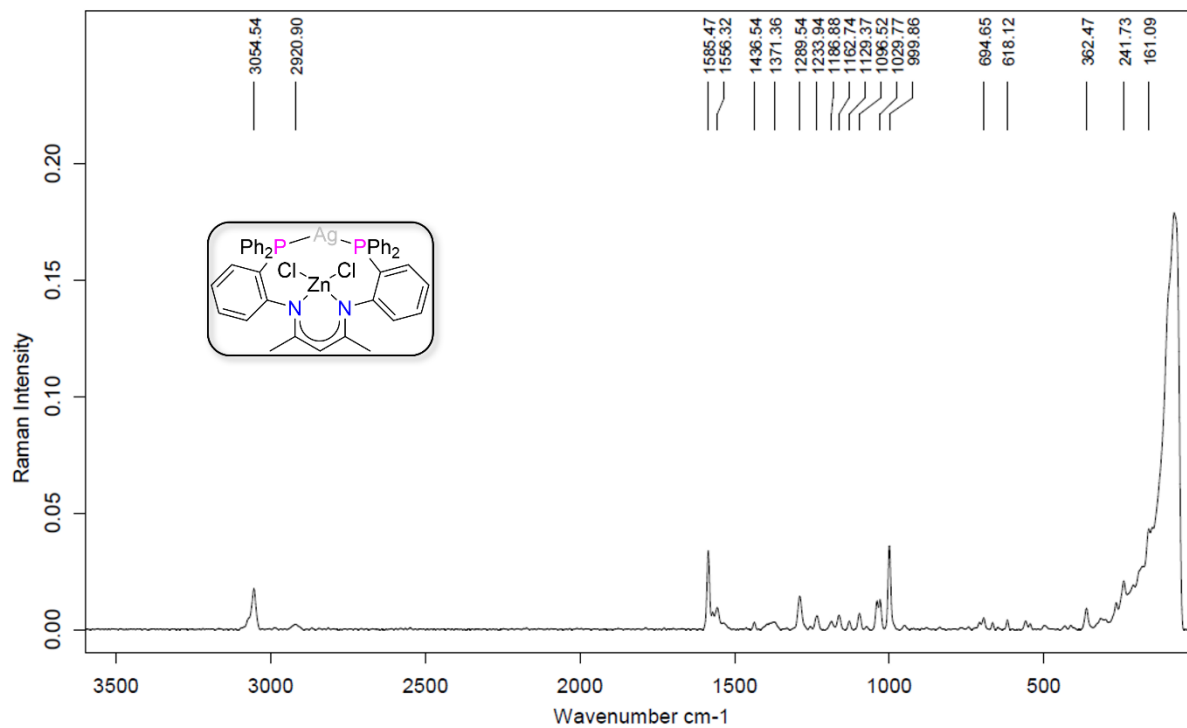


Figure S41: Raman spectrum of [PNacAgZn] (7).

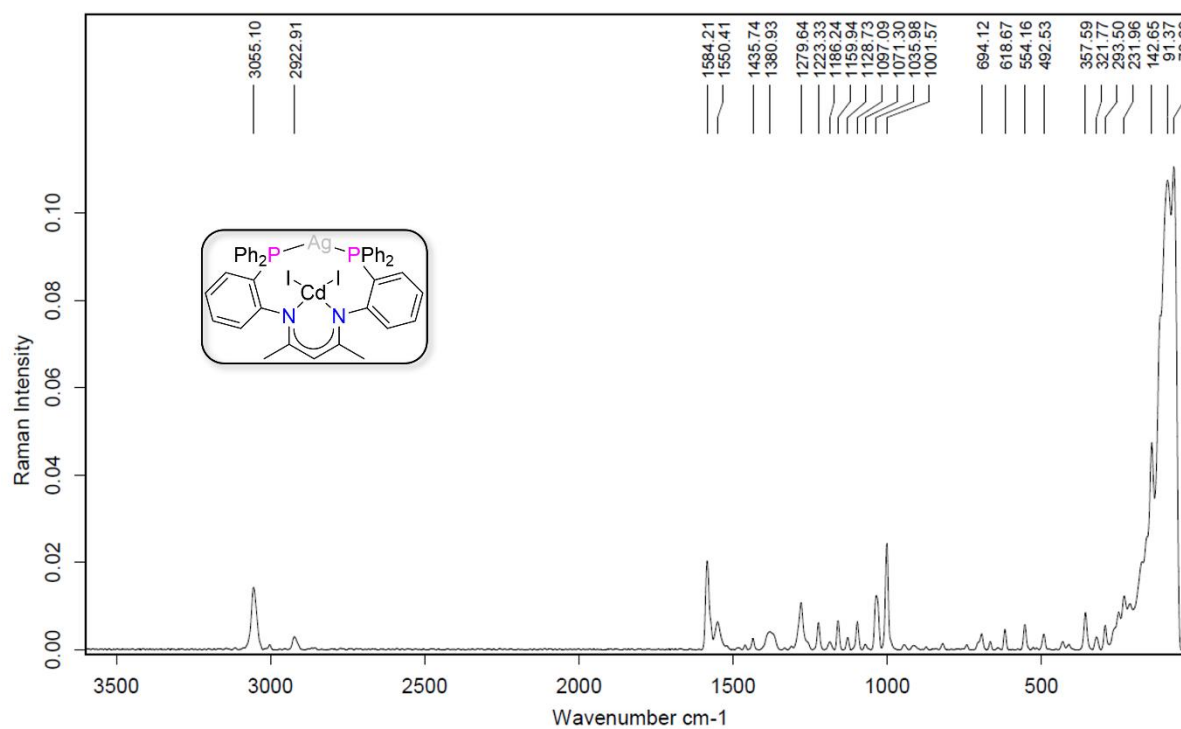


Figure S42: Raman spectrum of [PNacAgCd] (8).

UV/Vis spectra

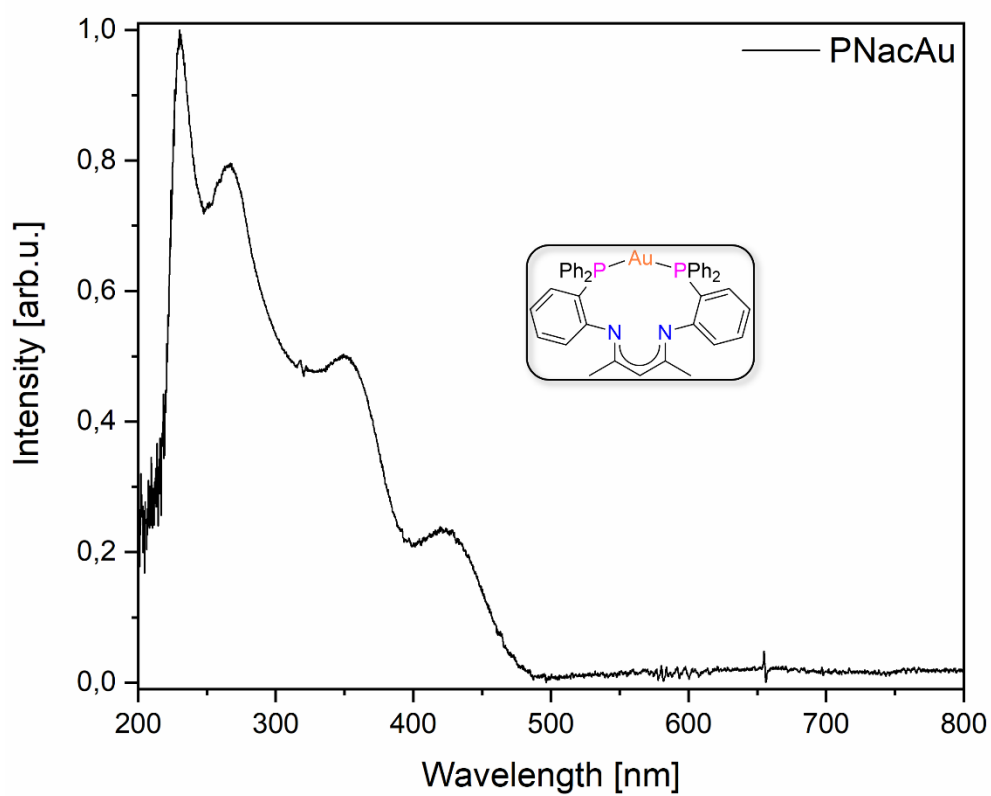


Figure S43: UV/Vis spectrum of [PNacAu] (1).

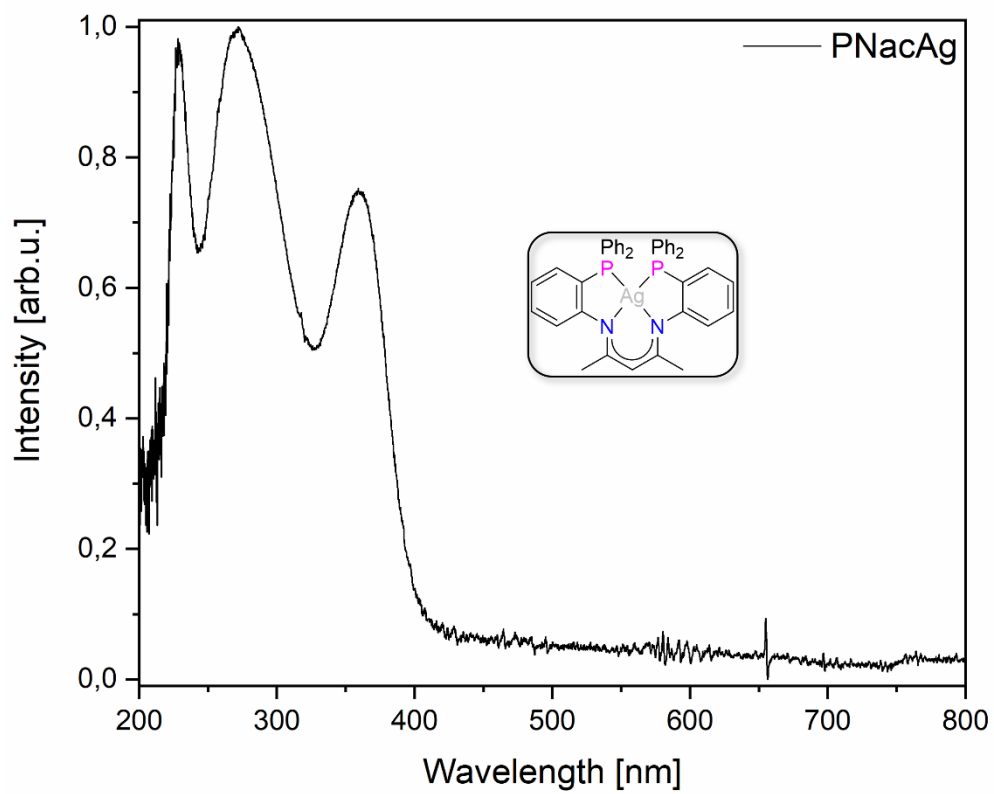


Figure S44: UV/Vis spectrum of [PNacAg] (2).

Supplementary Information

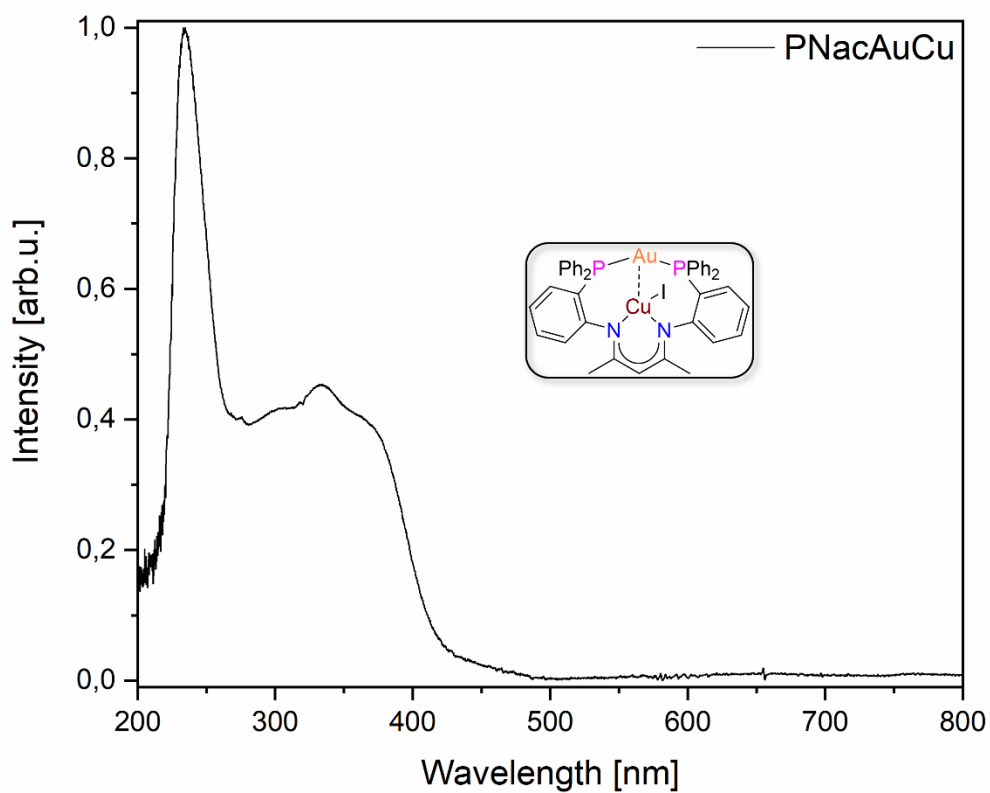


Figure S45: UV/Vis spectrum of [PNacAuCu] (3).

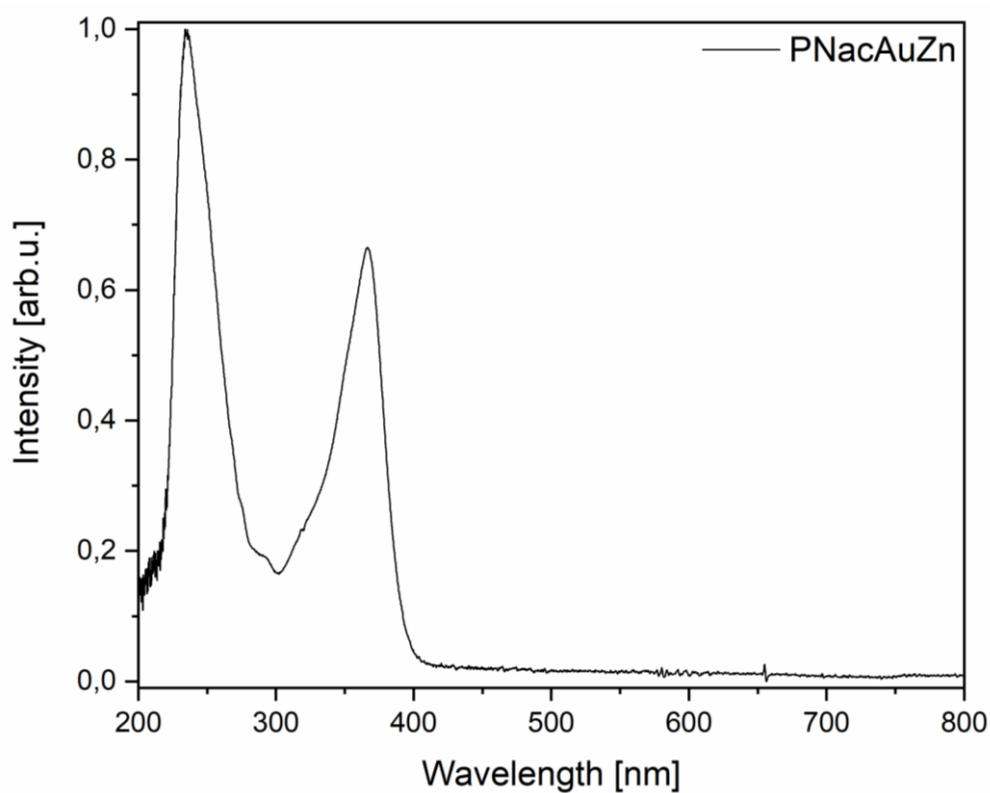


Figure S46: UV/Vis spectrum of [PNacAuZn] (4).

Supplementary Information

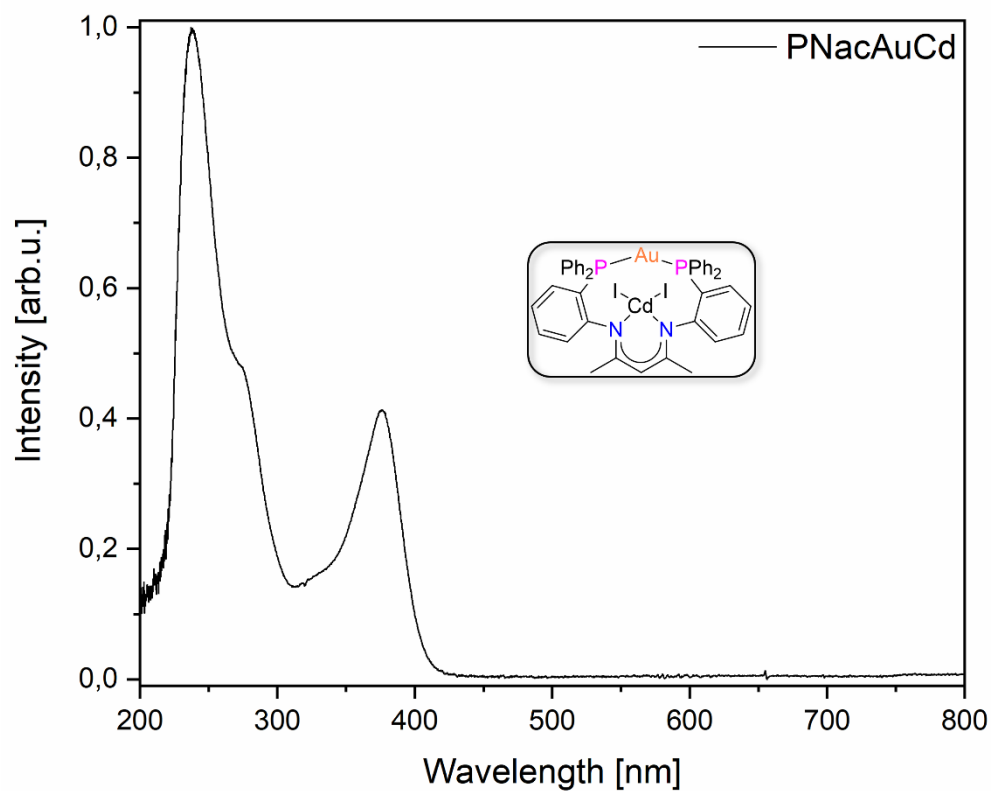


Figure S47: UV/Vis spectrum of [PNacAuCd] (5).

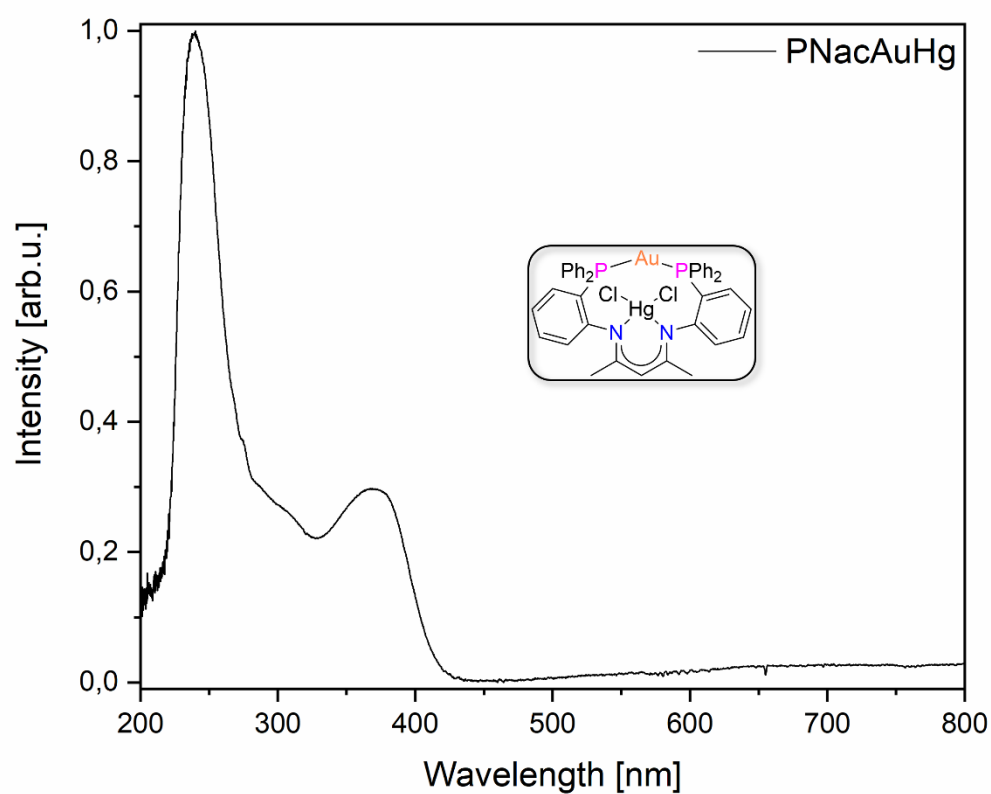


Figure S48: UV/Vis spectrum of [PNacAuHg] (6).

Supplementary Information

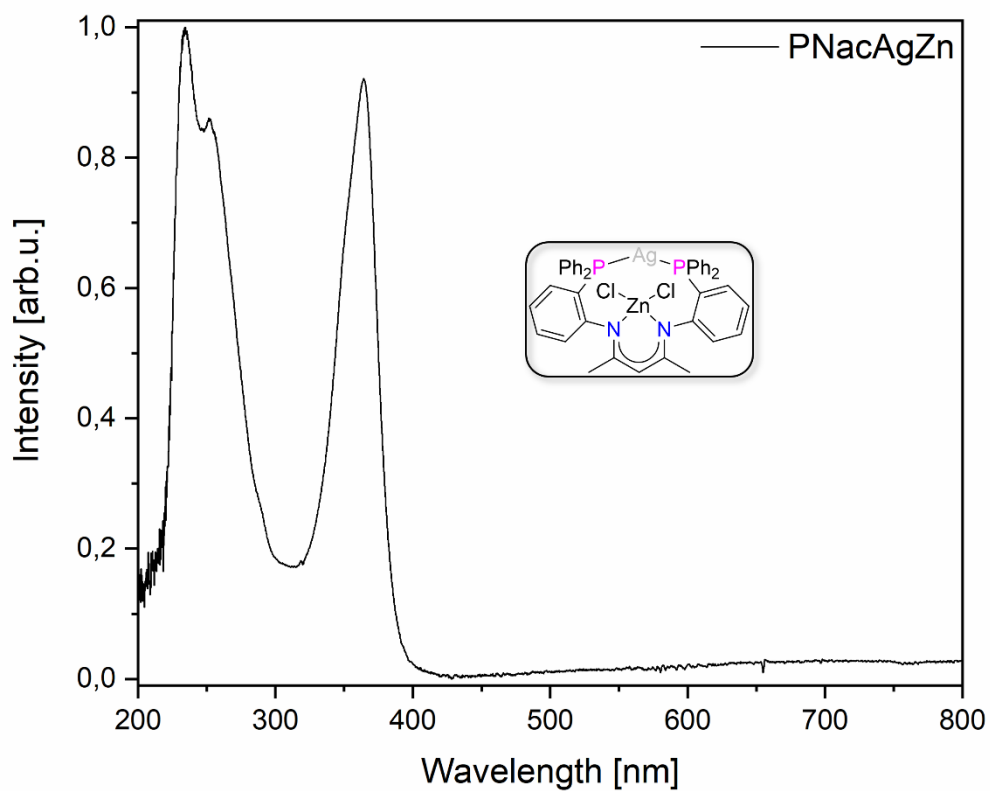


Figure S49: UV/Vis spectrum of [PNacAgZn] (7).

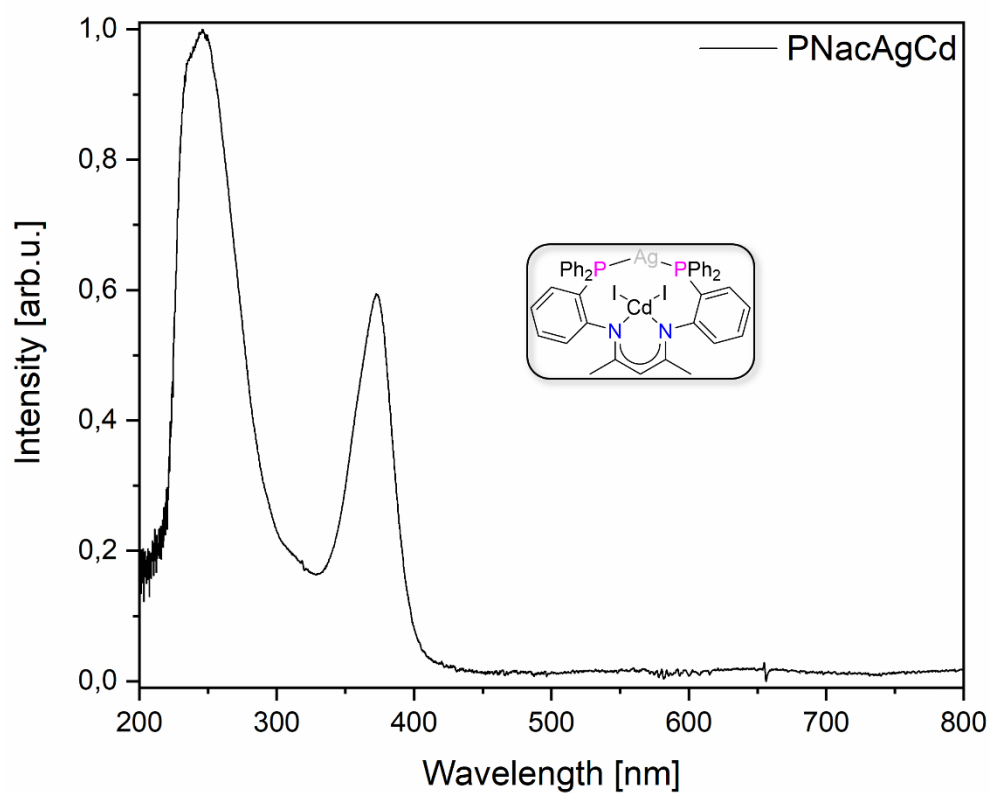


Figure S50: UV/Vis spectrum of [PNacAgCd] (8).

Photoluminescence

General methods

Photoluminescence was measured on a PTI Quanta Master™ 8075-22 fluorometer with double monochromator (*HORIBA Jobin Yvon GmbH*) in excitation and emission. For this purpose, the samples were placed in an inert gas atmosphere into a “J Young” NMR tube made of Suprasil® quartz glass. For measurements at 77 K the tube was placed directly in liquid nitrogen (in a specially designed dewar vessel). For the detection of the emission a R928 photomultiplier (*HORIBA Jobin Yvon GmbH*) in the range of 250 nm – 800 nm or a liquid nitrogen cooled DSS-IGA020L/CUS detector in the range of 800 nm – 1550 nm was used. All spectra were corrected for the wavelength-dependent response of the spectrometer and the detector. For the determination of the emission lifetime, the sample was either excited with a Delta Diode™ (*HORIBA Jobin Yvon GmbH*, model DD-370, $\lambda_{\text{Exc}} = 370$ nm, pulse width 800 ps, power 2 μW) or a PTI Xenon Flash™ (before the excitation monochromator, frequency max. 300 MHz, for lifetimes > 6 μs). When using the LED diode, the “Stop-Button” method was used, when using the xenon flash lamp 10.000 pulses were recorded. The obtained decay curves were plotted using Origin(Pro) (version 2020, OriginLab Corporation Northampton, MA, US) with an exponential function with one or two exponents. Quantum yields were determined at room temperature according to the method of Friend *et. al.* in an integrating sphere made of optical PTFE, which was installed in the sample chamber of the spectrometer.³ The quantum yield is determined with an accuracy of about $\pm 10\%$.

Photoluminescence spectra

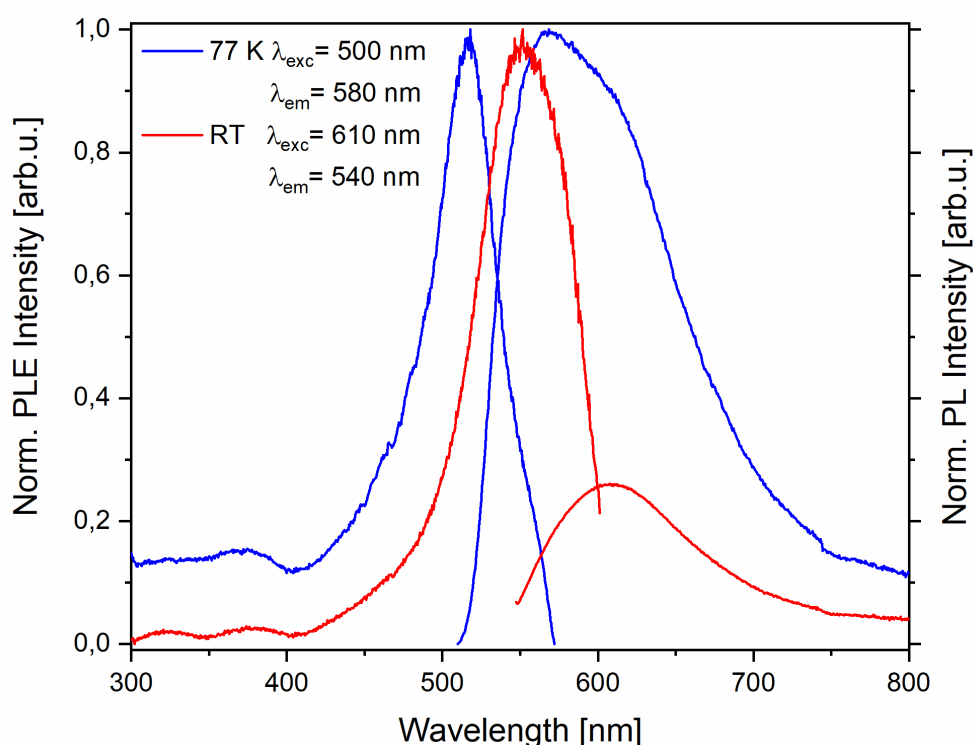


Figure S51: Solid-state photoluminescence emission (PL) and excitation (PLE) spectra of [PNack] from 300-800 nm at 77 K (blue) and RT, 293 K (red).

Supplementary Information

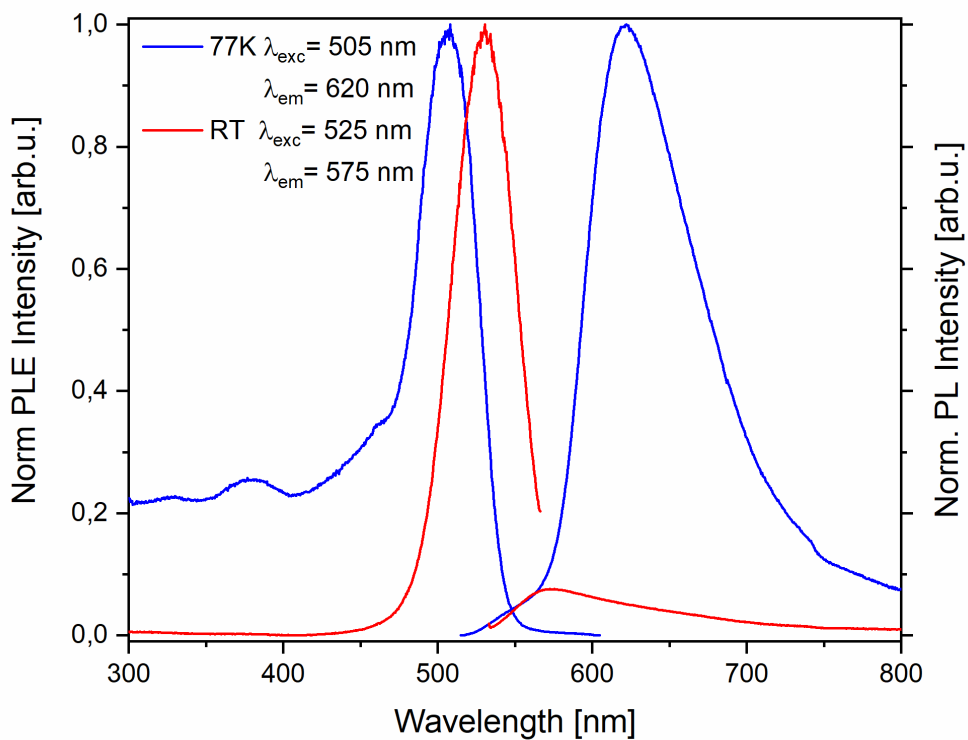


Figure S52: Solid-state photoluminescence emission (PL) and excitation (PLE) spectra of [PNacAu] (1) from 300-800 nm at 77 K (blue) and RT, 293 K (red).

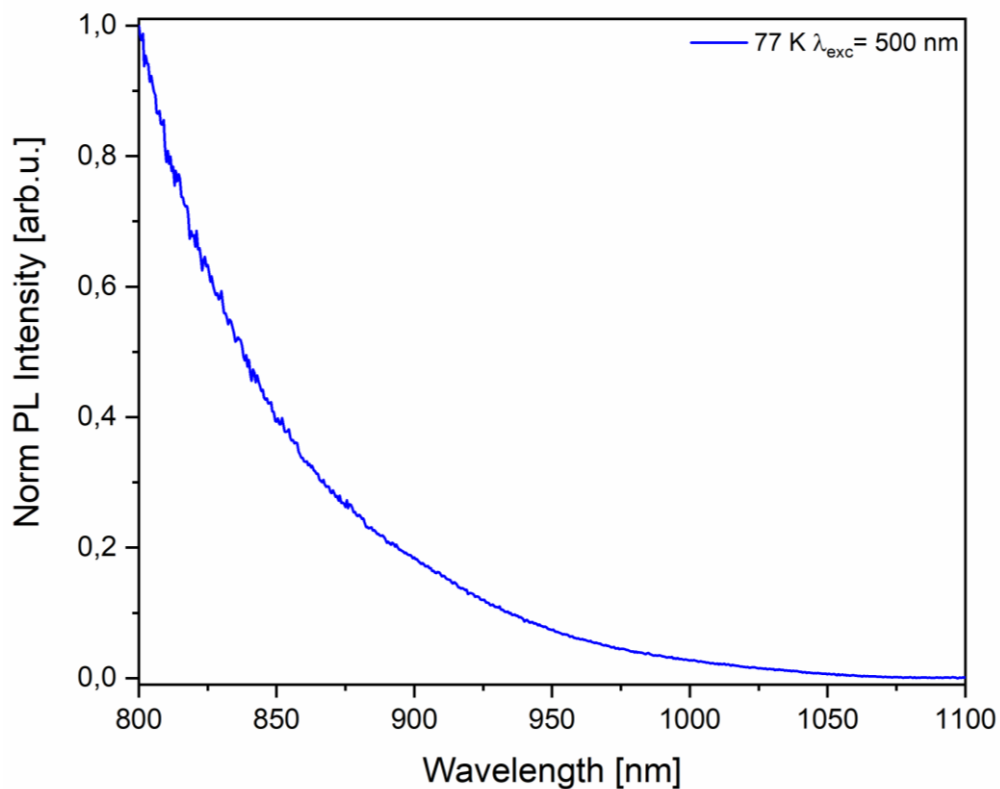


Figure S53: Solid-state photoluminescence emission (PL) spectrum of [PNacAu] (1) from 800-1100 nm at 77 K (blue).

Supplementary Information

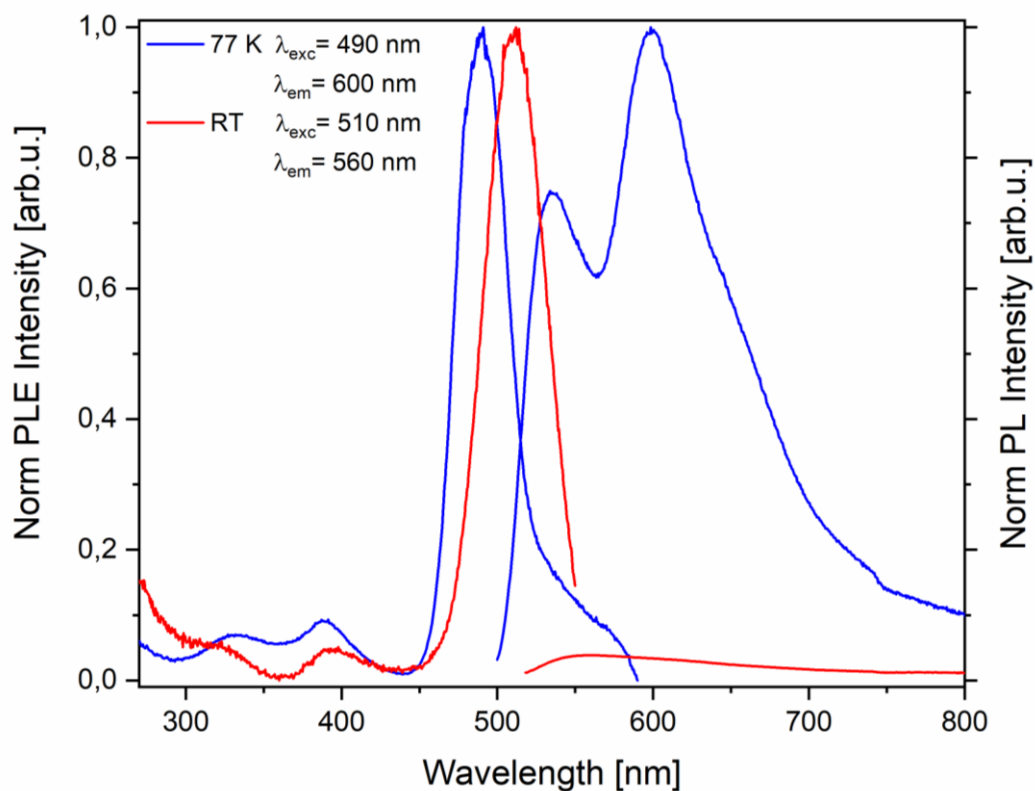


Figure S54: Solid-state photoluminescence emission (PL) and excitation (PLE) spectra of [PNacAg] (2) from 270-800 nm at 77 K (blue) and RT, 293 K (red).

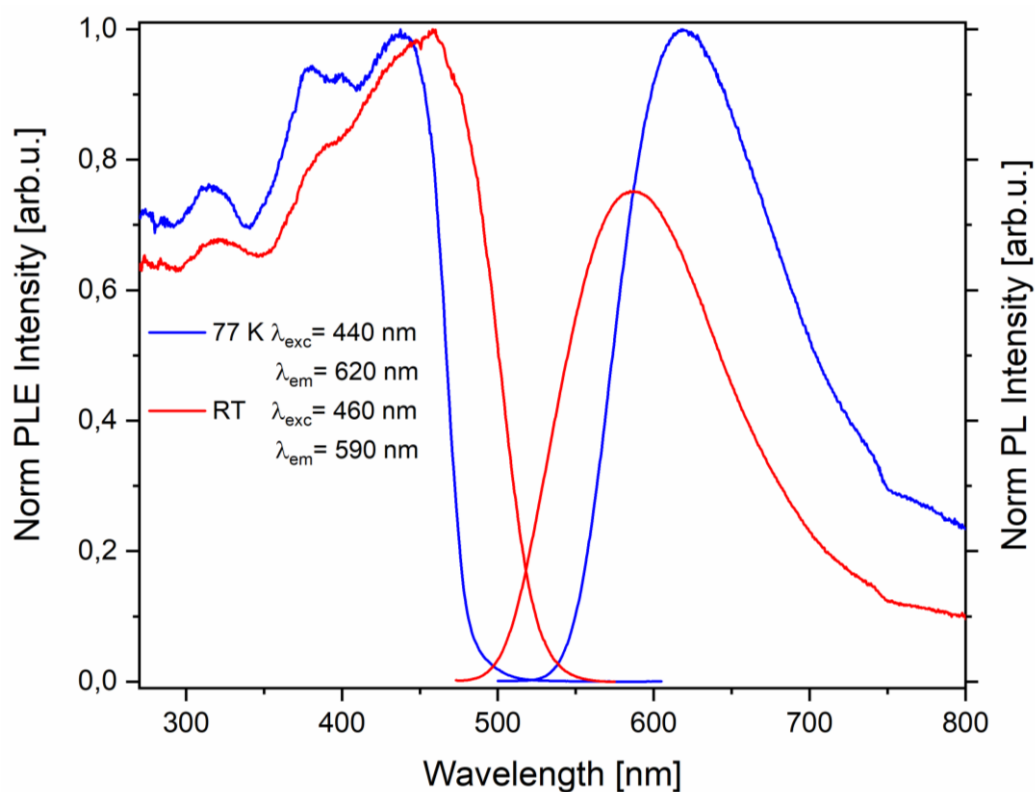


Figure S55: Solid-state photoluminescence emission (PL) and excitation (PLE) spectra of [PNacAuCu] (3) from 270-800 nm at 77 K (blue) and RT, 293 K (red).

Supplementary Information

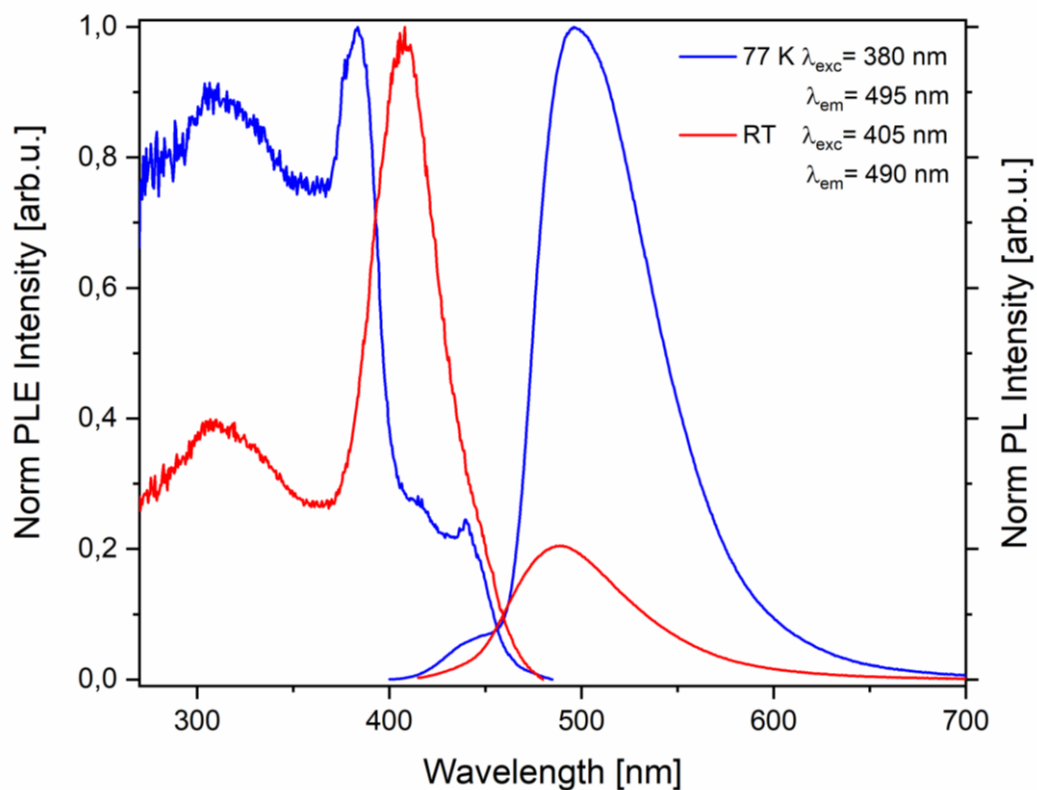


Figure S56: Solid-state photoluminescence emission (PL) and excitation (PLE) spectra of [PNacAuZn] (4) from 270-700 nm at 77 K (blue) and RT, 293 K (red).

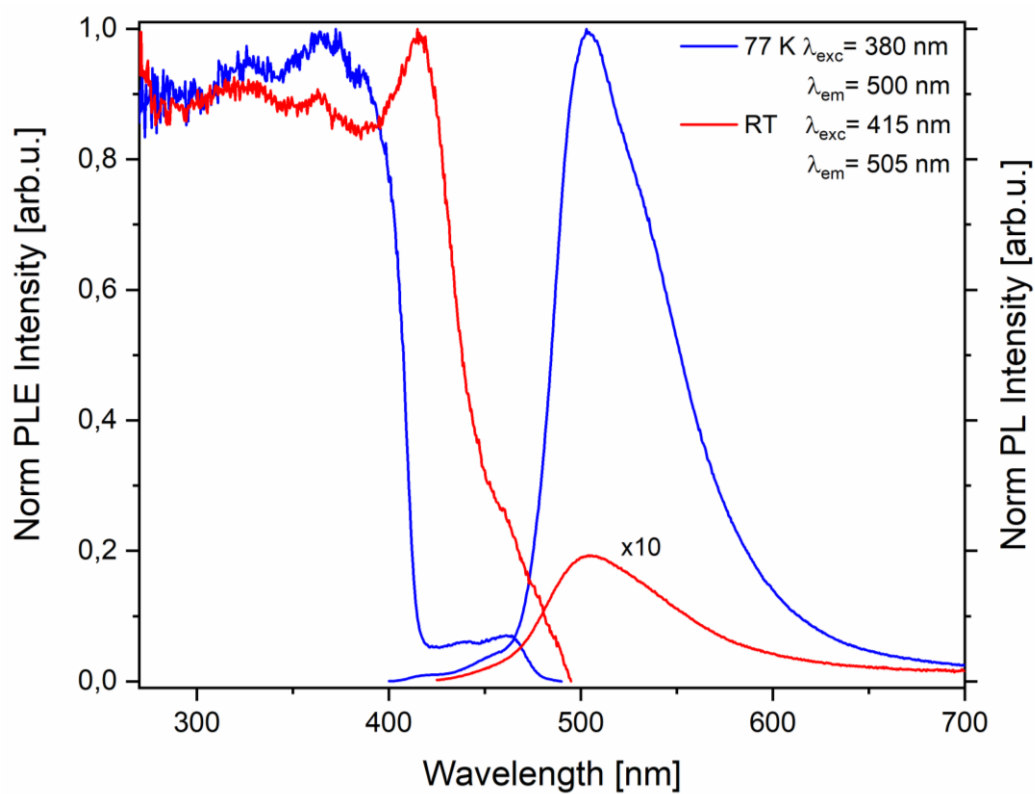


Figure S57: Solid-state photoluminescence emission (PL) and excitation (PLE) spectra of [PNacAuCd] (5) from 270-700 nm at 77 K (blue) and RT, 293 K (red).

Supplementary Information

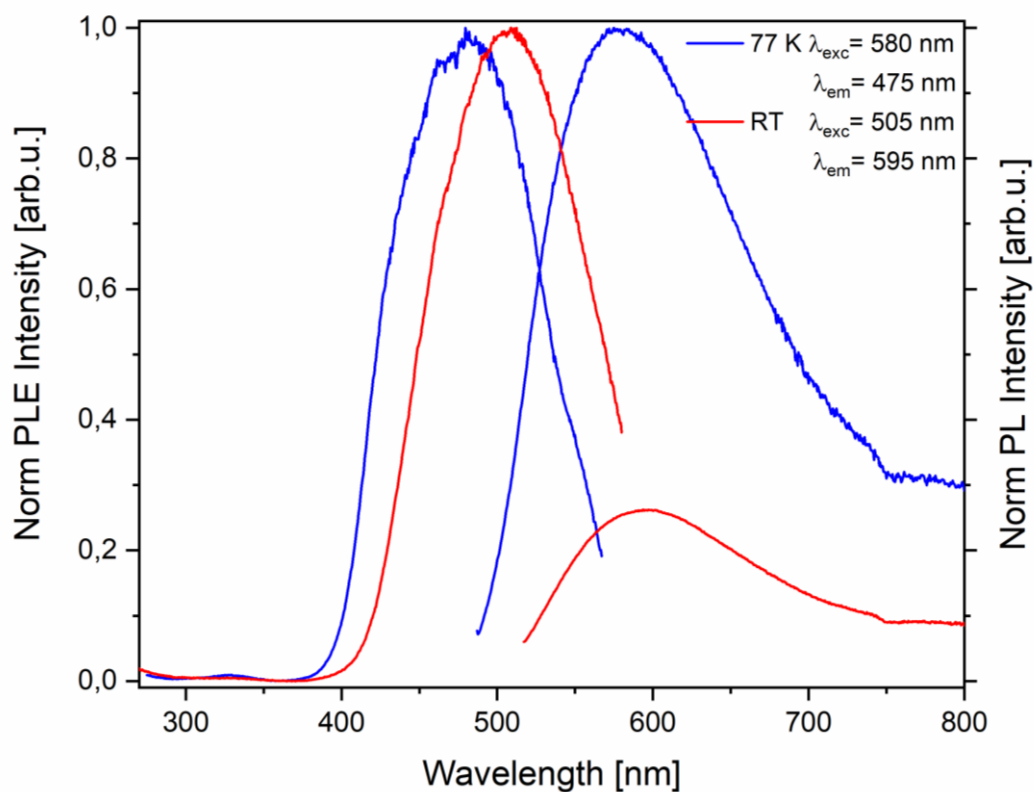


Figure S58: Solid-state photoluminescence emission (PL) and excitation (PLE) spectra of [PNacAuHg] (6) from 270-800 nm at 77 K (blue) and RT, 293 K (red).

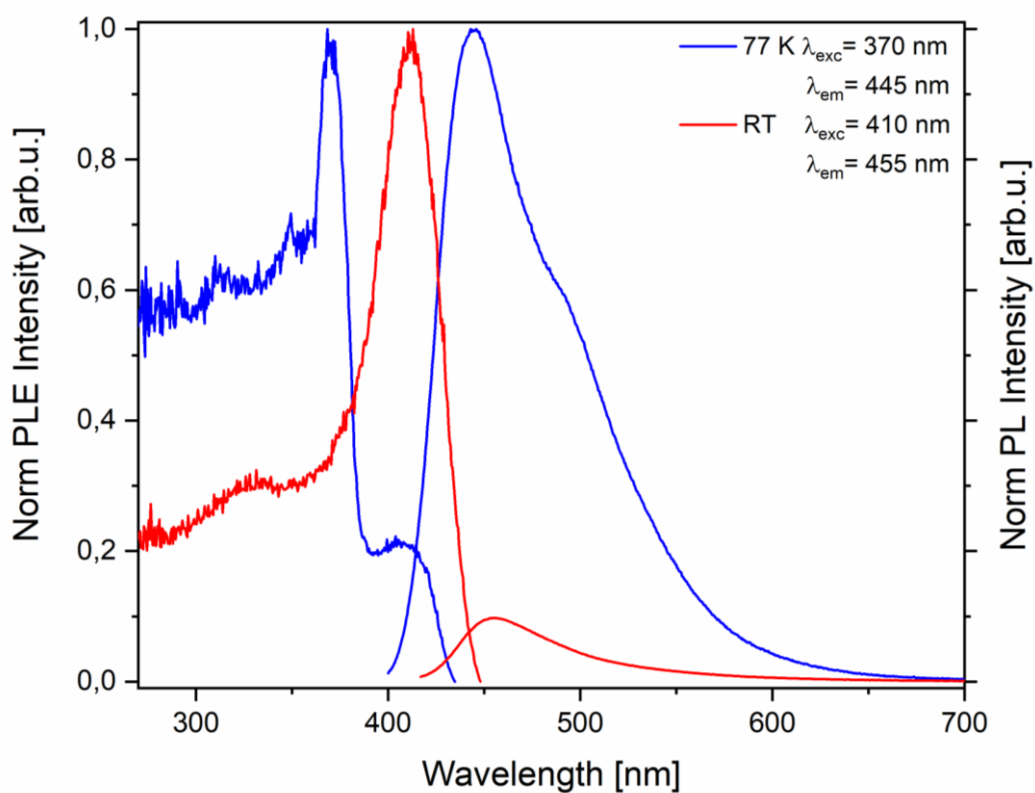


Figure S59: Solid-state photoluminescence emission (PL) and excitation (PLE) spectra of [PNacAgZn] (7) from 270-700 nm at 77 K (blue) and RT, 293 K (red).

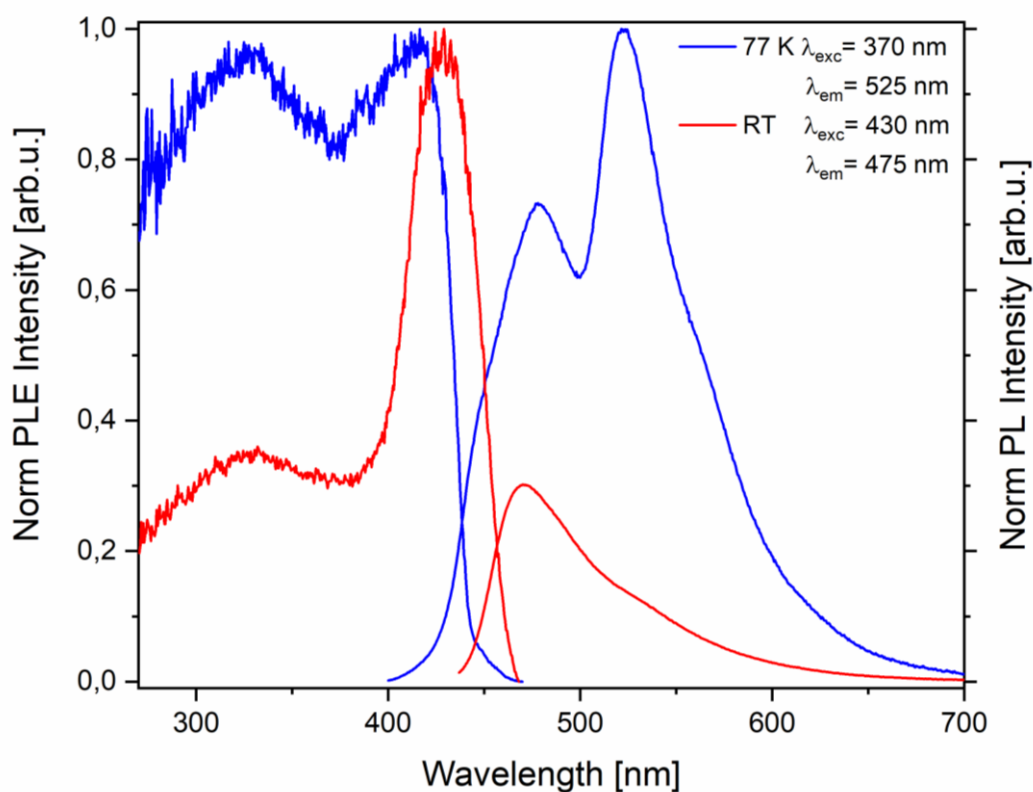


Figure S60: Solid-state photoluminescence emission (PL) and excitation (PLE) spectra of **[PNacAgCd] (8)** from 270-700 nm at 77 K (blue) and RT, 293 K (red).

Table S1: Experimental data of the PLE and PL spectra and decay times of compounds **1-8**.

	$\lambda_{\max, \text{exc}}$ [nm]		$\lambda_{\max, \text{em}}$ [nm]		τ_{eff} [μs]	
	77 K	293 K	77 K	293 K	77 K	293 K
[PNacK]	500	540	580	610	-	-
1: [PNacAu]	505	525	620	575	13/90/566	5/34
2: [PNacAg]	490	510	600	560	6	7/67
3: [PNacAuCu]	440	460	620	590	47/99	8
4: [PNacAuZn]	380	410	495	490	6/222/818	9/85
5: [PNacAuCd]	375	415	505	505	7/137/404	19
6: [PNacAuHg]	480	510	580	595	6	7
7: [PNacAgZn]	370	410	445	455	6	6
8: [PNacAgCd]	420	430	525	470	7/600	7

Photoluminescence decay curves

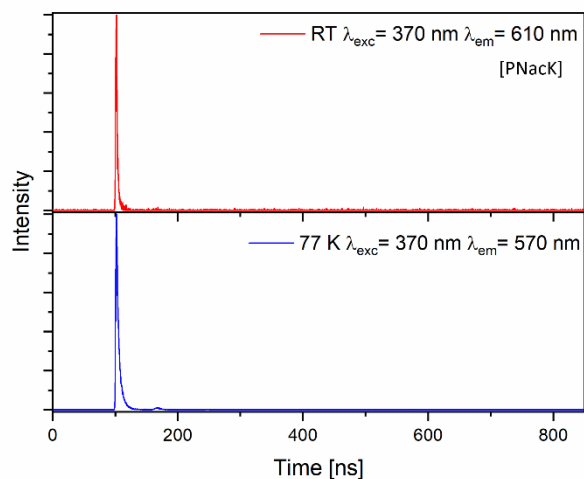


Figure S61: Solid state PL decay of complex [PNacK] at 77 K (blue) and at RT, 293 K (red). Lifetimes 4 ns (77 K), 2 ns (RT).

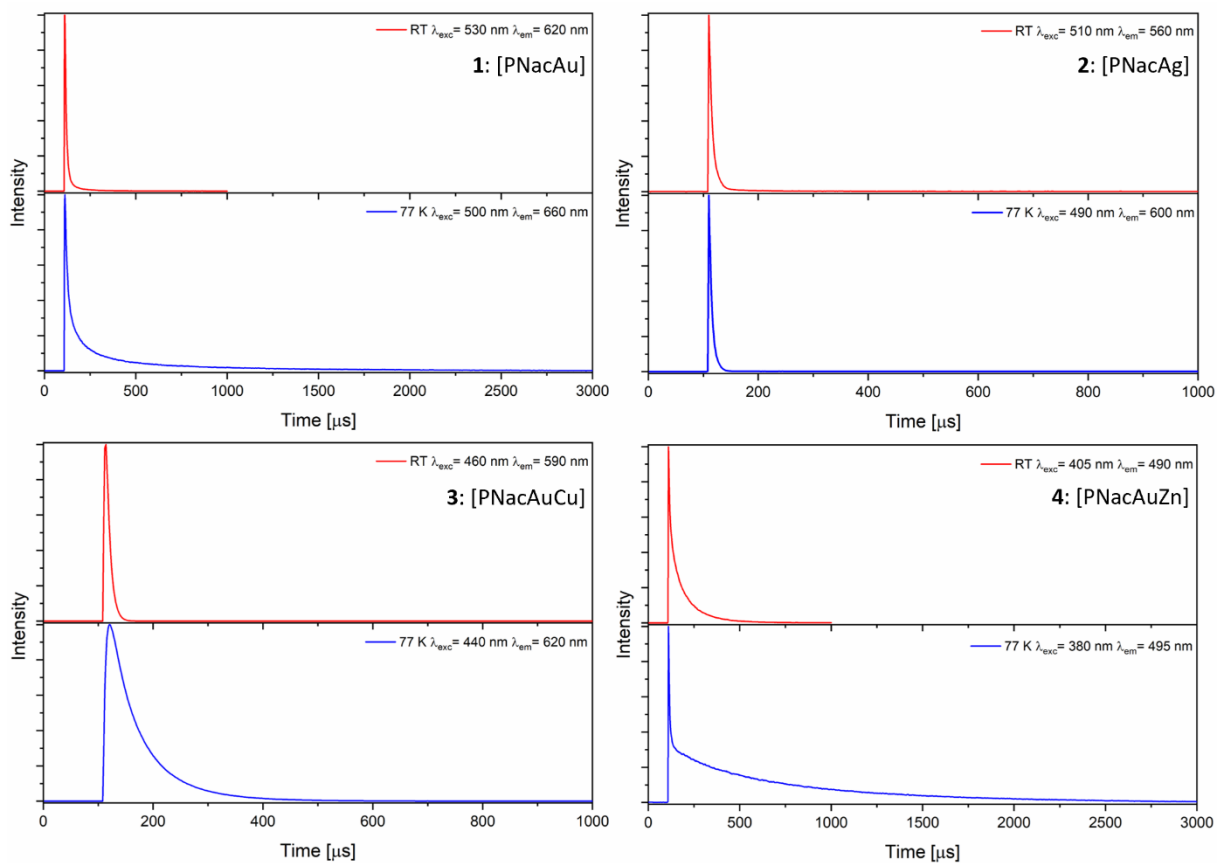


Figure S62: Solid state PL decay of complex 1-4 at 77 K (blue) and at RT, 293 K (red).

Supplementary Information

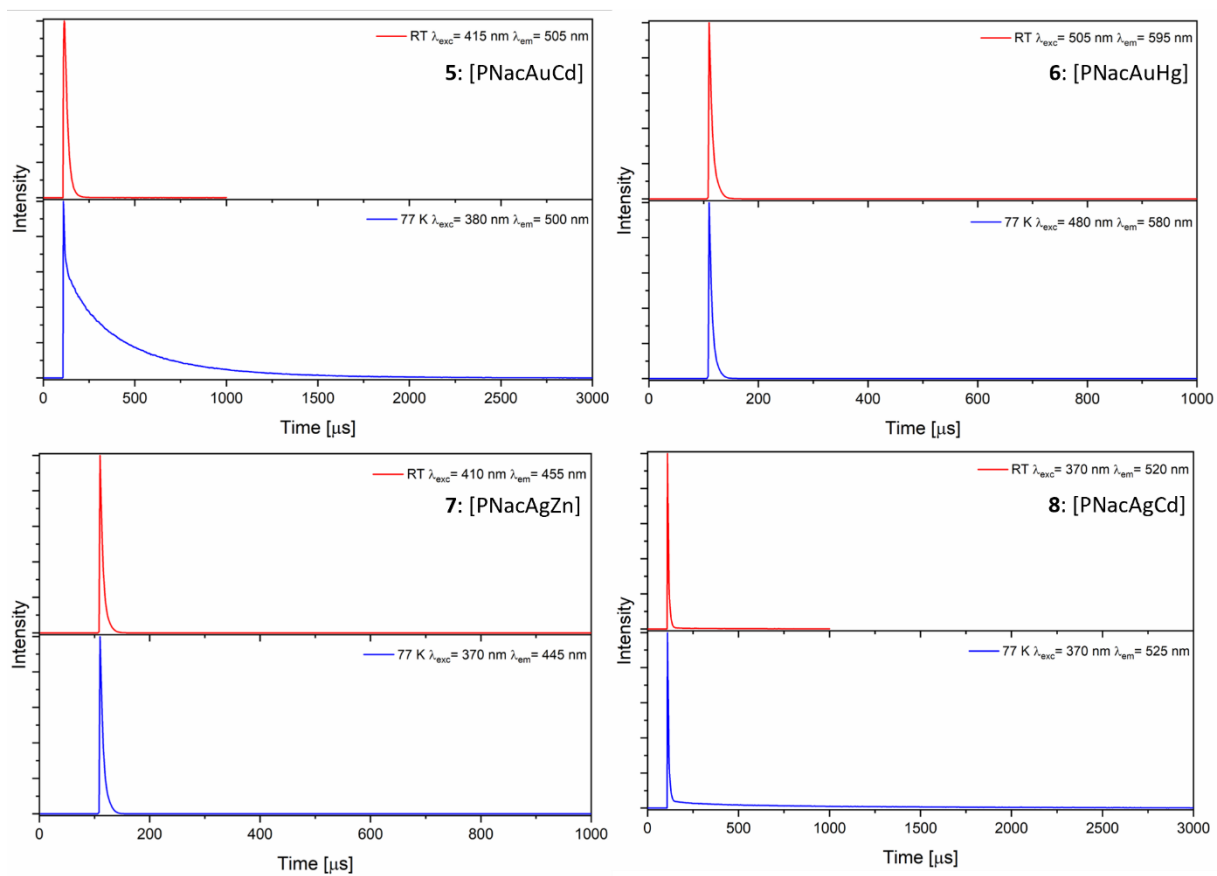


Figure S63: Solid state PL decay of complex 5-8 at 77 K (blue) and at RT, 293 K (red).

X-ray crystallography

General methods

Suitable crystals for the X-ray analysis of all compounds were obtained as described above. A suitable crystal was covered in mineral oil (Aldrich) and mounted on a glass fibre. The crystal was transferred directly to the cold stream of a STOE StadiVari (100, 130 or 150 K) diffractometer. All structures were solved by using the program SHELXS/T⁴ and Olex².⁵ The remaining non-hydrogen atoms were located from successive difference Fourier map calculations. The refinements were carried out by using full-matrix least-squares techniques on F^2 by using the program SHELXL.⁶ The H-atoms were introduced into the geometrically calculated positions (SHELXL procedures) unless otherwise stated and refined riding on the corresponding parent atoms. In each case, the locations of the largest peaks in the final difference Fourier map calculations, as well as the magnitude of the residual electron densities, were of no chemical significance. Specific comments for each data set are given below. Summary of the crystal data, data collection and refinement for compounds are given in Table S2 and Table S3. Crystallographic data for the structures reported in this paper have been deposited with the Cambridge Crystallographic Data Centre as a supplementary publication no. CCDC XXXX. Copies of the data can be obtained free of charge on application to CCDC, 12 Union Road, Cambridge CB21EZ, UK (fax: +(44)1223-336-033; email: deposit@ccdc.cam.ac.uk).

Supplementary Information

Summary of crystal data

Table S2: Crystal data, data collection and refinement for compounds **1-3**.

Compounds	1	2	3 (CH₂Cl₂)
Chemical formular	C ₄₁ H ₃₅ AuN ₂ P ₂	C ₄₁ H ₃₅ AgN ₂ P ₂	C ₄₂ H ₃₇ AuCl ₂ CuIN ₂ P ₂
CCDC Number			
Formular Mass	814.61	725.52	1089.98
Radiation type	Mo K α	Mo K α	Mo K α
Wavelength/nm	0.71073	0.71073	0.71073
Crystal system	monoclinic	monoclinic	monoclinic
<i>a</i> /Å	11.3333(12)	16.1322(6)	11.5181(10)
<i>b</i> /Å	16.3984(11)	9.0059(3)	21.4134(13)
<i>c</i> /Å	17.996(2)	23.0302(9)	15.9704(11)
α /°			
β /°	101.993(8)	94.494(3)	102.741(6)
γ /°			
Unit cell volume/Å ³	3271.5(5)	3336.1(2)	3842.0(5)
Temperatur/K	100	100	110
Space Group	<i>P</i> 2 ₁ / <i>n</i>	<i>P</i> 2 ₁ / <i>c</i>	<i>Cc</i>
Z	4	4	4
Absorption coefficient, μ /mm	4.628	0.733	5.428
No. of reflections measured	34720	20028	25870
No. of independent reflections	7876	8150	9934
<i>R</i> _{int}	0.0606	0.0197	0.0399
Final <i>R</i> ₁ values (<i>I</i> > 2 σ (<i>I</i>))	0.0422	0.0270	0.0461
Final <i>wR</i> (<i>F</i> ²) values (<i>I</i> > 2 σ (<i>I</i>))	0.0927	0.0725	0.1119
Final <i>R</i> ₁ values (all data)	0.0697	0.0345	0.0594
Final <i>wR</i> (<i>F</i> ²) values (all data)	0.1166	0.0751	0.1418
Goodness of fit on <i>F</i> ²	1.047	1.067	1.122

Supplementary Information

Table S3: Crystal data, data collection and refinement for compounds **4-6**.

Compounds	4 (2 CH₂Cl₂)	5 (2 C₄H₈O)	6 (2 C₄H₈O)
Chemical formular	C ₄₃ H ₃₉ AuCl ₆ N ₂ P ₂ Zn	C ₄₉ H ₅₁ AuCdI ₂ N ₂ O ₂ P ₂	C ₄₉ H ₅₁ AuCl ₂ HgN ₂ O ₂ P ₂
CCDC Number			
Formular Mass	950.88	1325.02	1230.31
Radiation type	Mo K α	Mo K α	Mo K α
Wavelength/nm	0.71073	0.71073	0.71073
Crystal system	orthorhombic	orthorhombic	monoclinic
<i>a</i> /Å	12.1617(3)	28.1026(6)	16.1508(5)
<i>b</i> /Å	22.4791(6)	16.7556(5)	12.0679(5)
<i>c</i> /Å	31.9607(12)	10.1411(2)	23.5979(7)
α /Å			
β /Å			97.498(2)
γ /Å			
Unit cell volume/Å ³	8737.5(5)	4775.2(2)	4560.0(3)
Temperatur/K	150	100	100
Space Group	<i>Pbca</i>	<i>Pnma</i>	<i>P2₁/c</i>
Z	8	4	4
Absorption coefficient, μ /mm	4.126	4.914	6.805
No. of reflections measured	46428	38812	47855
No. of independent reflections	9667	6111	11656
<i>R</i> _{int}	0.0260	0.0379	0.0250
Final <i>R</i> ₁ values (<i>I</i> > 2 σ (<i>I</i>))	0.0335	0.0286	0.0268
Final <i>wR</i> (<i>F</i> ²) values (<i>I</i> > 2 σ (<i>I</i>))	0.0823	0.0700	0.0656
Final <i>R</i> ₁ values (all data)	0.0401	0.0398	0.0314
Final <i>wR</i> (<i>F</i> ²) values (all data)	0.0873	0.0723	0.0686
Goodness of fit on <i>F</i> ²	1.130	1.021	1.137

Supplementary Information

Table S4: Crystal data, data collection and refinement for compounds **7** and **8**.

Compounds	7	8 (0.5 C₄H₈O)
Chemical formular	C ₄₁ H ₃₅ AgCl ₂ N ₂ P ₂ Zn	C ₄₃ H ₃₉ AgCdI ₂ N ₂ O _{0.5} P ₂
CCDC Number		
Formular Mass	861.79	1127.77
Radiation type	Mo K α	Mo K α
Wavelength/nm	0.71073	0.71073
Crystal system	monoclinic	monoclinic
<i>a</i> /Å	25.5385(11)	11.2940(4)
<i>b</i> /Å	19.9358(6)	29.8817(15)
<i>c</i> /Å	15.2535(7)	12.1200(5)
α /Å		
β /Å	103.974(4)	990.853(3)
γ /Å		
Unit cell volume/Å ³	7536.2(5)	4089.9(3)
Temperatur/K	110	100
Space Group	<i>P</i> 2 ₁ / <i>c</i>	<i>P</i> 2 ₁ / <i>n</i>
Z	8	4
Absorption coefficient, μ /mm	1.415	2.621
No. of reflections measured	82459	29523
No. of independent reflections	20016	10298
<i>R</i> _{int}	0.0479	0.0408
Final <i>R</i> ₁ values (<i>I</i> > 2 σ (<i>I</i>))	0.0549	0.0424
Final <i>wR</i> (<i>F</i> ²) values (<i>I</i> > 2 σ (<i>I</i>))	0.1306	0.1015
Final <i>R</i> ₁ values (all data)	0.0855	0.0607
Final <i>wR</i> (<i>F</i> ²) values (all data)	0.1427	0.1066
Goodness of fit on <i>F</i> ²	1.066	0.957

Crystal structures

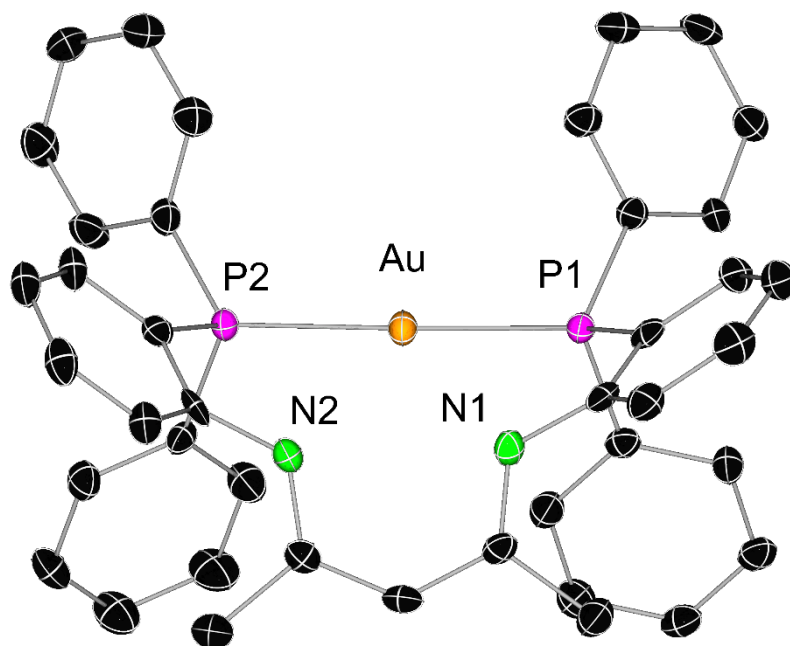


Figure S64: Molecular structure of **1** in the solid state with ellipsoids drawn at 40 % probability. Hydrogen atoms are omitted for clarity. Selected bond lengths [Å] and angles [°]: P1-Au 2.2909(15), P2-Au 2.2881(15); P1-Au-P2 169.12(6).

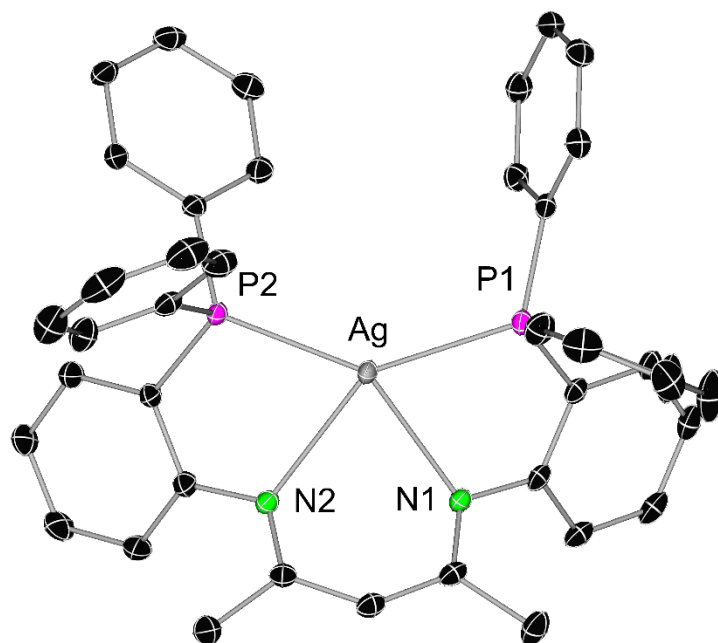


Figure S65: Molecular structure of **2** in the solid state with ellipsoids drawn at 40 % probability. Hydrogen atoms are omitted for clarity. Selected bond lengths [Å] and angles [°]: P1-Ag 2.4040(5), P2-Ag 2.4254(5), N1-Ag 2.4371(14), N2-Ag 2.4749(14); P1-Ag-P2 140.78(2), N1-Ag-N2 72.04(5).

Supplementary Information

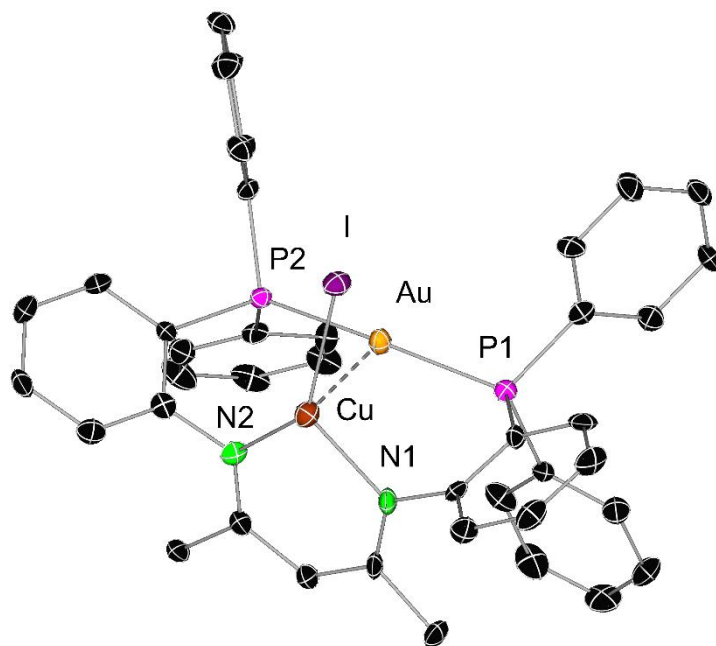


Figure S66: Molecular structure of **3** in the solid state with ellipsoids drawn at 40 % probability. Hydrogen atoms are omitted for clarity. Selected bond lengths [Å] and angles [°]: Au...Cu 2.634(2), P1-Au 2.293(3), P2-Au 2.290(3), N1-Cu 1.948(11), N2-Cu 1.970(12), I-Cu 2.46(2); P1-Au-P2 169.47(12), N1-Cu-N2 95.6(5).

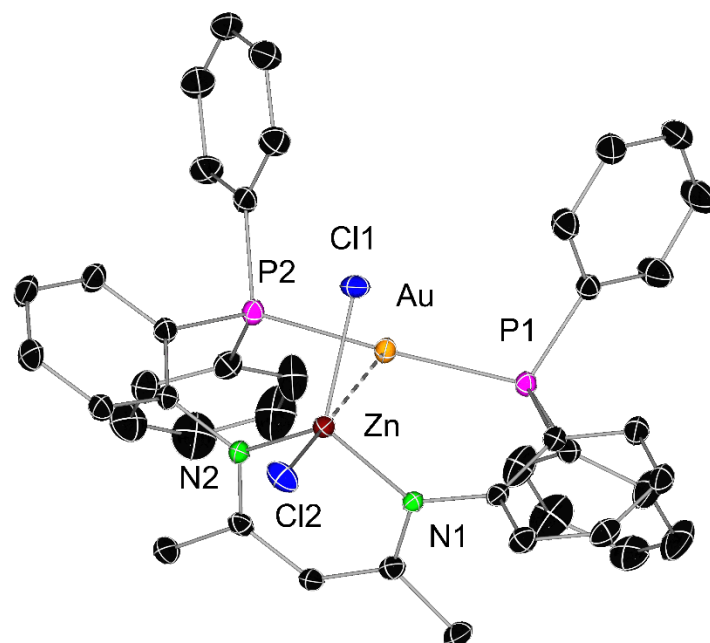


Figure S67: Molecular structure of **4** in the solid state with ellipsoids drawn at 40 % probability. Hydrogen atoms are omitted for clarity. Selected bond lengths [Å] and angles [°]: Au...Zn 3.2088(5), P1-Au 2.3019(11), P2-Au 2.3009(12), N1-Zn 2.001(4), N2-Zn 2.003(4), Cl1-Zn 2.2641(12), Cl2-Zn 2.2536(13); P1-Au-P2 169.01(4), N1-Zn-N2 93.46(15).

Supplementary Information

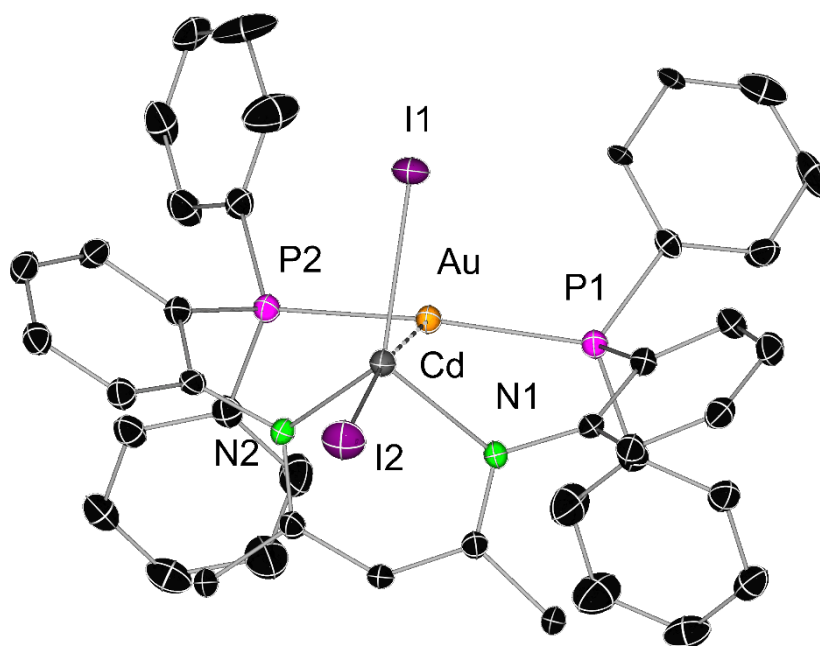


Figure S68: Molecular structure of **5** in the solid state with ellipsoids drawn at 40 % probability. Hydrogen atoms are omitted for clarity. Selected bond lengths [Å] and angles [°]: Au···Cd 3.3942(4), P-Au 2.3139(9), N-Cd 2.227(3), I-Cd 2.7253(4); P-Au-P' 167.68(5), N-Cd-N' 84.41(13).

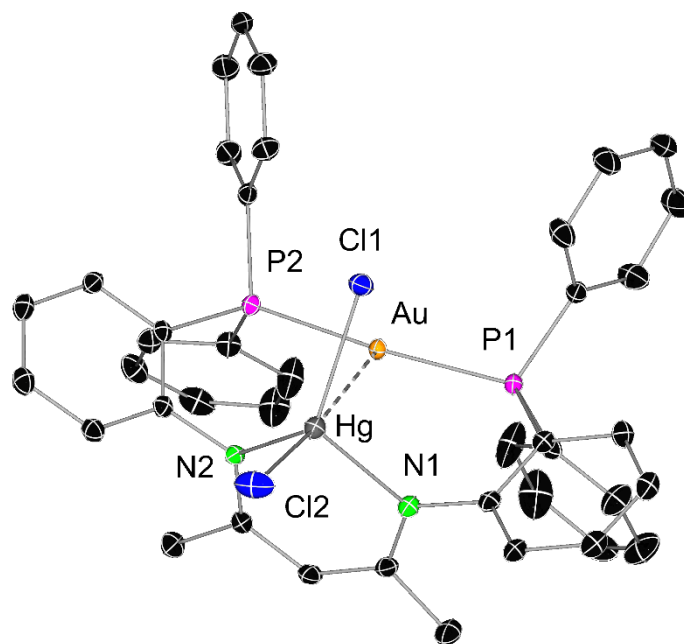


Figure S69: Molecular structure of **6** in the solid state with ellipsoids drawn at 40 % probability. Hydrogen atoms are omitted for clarity. Selected bond lengths [Å] and angles [°]: Au···Hg 3.2417(2), P1-Au 2.2968(9), P2-Au 2.2968(9), N1-Hg 2.251(3), N2-Hg 2.255(3), Cl1-Hg 2.4589(9), Cl2-Hg 2.4160(10); P1-Au-P2 167.38(3), N1-Hg-N2 84.80(10).

Supplementary Information

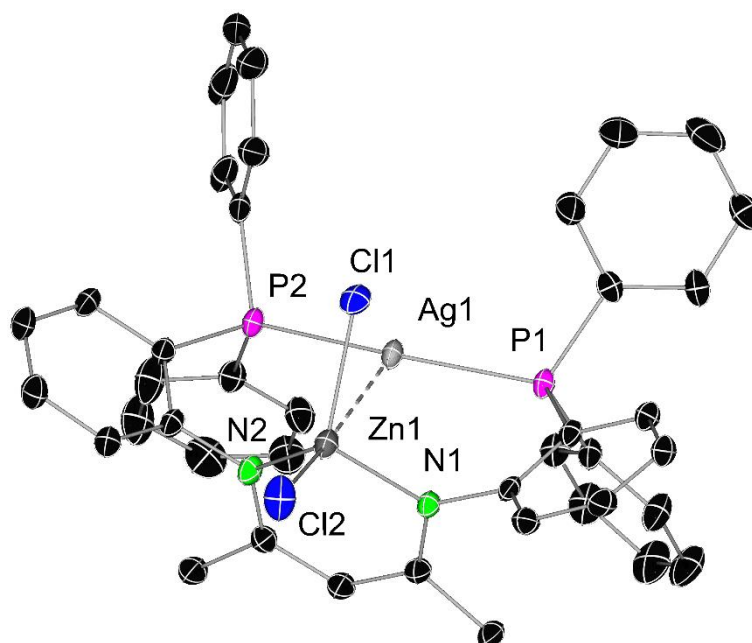


Figure S70: Molecular structure of **7** in the solid state with ellipsoids drawn at 40 % probability. Hydrogen atoms are omitted for clarity. Compound **7** crystallises with two molecules in the asymmetric unit with similar metric data. Only one is described. Selected bond lengths [Å] and angles [°]: Ag1···Zn1 3.0941(7), P1–Ag1 2.4054(12), P2–Ag1 2.3984(12), N1–Zn1 2.009(4), N2–Zn1 2.009(4), Cl1–Zn1 2.2138(15), Cl2–Zn1 2.2776(14); P1–Ag1–P2 160.97(4), N1–Zn1–N2 92.9(2).

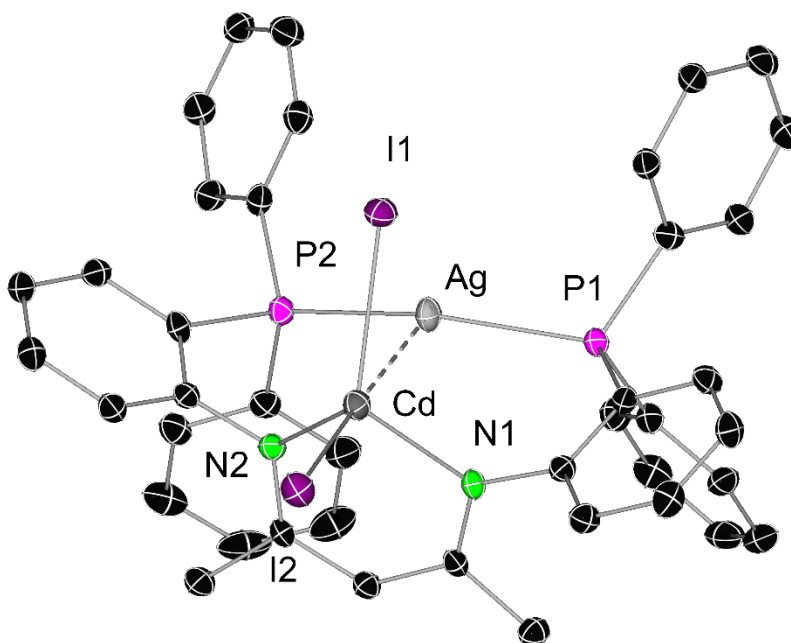


Figure S71: Molecular structure of **8** in the solid state with ellipsoids drawn at 40 % probability. Hydrogen atoms are omitted for clarity. Selected bond lengths [Å] and angles [°]: Ag···Cd 3.2077(5), P1–Ag 2.4282(12), P2–Ag 2.4271(12), N1–Cd 2.233(4), N2–Cd 2.248(4), I1–Cd 2.7502(5), I2–Cd 2.6841(5); P1–Ag–P2 154.76(4), N1–Cd–N2 83.82(13).

Quantum chemical calculations

Quantum chemical calculations were performed with the TURBOMOLE program package, version 7.6.⁷ The calculations were carried out in the framework of ground-state density-functional theory (DFT) and excited-state time-dependent density-functional theory (TDDFT). The TPSSh functional⁸ was used in conjunction with Grimme's D3 correction for dispersion including Becke–Johnson damping (D3(BJ)).⁹ For geometry optimizations, the def2-SV(P) basis set was used,¹⁰ but all calculations at the TDDFT level were performed in the def2-SVPD basis.¹¹ All optimised geometries displayed only real harmonic vibrational frequencies and thus were shown to be minima on the respective potential-energy hypersurface. At the ground-state equilibrium geometries, vertical excitation energies were computed for 200 singlet excited states to simulate the absorption spectra. These calculations were done in the def2-SVPD basis set, which is a property-optimised Gaussian basis set for molecular response calculations.^{Rappoport, 2010 #63} The equilibrium-geometry optimisations were performed with tight thresholds (energy and gradient were converged to within 10⁻⁸ Eh and 10⁻⁶ Eh/a₀, respectively), and derivatives of the weights of the quadrature grid (TURBOMOLE 's size 4 was used) were taken into account (other TURBOMOLE parameters were set to scfconv = 9, denconv = 1d-8, and rpaconv = 6).

Table S5: Natural population analysis (NPA) of the hole contribution to the unrelaxed difference density of the singlet excited state S_n , as obtained at the CAM-B3LYP/def2-SVPD//CAM-B3LYP/def2-SV(P) level. Also shown are the vertical excitation energy ΔE_S (in eV), the oscillator strength in the mixed length/velocity representation, and the weight of the dominant pair of hole/particle natural transition orbitals (NTOs). Displayed are the NPA populations of the s, p, and d shells of the coinage ions (Cu/Ag/Au) and of the metal ions of the metal halides (Cu/Zn/Cd/Hg).

		S_n				Cu/Ag/Au			Cu/Zn/Cd/Hg		
		n	ΔE_S (eV)	f_{mixed}	%	s	p	d	s	p	d
[PNacAu]	1	1	3.479	0.4579	92.7	0.005	0.002	0.002	--	--	--
[PNacAg]	2	1	3.549	0.4763	93.8	0.002	0.002	0.010	--	--	--
[PNacAuCu]	3	3	3.853	0.1557	48.9	0.001	0.001	0.002	0.000	0.028	0.273
[PNacAuZn]	4	1	4.034	0.3087	94.4	0.004	0.003	0.007	0.000	0.002	0.006
[PNacAuCd]	5	1	3.907	0.2530	93.6	0.005	0.003	0.007	0.000	0.003	0.005
[PNacAuHg]	6	1	3.841	0.2068	88.5	0.004	0.003	0.006	0.000	0.003	0.011
[PNacAgZn]	7	1	4.031	0.3463	94.8	0.003	0.004	0.005	0.000	0.002	0.006
[PNacAgCd]	8	1	3.928	0.2749	93.7	0.001	0.003	0.004	0.000	0.003	0.005
[PNacCu]	9	1	2.958	0.1468	97.8	0.000	0.018	0.185	--	--	--

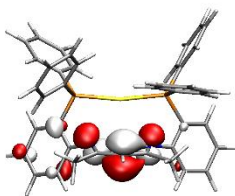
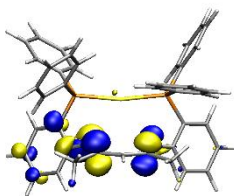
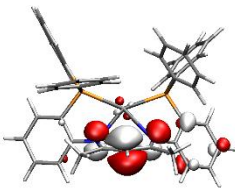
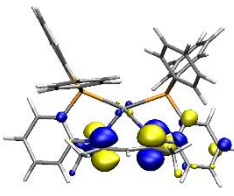
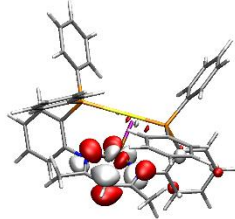
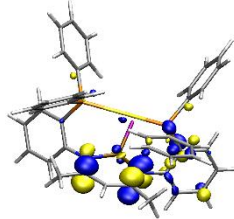
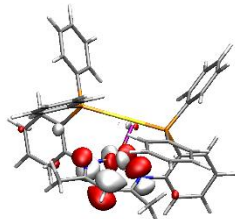
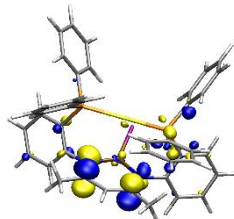
Table S6: Natural population analysis (NPA) of the particle contribution to the unrelaxed difference density of the singlet excited state S_n , as obtained at the CAM-B3LYP/def2-SVPD//CAM-B3LYP/def2-SV(P) level. Also shown are the vertical excitation energy ΔE_S (in eV), the oscillator strength in the mixed length/velocity representation, and the weight of the dominant pair of hole/particle natural transition orbitals (NTOs). Displayed are the NPA populations of the s, p, and d shells of the coinage ions (Cu/Ag/Au) and of the metal ions of the metal halides (Cu/Zn/Cd/Hg).

		S_n				Cu/Ag/Au			Cu/Zn/Cd/Hg		
		n	ΔE_S (eV)	f_{mixed}	%	s	p	d	s	p	d
[PNacAu]	1	1	3.479	0.4579	92.7	0.003	0.010	0.026	--	--	--
[PNacAg]	2	1	3.549	0.4763	93.8	0.004	0.017	0.028	--	--	--

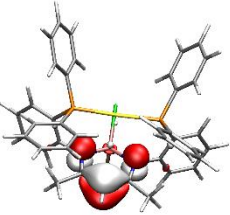
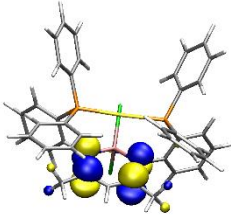
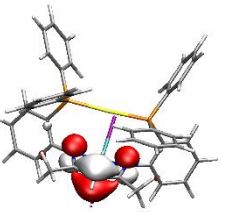
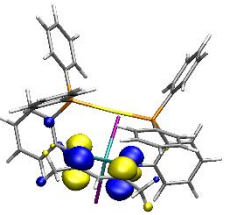
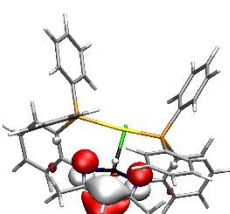
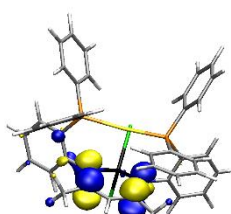
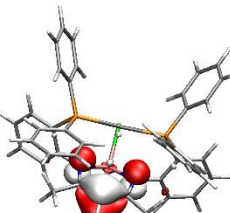
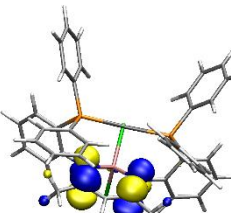
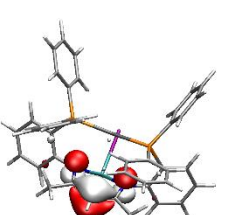
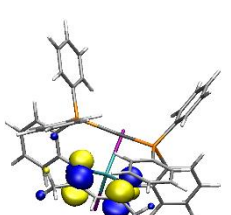
Supplementary Information

[PNacAuCu]	3	3	3.853	0.1557	48.9	0.011	0.058	0.013	0.001	0.004	0.020
[PNacAuZn]	4	1	4.034	0.3087	94.4	0.001	0.007	0.016	0.002	0.019	0.004
[PNacAuCd]	5	1	3.907	0.2530	93.6	0.001	0.006	0.017	0.005	0.028	0.005
[PNacAuHg]	6	1	3.841	0.2068	88.5	0.002	0.005	0.017	0.040	0.029	0.008
[PNacAgZn]	7	1	4.031	0.3463	94.8	0.001	0.007	0.022	0.002	0.023	0.004
[PNacAgCd]	8	1	3.928	0.2749	93.7	0.001	0.005	0.021	0.006	0.034	0.004
[PNacCu]	9	1	2.958	0.1468	97.8	0.004	0.014	0.018	--	--	--

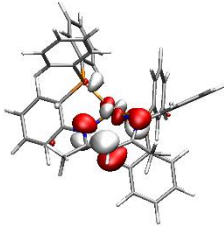
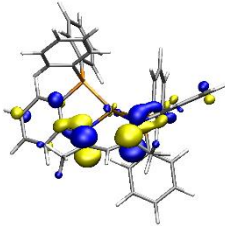
Table S7: Hole and particle natural transition orbitals (NTOs) of the singlet excited state S_n , as obtained at the CAM-B3LYP/def2-SVPD//CAM-B3LYP/def2-SV(P) level. Also shown are the vertical excitation energy ΔE_s (in eV) and the weight of the dominant pair of hole/particle natural transition orbitals (NTOs). Plotted at an isovalue of $\pm 0.05 a_0^{-3/2}$.

		n	ΔE_s (eV)	%	Hole NTO	Particle NTO
PNacAu	1	1	3.479	92.7		
PNacAg	2	1	3.549	93.8		
PNacAuCuI	3	3	3.853	48.9		
				47.7		

Supplementary Information

PNacAuZnCl ₂	4	1	4.034	94.4		
PNacAuCdI ₂	5	1	3.907	93.6		
PNacAuHgCl ₂	6	1	3.841	88.5		
PNacAgZnCl ₂	7	1	4.031	94.8		
PNacAgCdI ₂	8	1	3.928	93.7		

Supplementary Information

PNacCu	9	1	2.958	97.8		
--------	----------	----------	-------	------	--	---

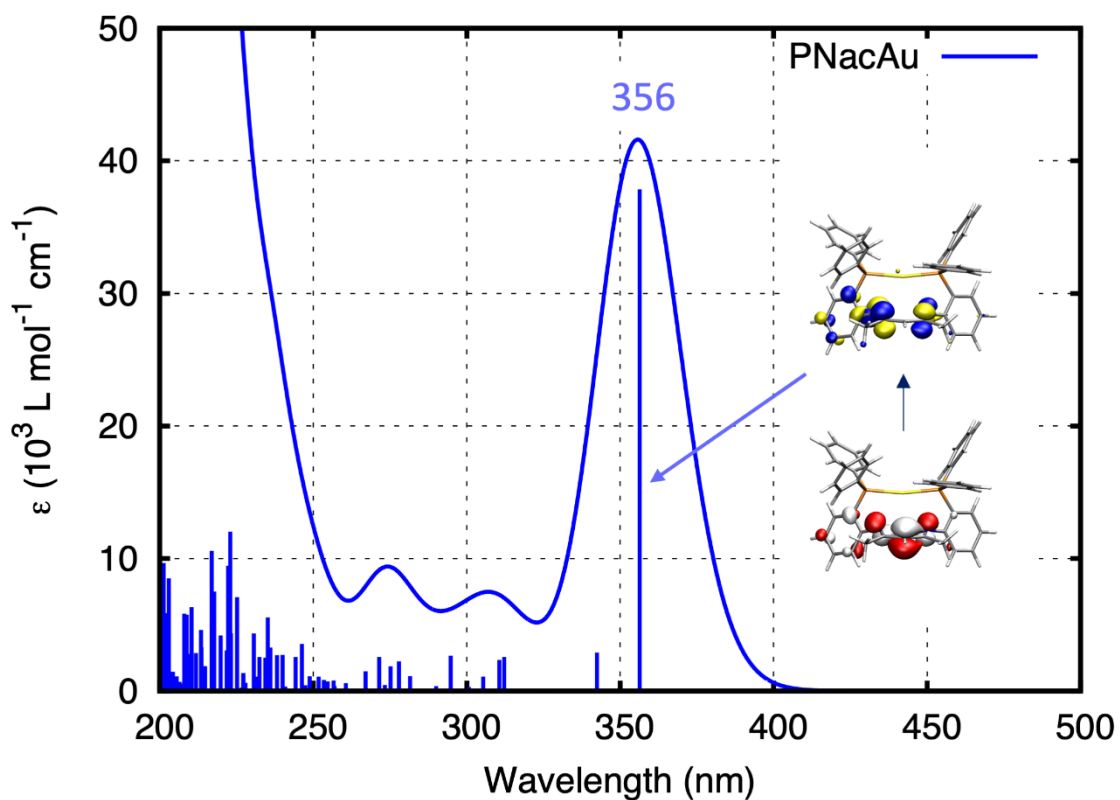


Figure S72: Simulated absorption spectrum of the [PNacAu] (1). Obtained from CAM-B3LYP/def2-SVPD//CAM-B3LYP/def2-SV(P) calculations by applying Gaussian broadening with a full width at half maximum of 2500 cm^{-1} . Oscillator strengths were computed in the mixed length/velocity representation. The dominant pair of natural transition orbitals (NTOs) is plotted at an isovalue of $\pm 0.05 a_0^{-3/2}$.

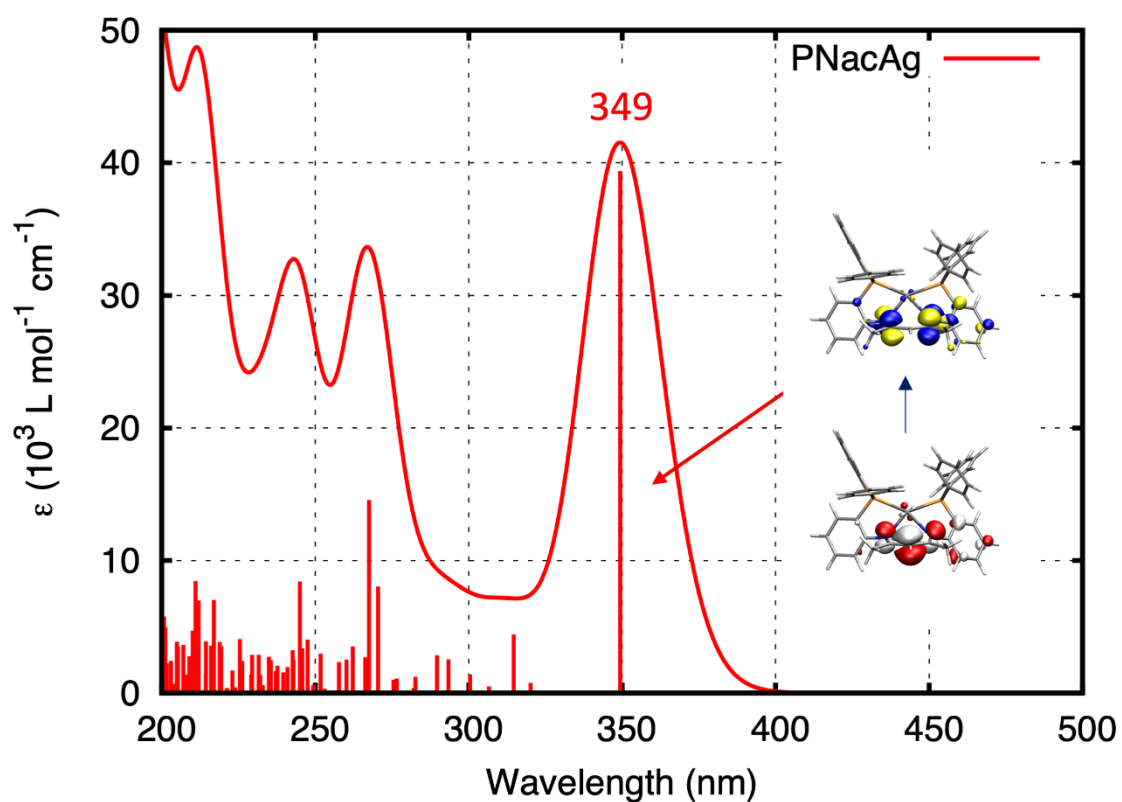


Figure S73: Simulated absorption spectrum of the [PNacAg] complex **2**. Obtained from CAM-B3LYP/def2-SVPD//CAM-B3LYP/def2-SV(P) calculations by applying Gaussian broadening with a full width at half maximum of 2500 cm^{-1} . Oscillator strengths were computed in the mixed length/velocity representation. The dominant pair of natural transition orbitals (NTOs) is plotted at an isovalue of $\pm 0.05 a_0^{-3/2}$.

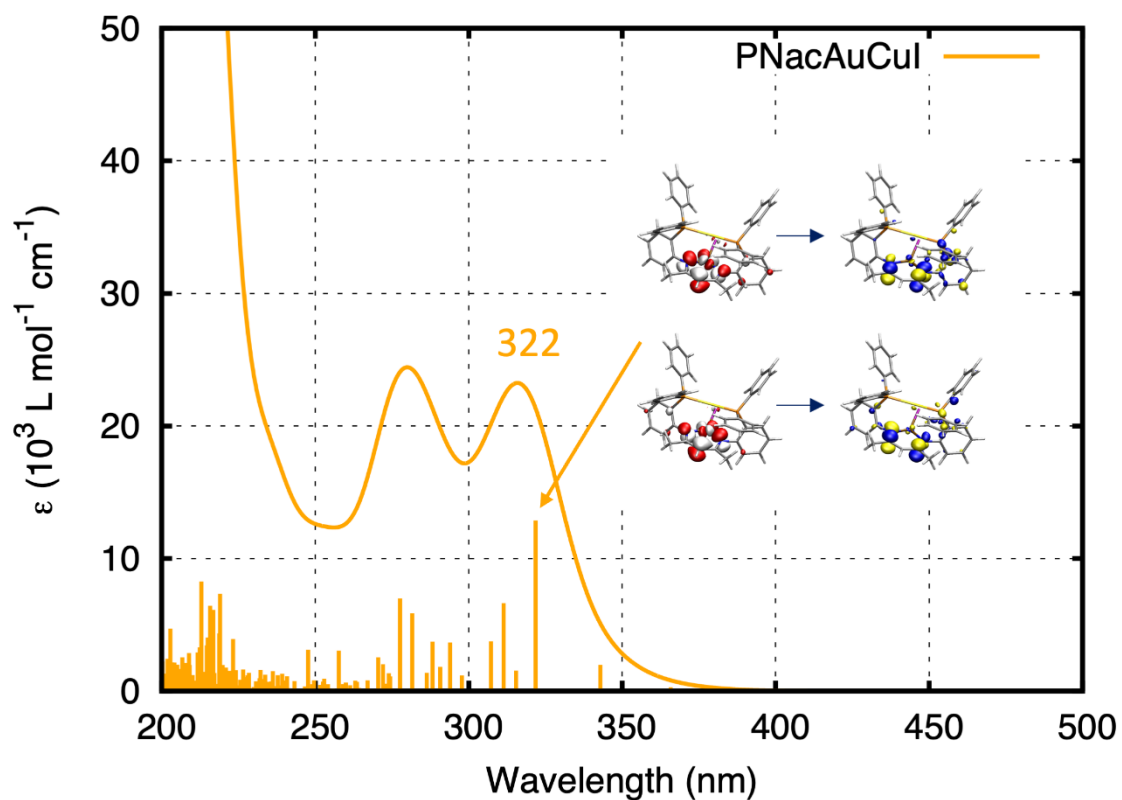


Figure S74: Simulated absorption spectrum of the [PNacAuCu] complex **3**. Obtained from CAM-B3LYP/def2-SVPD//CAM-B3LYP/def2-SV(P) calculations by applying Gaussian broadening with a full width at half maximum of 2500 cm^{-1} . Oscillator strengths were computed in the mixed length/velocity representation. The two dominant pairs of natural transition orbitals (NTOs) are plotted at an isovalue of $\pm 0.05 a_0^{-3/2}$.

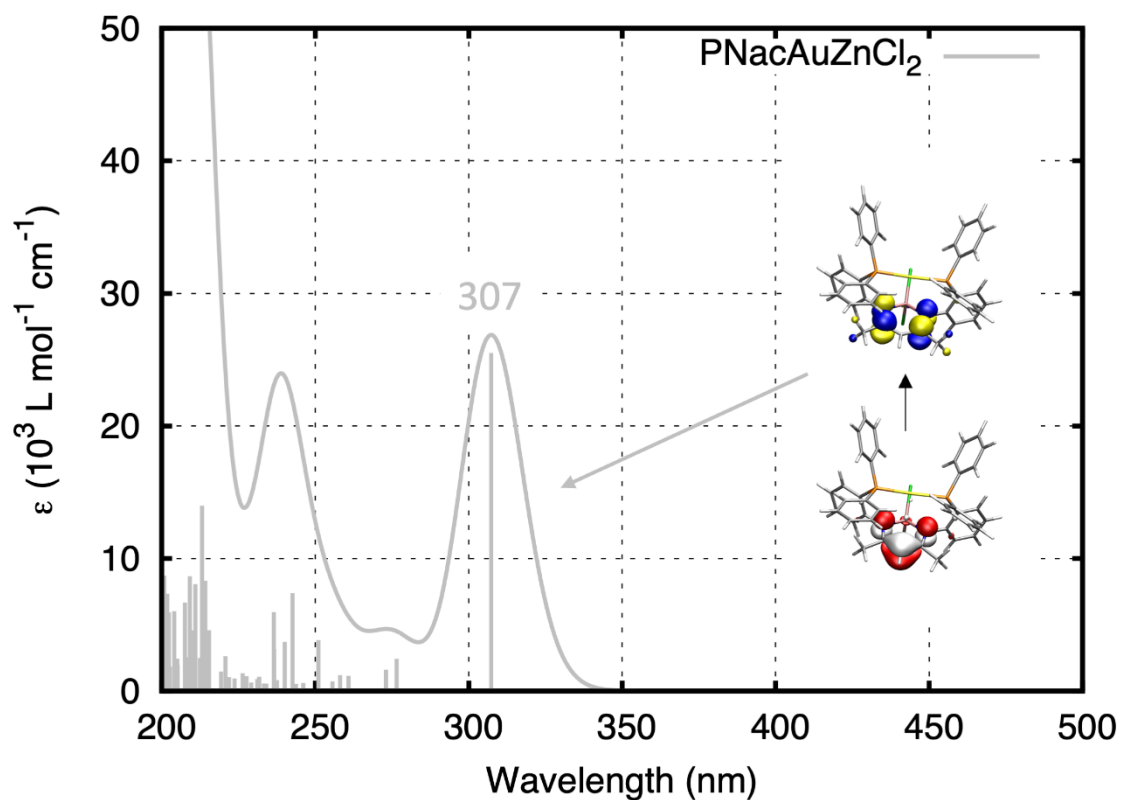


Figure 75: Simulated absorption spectrum of the [PNacAuZnCl₂] complex **4**. Obtained from CAM-B3LYP/def2-SVPD//CAM-B3LYP/def2-SV(P) calculations by applying Gaussian broadening with a full width at half maximum of 2500 cm⁻¹. Oscillator strengths were computed in the mixed length/velocity representation. The dominant pair of natural transition orbitals (NTOs) is plotted at an isovalue of $\pm 0.05 a_0^{-3/2}$.

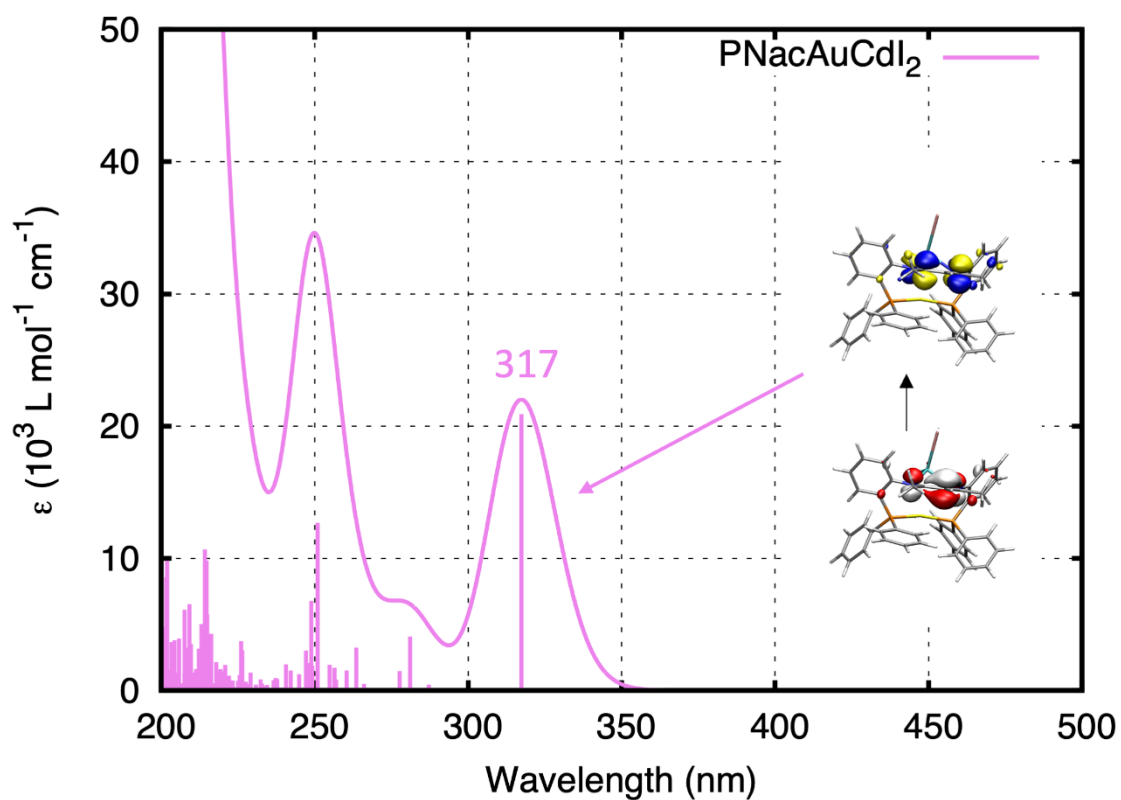


Figure S76: Simulated absorption spectrum of the [PNacAuHgCl₂] complex 5. Obtained from CAM-B3LYP/def2-SVPD//CAM-B3LYP/def2-SV(P) calculations by applying Gaussian broadening with a full width at half maximum of 2500 cm^{-1} . Oscillator strengths were computed in the mixed length/velocity representation. The dominant pair of natural transition orbitals (NTOs) is plotted at an isovalue of $\pm 0.05 a_0^{-3/2}$.

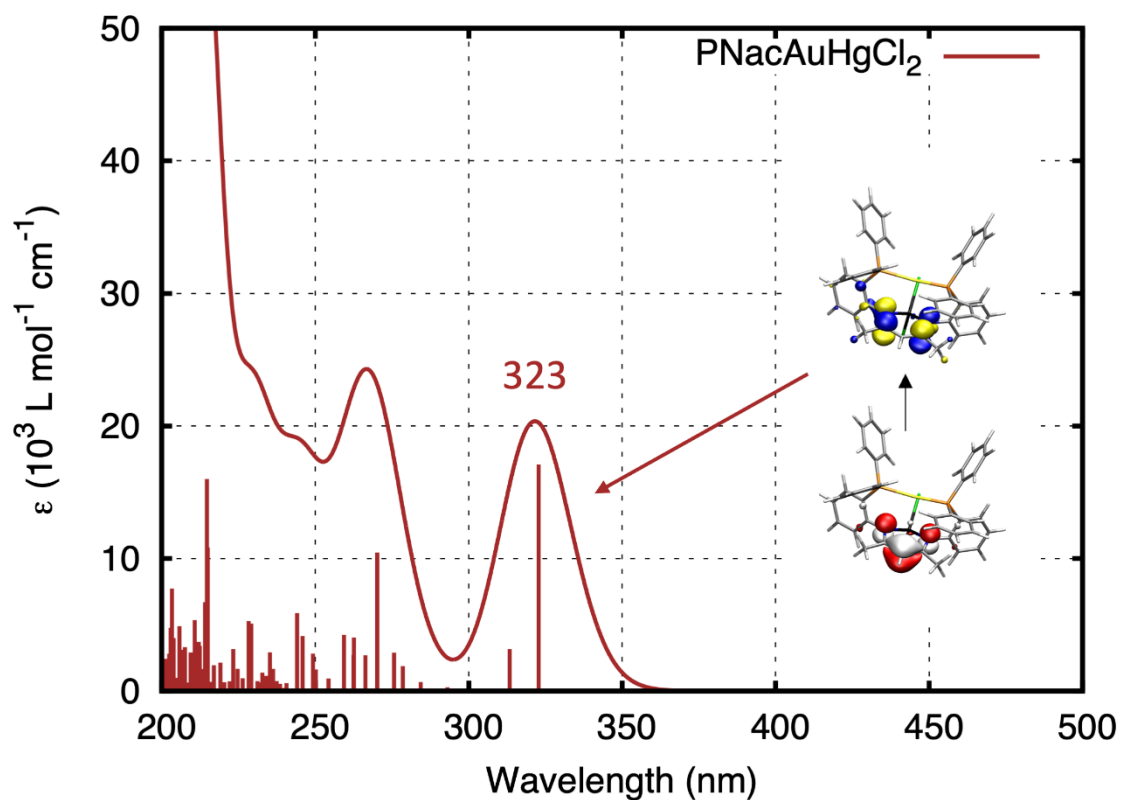


Figure S77: Simulated absorption spectrum of the [PNacAuHgCl₂] complex **6**. Obtained from CAM-B3LYP/def2-SVPD//CAM-B3LYP/def2-SV(P) calculations by applying Gaussian broadening with a full width at half maximum of 2500 cm⁻¹. Oscillator strengths were computed in the mixed length/velocity representation. The dominant pair of natural transition orbitals (NTOs) is plotted at an isovalue of $\pm 0.05 a_0^{-3/2}$.

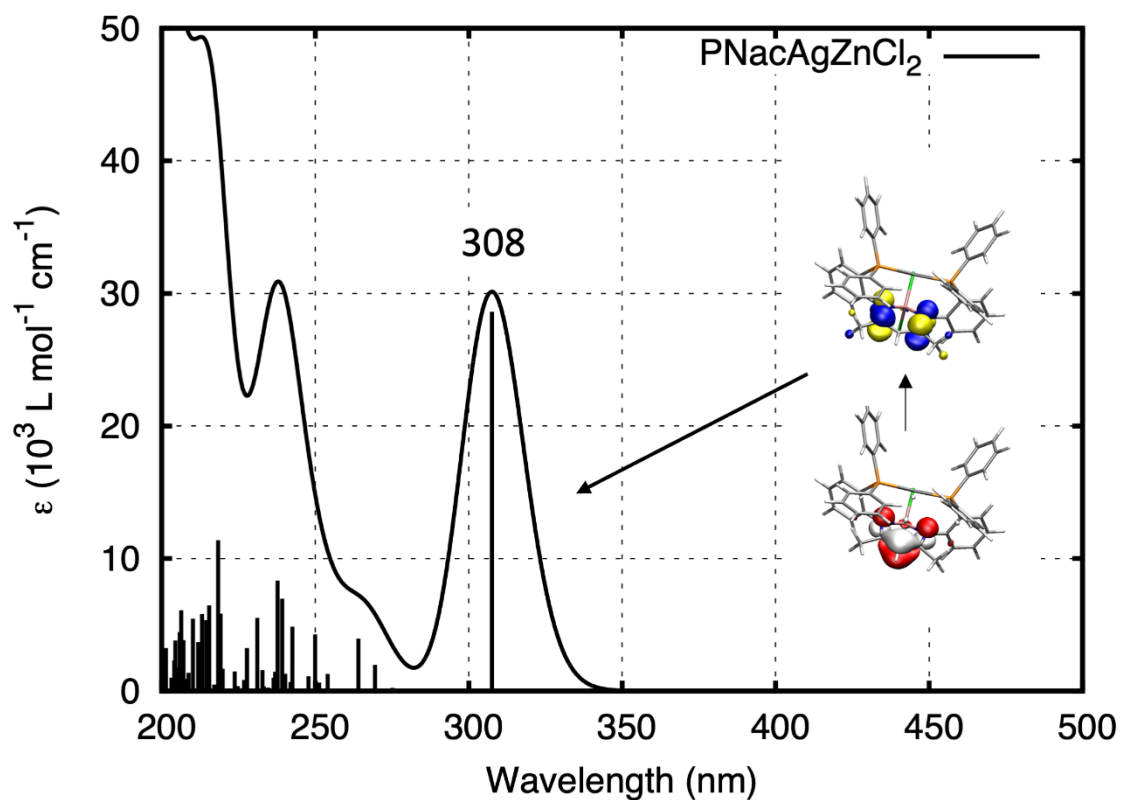


Figure S78: Simulated absorption spectrum of the [PNacAgZnCl₂] complex 7. Obtained from CAM-B3LYP/def2-SVPD//CAM-B3LYP/def2-SV(P) calculations by applying Gaussian broadening with a full width at half maximum of 2500 cm⁻¹. Oscillator strengths were computed in the mixed length/velocity representation. The dominant pair of natural transition orbitals (NTOs) is plotted at an isovalue of $\pm 0.05 a_0^{-3/2}$.

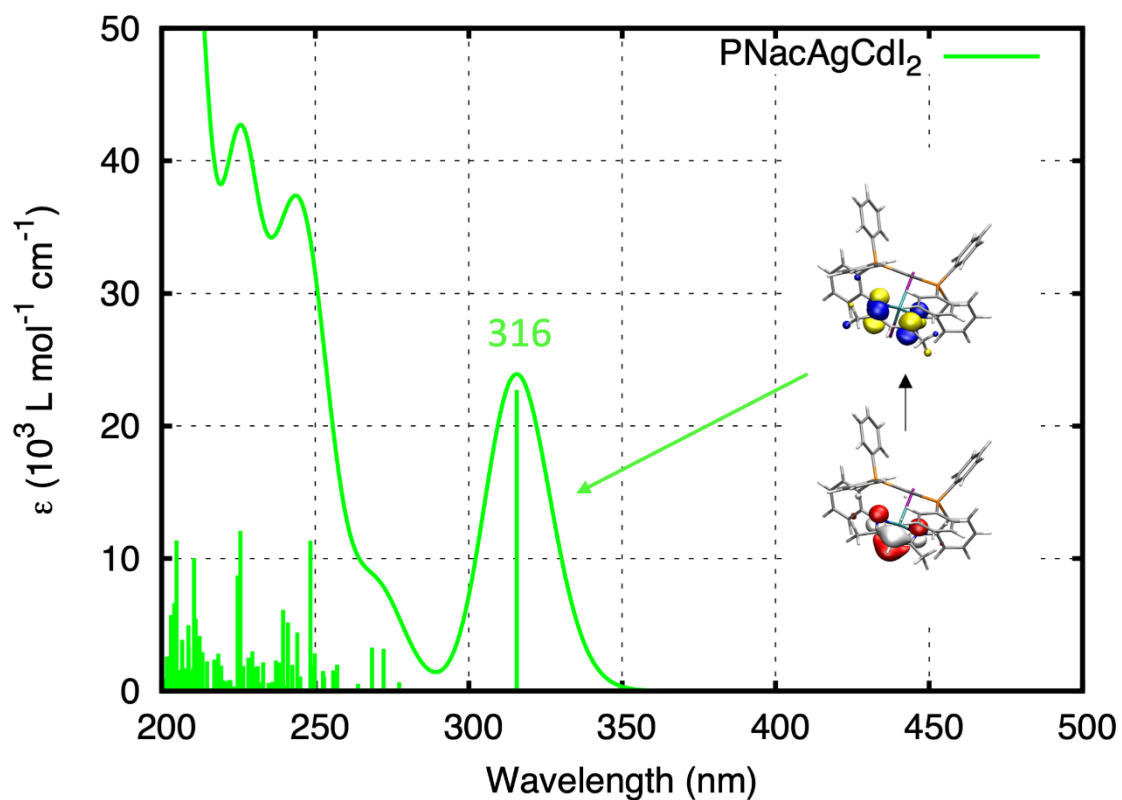


Figure S79: Simulated absorption spectrum of the [PNacAgCdI₂] complex **8**. Obtained from CAM-B3LYP/def2-SVPD//CAM-B3LYP/def2-SV(P) calculations by applying Gaussian broadening with a full width at half maximum of 2500 cm⁻¹. Oscillator strengths were computed in the mixed length/velocity representation. The dominant pair of natural transition orbitals (NTOs) is plotted at an isovalue of $\pm 0.05 a_0^{-3/2}$.

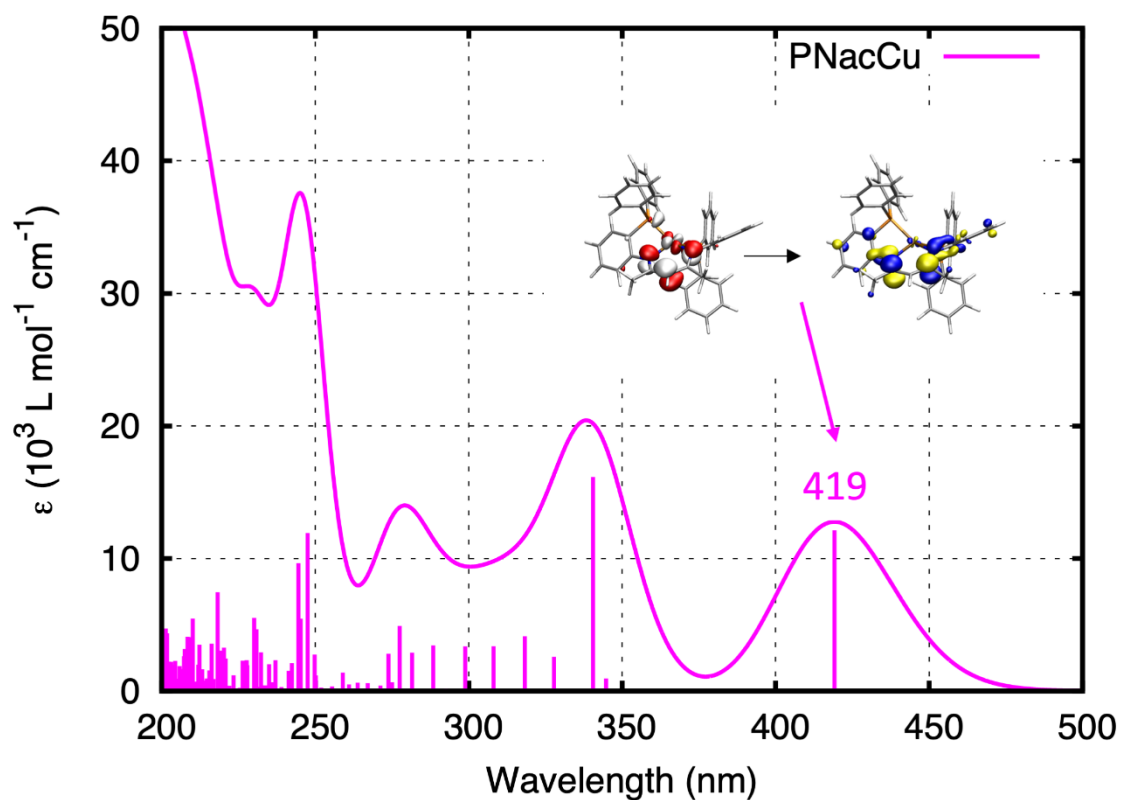


Figure S80: Simulated absorption spectrum of the [PNacCu] complex **9**. Obtained from CAM-B3LYP/def2-SVPD//CAM-B3LYP/def2-SV(P) calculations by applying Gaussian broadening with a full width at half maximum of 2500 cm^{-1} . Oscillator strengths were computed in the mixed length/velocity representation. The dominant pair of natural transition orbitals (NTOs) is plotted at an isovalue of $\pm 0.05 a_0^{-3/2}$.

Supplementary Information

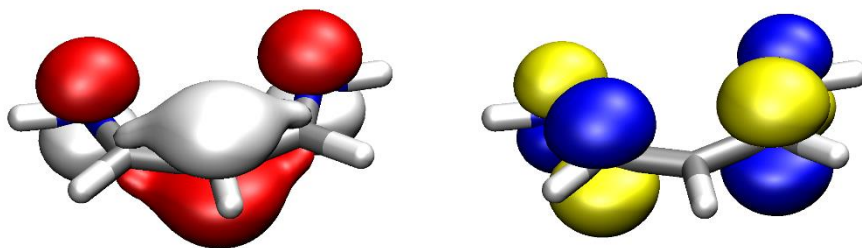


Figure S81: Highest occupied molecular orbital (HOMO, left) and lowest unoccupied molecular orbital (LUMO, right) as obtained from Hückel molecular-orbital (HMO) theory for the model system $[\text{NH}-(\text{CH})_3\text{-NH}]^-$. Plotted at an isovalue of $\pm 0.05 a_0^{-3/2}$.

References

1. F. Krätschmer, *Synthese von multinuklearen mono- und bimetallichen Verbindungen der Münzmetalle sowie die Untersuchung von Metall-Metall Wechselwirkungen auf photophysikalische Eigenschaften*, Cuvillier Verlag, 2023.
2. a) C. Zovko, S. Bestgen, C. Schoo, A. Görner, J. M. Goicoechea and P. W. Roesky, *Chem. Eur. J.*, 2020, **26**, 13191; b) S. Ahrland, K. Dreisch, B. Norén and Å. Oskarsson, *Mater. Chem. Phys.*, 1993, **35**, 281; c) M. Kuprat, M. Lehmann, A. Schulz and A. Villinger, *Organometallics*, 2010, **29**, 1421; d) R. Usón, A. Laguna and J. Vicente, *J. Chem. Soc., Chem. Commun.*, 1976, DOI: 10.1039/c39760000353, 353.
3. J. C. De Mello, H. F. Wittmann and R. H. Friend, *Adv. Mater.*, 1997, **9**, 230.
4. a) G. M. Sheldrick, *Acta Crystallogr. A*, 2015, **71**, 3; b) G. M. Sheldrick, *Acta Crystallogr. A*, 2008, **64**, 112.
5. O. V. Dolomanov, L. J. Bourhis, R. J. Gildea, J. A. K. Howard and H. Puschmann, *J. Appl. Crystallogr.*, 2009, **42**, 339.
6. G. M. Sheldrick, *Acta Crystallogr. C*, 2015, **71**, 3.
7. TURBOMOLE V7.72022, a development of University of Karlsruhe and Forschungszentrum Karlsruhe GmbH, 1989–2007, TURBOMOLE GmbH, since 2007, <https://www.turbomole.org>, (accessed September 16, 2022).
8. a) T. Yanai, D. P. Tew and N. C. Handy, *Chem. Phys. Lett.*, 2004, **393**, 51; b) F. Weigend and R. Ahlrichs, *PCCP*, 2005, **7**, 3297.
9. a) S. Grimme, J. Antony, S. Ehrlich and H. Krieg, *J. Chem. Phys.*, 2010, **132**, 154104; b) S. Grimme, S. Ehrlich and L. Goerigk, *J. Comput. Chem.*, 2011, **32**, 1456.
10. D. Rappoport and F. Furche, *J. Chem. Phys.*, 2010, **133**, 134105.
11. R. L. Martin, *J. Chem. Phys.*, 2003, **118**, 4775.